

ELECTROCHEMICAL DECOMPOSITION OF CHLORINATED HYDROCARBONS.

by

Gerard Anthony McGee


A Thesis Presented to
Dublin City University
for the award of MSc.

Prepared under the supervision of Dr. John Cassidy, Chemistry
Department, Dublin Institute of Technology, Kevin Street and under the
direction of Dr. Johannes G. Vos, School of Chemical Sciences,
Dublin City University.

June 1993.

Declaration.

This thesis has not been submitted as an exercise for a degree at any other University. Except where otherwise indicated, the work described herein has been carried out by the author alone.



Gerard Anthony McGee

CHAPTER 1. GENERAL INTRODUCTION.	1
1.1 General Introduction	1
1.1 Introduction	1
1.1.1 The Need for Alternative Technology	2
1.2 General Electrochemical Introduction	5
1.2.1 Basic Introduction to Electrochemical Cells and Reactions	5
1.2.2 Factors Which Affect Electrode Reaction Rate and Current	9
1.2.3 Electrode Materials	11
1.2.4 Advantages of the Three Electrode Configuration	12
1.2.5 Working Electrodes	14
1.2.6 Reference Electrodes	16
1.2.7 Auxiliary Electrodes	19
1.2.8 Factors Affecting Mass Transport	19
1.2.9 Electrochemical Cells	20
1.2.10 Solvents	21
1.2.11 Supporting Electrolyte	23
1.2.12 Potentiostats	25
1.3 Electrochemical Techniques	
1.3.1 Cyclic Voltammetry	27
1.3.2 Rotating Disk Electrochemistry	32
1.4 Conducting Polymers, General Introduction	36

1.4.1 Polymer Modified Electrodes	36
1.4.2 Polypyrrole	37
1.4.3 Mechanism of Growth of Polypyrrole Films on Electrodes	40
1.4.4 Charge Transport Through Conducting Polymers	42
1.5 Electrochemical Mediation	42
1.6 References	45

CHAPTER 2. CHARACTERISATION OF POLYPYRROLE LAYERS

2.1 Introduction	49
2.2 Theory	53
2.2.1 Electronic Spectroscopy of Conducting Polymers	53
2.2.2 Optical Spectroelectrochemistry	60
2.3 Experimental	
2.3.1 Instrumentation, Cells, Electrodes, and Chemicals	63
2.3.2 Polymer Layer Formation	63
2.3.3 UV-Vis Spectroelectrochemistry	64
2.4 Results and Discussion	65
2.4.1 Cyclic Voltammetry of Polypyrrole Layers	65
2.4.2 Spectroelectrochemistry of Polypyrrole Layers	79
2.4.3 Nernst Model of Polypyrrole System	87

2.4.4 Bandgap Energy Estimation for Polypyrrole	91
2.5 Conclusions	100
2.6 References	103

CHAPTER 3. PLATINUM-CONTAINING POLYPYRROLE LAYERS FOR THE FORMATION OF SUPEROXIDE ION IN

APROTIC MEDIA.	105
3.1 Introduction	105
3.1.1 Introduction	105
3.1.2 The Chemistry of the Superoxide Ion	106
3.2 Experimental	106
3.2.1 Electrodes, Cells Instrumentation and Chemicals	106
3.2.2 Polymer Layer Formation	107
3.3 Results and Discussion	108
3.3.1 Current-Time Analysis of PPy/Pt Layers	108
3.3.2 Cyclic Voltammogram of PPy/Pt Modified Electrodes	111
3.3.3 Rotating Disk Electrode Experiments	116
3.3.4 PPy/Pt Modified Stainless Steel Electrodes	118
3.4 Conclusions	124
3.5 References	126

CHAPTER 4. DECOMPOSITION OF CHLORINATED ORGANIC MOLECULES IN A HOMOGENEOUS MEDIATOR SYSTEM	128
4.1 Introduction	128
4.2 Experimental	130
4.2.1 Instrumentation, Cells, Electrodes and Chemicals	130
4.2.2 Catalyst Incorporation in Surfactant Micelles	130
4.2.3 Bulk Electrolysis Experiments	131
4.3 Results and Discussion	133
4.3.1 Cyclic Voltammetry Experiments	133
4.3.2 Bulk Electrolysis	145
4.4 Conclusions	150
4.5 References	152
 CHAPTER 5. GENERAL CONCLUSION	 153

Electrochemical Decomposition of Chlorinated Hydrocarbons

Gerard Anthony McGee.

Abstract.

This work involves the characterisation of the electrochemical decomposition of chlorinated hydrocarbons. A variety of methods were employed involving the use of catalytic reagents to enhance the rate at which chlorinated organic compounds are reduced. The first reagent used was oxygen which was electrochemically reduced to superoxide in nonaqueous solvents. Superoxide is a reactive intermediate and decomposes chlorinated hydrocarbons. However it was found that since the rate of reaction between the superoxide and water is much greater than between superoxide and the chlorinated hydrocarbons, that the waste organics would need to be dried rigorously before decomposition. Initially oxygen was reduced at platinum but since this process is not economically feasible, it was decided to attempt to reduce the oxygen at an array of platinum microelectrodes supported on a conducting polymer. For this reason the deposition and characteristics of conducting polymers were examined voltammetrically and spectroscopically. It was found that the platinum particles behaved like an array of microelectrodes and that superoxide could be successfully evolved at a platinum containing polypyrrole coating on stainless steel.

A second system was also tried, consisting of a water soluble mediator. In this latter system, the mediator and the chlorinated organic substrate were both confined in a micelle. It was hoped by using this microencapsulation that the reaction of the electrochemically generated mediator and the chlorinated organic would be more efficient. The mediator was a $[\text{Co}(\text{bpy})_3]^{2+}$ complex where bpy is 2,2'-bipyridyl. It was found that the surfactant didodecyldimethylammonium bromide was better than cetyltrimethylammonium bromide for the mediated reduction of carbon tetrachloride using the mediator. Analysis of the bulk electrolysis solution by a potentiometric titration confirmed that the carbon tetrachloride was decomposed to chloride. However the efficiency was low due to the small area of the electrode.

CHAPTER 1. GENERAL INTRODUCTION

1.1 INTRODUCTION:

As humanity moves towards the 21st century people are turning towards the scientific community and appealing for “greener”, more environmentally -friendly technology. Mankind has realised the environmental folly of much of what industrial “progress” has achieved for society. Global pollution on an ever upwardly spiraling scale, the depletion of the ozone layer, the greenhouse effect etc. are all concepts with which the modern non-scientific layperson is all too familiar.

The furore that arose in the Northwest of Ireland last year with the proposed siting of a waste incinerator at the DuPont factory in Derry shows that the “greening” of many existing technological processes and methods is a concern of more than just technologists. With this in mind there are groups in various branches of chemical research working on the development of “cleaner” technology.

There are many different groups working on the development of electrochemical methods of chemical waste disposal [1]. Such processes under study include the treatment of water using UV-Vis/Ozone techniques, nitrate treatment, the electrochemical destruction of organic molecules and the removal of metal ions from dilute solutions [1]. The removal of heavy metal ions such as Pb^{2+} , Cd^{2+} and Cu^{2+} from solutions is a very important process as public interest in the occurrence and effects of such ions in domestic water supplies is high.

The area of interest in this work was the destruction of chlorinated organic molecules using electrochemical techniques. There are many reports of organic molecule decomposition by electrochemical methods in the literature [1-5]. Sawyer, et al [2], reported the destruction of a number of polychlorinated organic molecules by employing electrochemically generated superoxide ion as a reagent. Rusling et al, dehalogenated 4-4' dibromobiphenyl at clay modified electrodes utilizing a surfactant system [3]. Furthermore he investigated electrochemical decomposi-

tion of 4-bromobiphenyl [4] and trichloroacetic acid [5], to name but two. Organic wastes with a high water content may prove difficult to incinerate. A method of treatment for such wastes has been developed [1]. This method consists of a membrane electrolyser into which is pumped an electrolyte consisting of nitric acid containing a silver salt. At the anode the silver salt is oxidized, and the highly reactive Ag(II) species formed destroys the carbon-chlorine bond. The work presented here is concerned with the development of a system, utilizing electrochemical techniques, to decompose polychlorinated organic molecules. A system based on superoxide is examined followed by the use of organometallics, both of which decompose a carbon halogen bond.

1.1.1 The need for alternative technology

Rusling investigated the electrochemical removal of chlorine from 4-chlorobiphenyl and 4,4'-dichlorobiphenyl [6]. Polychlorinated biphenyls, (PCB's), were used extensively in electrical equipment until their toxicity and persistence were recognised in 1966 [7] PCB's may be dechlorinated by chemical, photochemical or electrochemical means, but extreme conditions and/or excess reagents are often necessary [6]. The problem that exists is that much of the PCB pollutant levels in the environment are due to PCB's which were in inks, adhesives, plasticisers etc. which are buried in landfill sites. Landfill sites emit gaseous fermentation products, such as methane, which carry volatile compounds like PCB's into the atmosphere. The preferred environmental solution would be some method that decreases, rather than contains, the level of PCB contamination [7].

The method usually used to decompose polychlorinated organic molecules is incineration. The method has a number of disadvantages [8];

- (1) Incineration is relatively expensive. Very high temperatures are needed to incinerate heavily chlorinated wastes.
- (2) Requires combustible fuel or fuel solution.
- (3) May produce residues which must be scrubbed and stored or disposed of.

- (4) Incineration frequently requires pollution control devices that can produce additional wastes.

One of the unwanted wastes that can be formed in incinerator stacks are dioxins [8]. The term “dioxin” is a synonym for the group of polychlorinated dibenzo-p-dioxins, (PCDD's), containing seventy-five isomers with chlorine substitution ranging from one to eight atoms. Dioxins are extremely toxic. The key sources of dioxins are chemical manufacture and incineration [9]. Dioxins have also been identified as trace contaminants in commercial PCB formulations. The levels of dioxin concentration necessary for toxicity are in the order of nanograms. A figure for grammes of dioxins formed per tonne of waste incinerated of 1173 $\mu\text{g}/\text{tonne}$ was obtained from studies in the U.S. and Europe. There is an average of approximately 3×10^6 tonnes of waste incinerated per annum in the U.K. [9]. So any technology which would minimise the use of incineration for waste disposed would be at least environmentally welcome.

Finally a method of organic waste decomposition worthy of mention is the process of Bioremediation [10]. This appears to be a very attractive and in many cases, a cost effective, treatment process. The process involves the stimulation of microorganisms to degrade chemical wastes. There are “blends” of microorganisms being developed to degrade petroleum hydrocarbons [11]. The final products are expected to be carbon dioxide, small organic compounds or water-soluble microbial products. It has been found, in the case of chlorinated organic molecules, that the ease of biodegradation decreases as the number of chlorine atoms increases [10]. Therefore, compounds such as PCB's, chloroform and carbon tetrachloride are not easily biodegraded.

Sawyer, et al [2], found when using electrochemically generated superoxide ion as a reagent that highly chlorinated molecules were easier to decompose than those containing less chlorine. With this in mind this work proposed to develop an electrochemical method, using polypyrrole modified electrodes, to decompose some model polychlorinated compound, eg. CCl_4 , then to extend analysis to some actual organic wastes with a view to the design and development of a reactor

system for the decomposition. Since there is a considerable electrochemical content in this work, it is necessary to review some fundamentals. This will be done in the next section.

1.2 GENERAL ELECTROCHEMICAL INTRODUCTION

1.2.1 Basic introduction to electrochemical cells and reactions.

Electrochemical measurements may be made on a system for a number of reasons. These include obtaining thermodynamic data for a reaction, generating some intermediate, such as a cation radical, to study its properties or analysis of a solution for traces of some metal ion or organic species, or electrosynthesis of some product of interest [12]. All of these processes require an understanding of the basic principles of electrode reactions the electrical properties of electrode/solution interfaces.

In potentiometric experiments, the current is equal to zero and potential is determined as a function of concentration. As no current flows in the experiment no net faradaic reaction occurs. When the current is equal to zero the Nernst equation applies

$$E = E^0 + \frac{RT}{nF} \ln \left\{ \frac{[\text{Oxidized}]}{[\text{Reduced}]} \right\} \quad 1.1$$

Where activity coefficients are assumed to be 1, and symbols having their usual meaning. Potentiometry involves measuring the interfacial potential difference across a membrane with a pair of reference electrodes.

Electrochemical analysis is also concerned with the processes and factors affecting the transport of charge across interfaces between chemical phases. One of the contributing phases will be electrolyte, which is the phase through which charge is carried by the movement of ions. The second phase at an interface may be an electrode, which is a phase through which charge is carried by electronic movement. Electrodes are usually metals or semiconductors. One must study the properties of collections of interfaces, called electrochemical cells. Generally there are two electrodes separated by at least one electrolyte phase. There is generally a measurable difference in potential between the two electrodes. The transition in

electric potential in crossing from one conducting phase to another occurs almost entirely at the interface itself. So the measurement and control of cell potentials is a very important part of experimental electrochemistry. In a two electrode cell one is generally only interested in one half reaction and the electrode at which it occurs. This electrode is termed the working electrode. To focus on it the other electrode is “standardised” and is called the reference electrode. So one observes or controls the potential of the working electrode with respect to the reference electrode. Generally by driving the electrode to potentials more negative than the equilibrium potential, the energy of the electrons is raised until they occupy a level high enough to occupy vacant sites on species in the electrolyte. This leads to a flow in electrons from electrode to solution, i.e. reduction occurs, see figure 1.1(a) [12]. In a similar manner application of a more positive potential leads to an oxidation current due to movement of electrons from electrolyte to the electrode, figure 1.1(b)

On the application of a potential which is different to the equilibrium potential of a redox couple, a current will flow which, in the absence of mass transport control, is governed by the Butler-Volmer equation [13]

$$i = i_0 \{ \exp(-\alpha f h) - \exp(1 - \alpha) n f h \}$$
1.2

where i_0 is the exchange current density, h is the overpotential, α is the transfer coefficient and

$$f = \frac{nF}{RT}$$
1.3

The overpotential, h , is the difference between the applied potential and the equilibrium value. At potentials close to the equilibrium potential the rate of electron transfer may be slow, and in this region the electron transfer may be said to be kinetically controlled.

The product of the electron transfer reaction is contained within a layer in

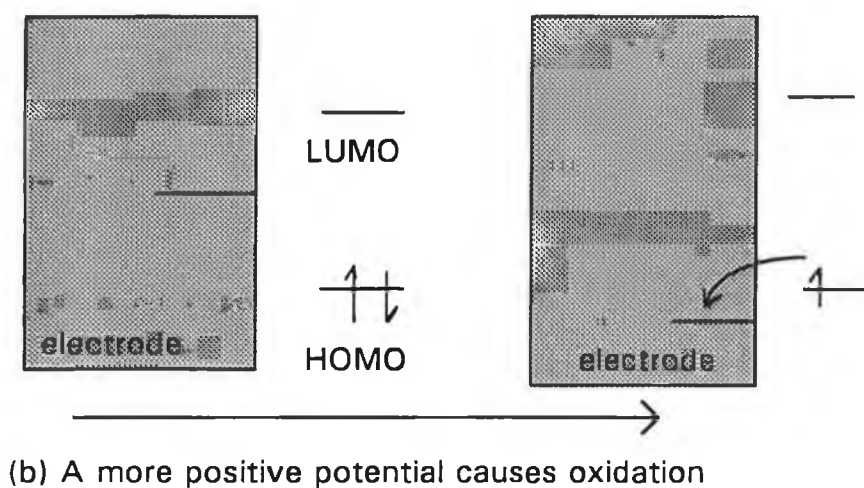
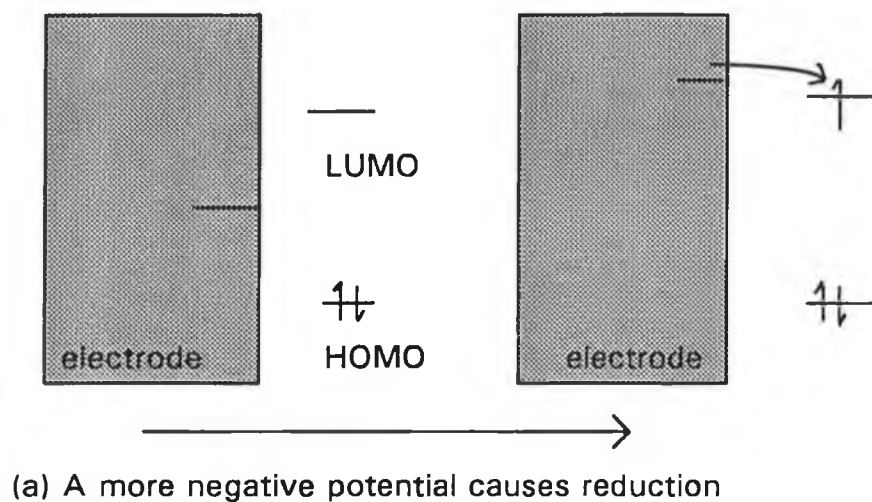


Figure 1.1 Schematic representation of, (a) oxidation and (b) reduction processes of a species A in solution at an electrode surface.

solution at the electrode surface. This layer is commonly termed the diffusion layer. As the potential is scanned in a positive/negative direction from the equilibrium potential the rate of consumption of reduced/oxidized species increases exponentially. Therefore the rate of electron transfer increases exponentially with potential causing the resulting current to increase in a similar manner if the reaction is not mass transport controlled. As the production of reaction product increases the diffusion layer extends out into the solution. The reactant therefore has further to diffuse to reach the electrode surface. Electron transport is therefore mass transport, ie. diffusion, controlled. Amperometry involves maintaining the potential of an electrode at a constant value with respect to the reference electrode and observing changes in current [14].

Virtually any surface in contact with an electrolyte solution acquires a charge and therefore an electric potential different to that of the bulk solution. There are four ways in which a surface may acquire a charge;

- (1) Imposition of a potential difference from an external potential source.
- (2) Adsorption of ions on a solid surface or on the surface of a colloidal particle.
- (3) Electron transfer between a metallic conductor and the solution
- (4) In the case of micelles and biological macromolecules and membranes, ionization of functional groups such as carboxylate, phosphate or amino groups [14].

A charged surface in contact with an electrolyte solution will be expected to attract ions of opposite charge and repel ions of like charge. An ion atmosphere is established in the immediate vicinity of the surface. Two parallel layers of charge are formed, the charge on the surface itself and the layer of oppositely charged ions near the surface. This is the double layer or the electric double layer. This layer is akin to a capacitor and therefore at a given potential the electrode/solution interface is characterised by a double-layer capacitance, C_d , typically of the order of a 10 to 40 $\mu\text{F}/\text{cm}^2$ [12]. There are a number of reviews of double-layer theory [14] Stern suggested that the double-layer consisted of some ions immobilised

on the surface (the Helmholtz layer), while the remainder of the charge is neutralised by a diffuse layer extending out into the solution [14]

Here it might be worth mentioning the difference between the two types of processes which occur at electrodes. In one type, electrons are transferred across the metal/solution interface. The electron transfer causes oxidation or reduction to occur. These reactions are governed by Faraday's law and are hence termed Faradaic processes. Under some condition no charge transfer reaction occurs because such reactions are thermodynamically or kinetically unfavourable. Processes such as adsorption and desorption can occur, and the structure of the solution/electrode interface can change with changing potential or solution composition. These processes are termed non-faradaic processes

1.2.2 Factors affecting electrode reaction rate and current

An overall electrode reaction is considered

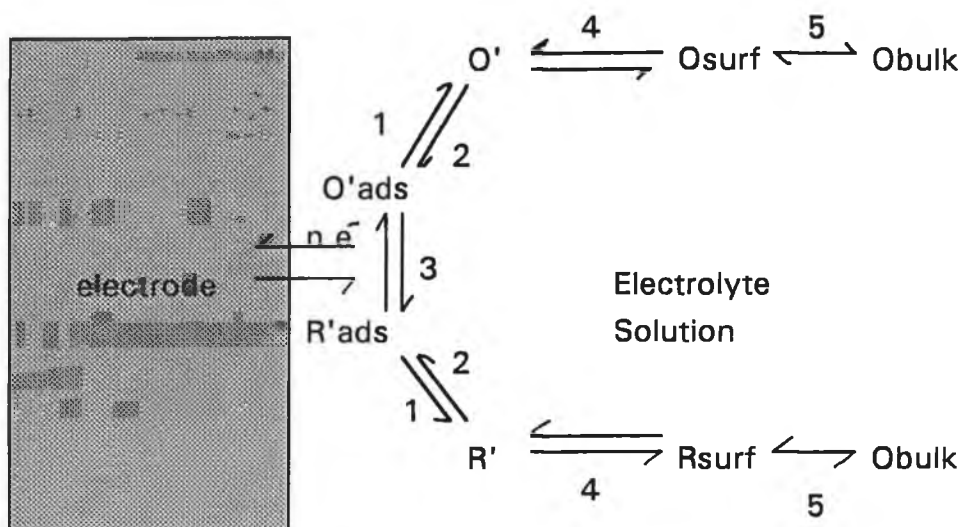


Composed of a series of steps which lead to the conversion of the dissolved oxidized species, O, to the reduced form, R, in solution. The current is affected by the rates of processes, such as

- (1) mass transfer of O from the bulk solution to the electrode surface,
- (2) electron transfer at the electrode surface,
- (3) chemical reactions preceding or following electron transfer,
- (4) other surface reactions such as adsorption, desorption electrodeposition.

The schematic representation of the pathway of a general electrode reaction is shown in figure 1.2 The simplest reaction involves only mass transfer of a reactant to the electrode, heterogeneous electron transfer involving non-adsorbed species and mass transfer of the product to the bulk solution.

There are two types of electrodes, polarizable and non-polarizable



- 1 Adsorption
- 2 Desorption
- 3 Electron Transfer
- 4 Chemical Reactions
- 5 Mass Transport

Figure 1.2 Pathway of a general electrode reaction
 1. Adsorption 2. Desorption 3. Electron Transfer

electrodes. An electrode at which no charge transfer occurs across the metal/solution interface regardless of potential imposed by an outside source of voltage is called a polarizable electrode. This type of electrode shows a large change in potential for the passage of an infinitesimal current. An electrode whose potential does not change upon passage of current is termed a non-polarizable electrode. Such electrodes are reference electrodes.

1.2.3 Electrode Materials

In order to obtain cell potentials of thermodynamic significance the potential must be measured under reversible conditions. A reversible process is one which can be reversed in direction by an infinitesimal change in the conditions of the surroundings. An electrochemical cell is regarded as reversible if a small amount of current can be passed in either direction without appreciably affecting the measured potential. Irreversible behaviour usually results from an electrode process having slow reaction kinetics, either in the electron transfer process, in a coupled chemical reaction or in the delivery of reactants to the electrode [15]. The reversibility or irreversibility of an electron transfer reaction is a function of the electrode material and will be discussed below. Firstly some important properties of electrode materials will be discussed and then working, reference and auxiliary electrodes will be discussed in greater detail.

The important properties of electrode materials include [16];

- (1) Physical stability: Material chosen must be of adequate mechanical strength. The material must not be subject to corrosion by the electrolyte, reactants or products and should be crack resistant.
- (2) Chemical stability: The material must be corrosion resistant, resistant to the formation of unwanted hydride or oxide layers and resistant to the deposition of unwanted organic films under all conditions.
- (3) Suitable physical form: It must be possible to fabricate the material into the form as required by the cell or reactor design. The material must facilitate sound

electrical connections.

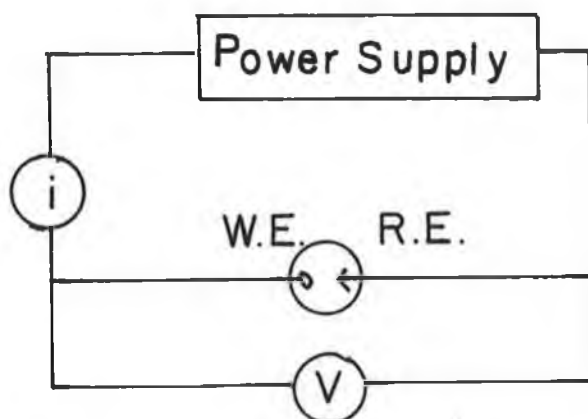
- (4) Rate and product selectivity. The electrode material must support the desired reaction and in some processes electrocatalytic processes are necessary. The electrode material must support the desired chemical change while inhibiting all competing chemical changes
- (5) Electrical conductivity: The material used for an electrode must have sufficiently high electrical conductivity throughout the electrode system in order to maintain a uniform current and potential distribution. This helps to minimise voltage losses leading to energy inefficiencies.
- (6) In the case of industrial processes the cost and lifetime of the material is important.

1.2.4 Advantages of the three electrode cell configuration

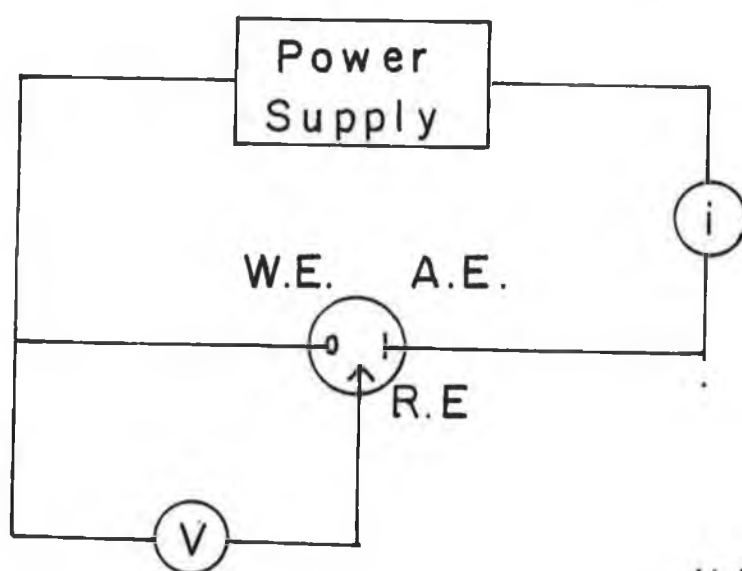
When the potential of an electrode of interest is measured against a nonpolarizable, reference, electrode, during the passage of current, a voltage drop of iR_s , by Ohm's law, is observed. R_s is the resistance of the solution which lies between the two electrodes and is therefore dependant on the distance between the electrodes.

The simplest electrode system is the two electrode system, and is schematically depicted in figure 1.3(a). The two electrode system works reasonably well for aqueous polarography where R_s is low and the current is small. When for example, nonaqueous solvents are used or the experiment generates a large current, iR_s drop may become a serious problem [2]. In these cases it is necessary to introduce a three electrode cell configuration, figure 1.3(b). In this configuration an auxiliary or counter electrode is introduced. Basically this acts as a sink for any current passed.

The device used to measure the potential difference between the working and reference electrodes must have a high input impedance, so that a negligible current is drawn through the reference. This means that the potential of the



(a)



(b)

Figure 1.3 Schematic representation of two and three-electrode cell configurations.

Figure 1.3(a) Schematic representation of a two-electrode cell configuration.

Figure 1.3 (b) Schematic representation of a three-electrode cell.

reference electrode will remain constant as relatively no current is passed. However, even such an arrangement does not remove all of the iR_s drop from the reading observed by the potential reading device. For the reference electrode placed anywhere but exactly at the working electrode surface, some fraction of iR_s , called the uncompensated resistance, will be observed in the measured potential. This can be minimised by using a very fine capillary tip called a luggin capillary.

1.2.5 Working Electrodes

The surface of the working electrode defines the interface at which an electrochemical reaction under study is occurring. Many materials can be used as working electrode materials. During this work platinum and carbon were used as working electrode materials. Also used were modified platinum and glassy carbon electrodes. For spectroelectrochemical work, optically transparent Indium tin oxide, (ITO), electrodes were used. These ITO electrodes will be discussed in a later chapter.

Previous workers [16], have suggested that the physical and chemical properties of the electrode material affect the rate of electron transfer across an electrode/solution interface. For example surface roughness of the glassy carbon electrode will present different sites for reaction to occur for an incoming reagent molecule. Ultimately this would lead to a distribution of heterogeneous rates of reaction at an electrode surface. It be therefore logical to assume a Gaussian distribution of heterogeneous rate constants and there has been studies on the cyclic voltammetry of such systems [17].

The reduction of the supporting electrolyte or the solvent is what normally limits the accessible potential on the negative side, for a particular electrode material. Similarly the oxidation of solvent or supporting electrolyte limits the potential attainable on the positive side, or oxidation of electrode material itself. There are tables of useful potential ranges for different electrode materials available [18]. For a study of a particular system the choice of working

electrode material is very important.

Commonly used working electrodes are platinum, gold, silver, mercury and various forms of carbon. Mercury is used for cathodic processes because it has a high overpotential for hydrogen evolution. Mercury has the advantage of being a liquid at room temperature and therefore can be used in a pool or hanging drop configuration or plated as a thin film on other solid electrode materials [19]. Mercury is rarely used for anodic processes as it is easily oxidized. A useful application here is the technique of anodic stripping voltammetry. There have been reports of anodic stripping voltammetry being carried out at mercury-containing zeolite layers on glassy carbon and gold support electrodes [20]

Platinum has a low overpotential for hydrogen evolution. In polar aprotic solvents, if water-free, platinum exhibits a greater positive potential limit than most other commonly used electrode materials. In aqueous solutions the platinum forms a conductive oxide film thought to consist of chemisorbed oxygen [18].

The most commonly used form of carbon as a working electrode is glassy carbon. This form of carbon is highly conductive and physically and chemically complies with the ideal properties of an electrode material as mentioned in section 1.2.3.

The advantages of glassy carbon over gold, silver or platinum electrodes include,

- (1) It is much cheaper,
- (2) It is very easy to polish,
- (3) It has a high overpotential for hydrogen evolution and
- (4) some redox systems exhibit a greater reversibility at glassy carbon than at other electrodes.

Glassy carbon electrodes have the disadvantages of exhibiting a high residual current in sulphuric acid and surface roughening can occur at high current densities [21, 22]. This surface roughening may then lead to the distribution of heterogeneous rate constants mentioned earlier [17].

It is necessary that the surface area of the working electrode be smaller than

the area of the auxiliary electrode. Pretreatment of the working electrode is required to remove surface impurities. Generally the pretreatment step consists of polishing the electrode on cloth or felt which is impregnated with a polishing substance such as alumina powder of a specific particle size. Generally polishing is initiated by polishing with alumina of a large particle size working down through the grades until the final polishing with alumina of the smallest particle size. Other methods of pretreatment may involve electrochemical cycling of the electrode in supporting electrolyte solutions.

It is usual to find solid electrodes fabricated as discs. These discs are mounted by sealing a rod of the solid electrode material in a cylinder of some inert substance such as Teflon or glass. In this way a reproducible and easily polished area of the electrode is exposed. In most of the experiments carried out in this work glassy carbon or platinum disc electrodes mounted in Teflon were used for stationary and rotating disc electrode studies.

The geometric surface area of these electrodes were of the order of 0.07 cm^2 . Prior to analysis the exposed electrode surface was polished using $0.3 \mu\text{m}$ alumina slurry on felt to a mirror finish.

1.2.6 Reference Electrodes

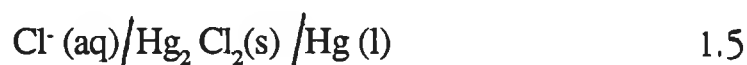
The characteristics of a ideal reference electrode are;

- (1) the electrode should be easily and reproducibly prepared and maintained,
- (2) should be relatively inexpensive,
- (3) the potential should be stable over time,
- (4) the electrode should be usable over a wide variety of conditions,
- (5) the reference electrode should contain both the oxidized and reduced form of the couple, both of which should be stable
- (6) the potential should return to original value after a small amount of current has passed through the electrode and,

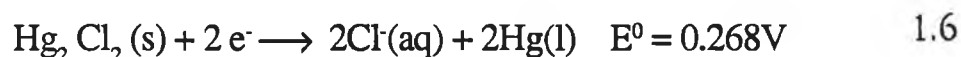
(7) there should be little temperature dependence.

The reference electrode is a source of a fixed potential. As the potential of the reference electrode is fixed, any change of potential observed in the cell potential must therefore be due to a change in voltage at the working electrode/solution interface.

Two types of electrodes which comply with the characteristics of an ideal reference electrode are the calomel electrode and the silver-silver chloride electrode. Schematic representations of these two electrodes are shown in figure 1.4. The calomel electrode is represented in shorthand notation by [23]

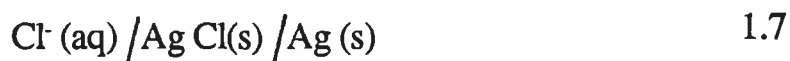


The half-cell reaction is

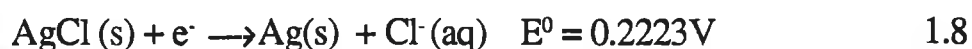


In practice it is usually more convenient to use saturated KCl solution as the electrolyte with a few crystals of solid KCl present in the solution to maintain saturation. In this way the chloride concentration is held constant.

The silver-silver chloride electrode provides a stable potential in halide solutions provided the halide concentration is not too high. In shorthand notation the silver-silver chloride electrode can be represented by



The half-cell reaction is



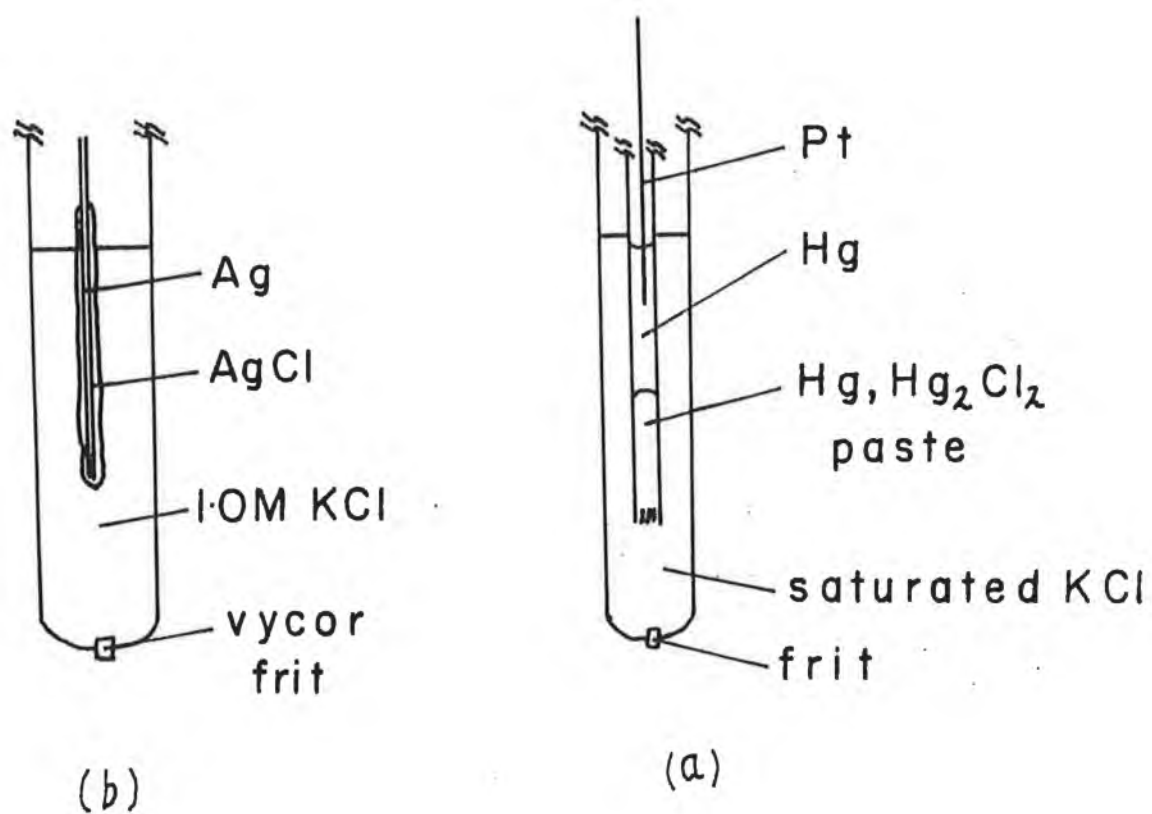


Figure 1.4 Reference Electrodes

Figure 1.4 (a) Saturated Calomel Electrode.

Figure 1.4 (b) Silver/Silver Chloride Reference Electrode.

In an operational sense the Ag/AgCl electrode is easily miniaturised and is thus convenient for biological applications and for microlithographic applications [23]. A Ag/AgCl electrode is normally prepared by coating a clean silver wire with AgCl. The electrode is washed and allowed to age for 3 days. The electrode is then placed in saturated KCl solution, (saturated with AgCl), in a tube fitted with a glass frit to prevent leakage [23]. Temperature fluctuations can result in concentration gradients when using saturated solutions. It is therefore recommended that solutions of 3.5 mol dm^{-3} KCl, (saturated with AgCl) be used, as opposed to saturated KCl solutions. In most of this work reference electrodes of calomel in saturated KCl or NaCl solutions were used.

1.2.7 Auxiliary Electrodes

An auxiliary electrode acts as a current sink. Basically, any current generated at the working electrode flows through the auxiliary electrode. This prevents any current flowing into the reference electrode leading to a potential drop being observed. The area of the auxiliary electrode should be greater than that of the working electrode to allow the current to pass easily through the auxiliary electrode. The material chosen for the auxiliary electrode must be such that it does not contaminate the test solution. Commonly carbon or platinum are used. Ideally a separate compartment should be used for the auxiliary electrode. However in this work for voltammetry, a 3-electrode, a two compartment cell was used. The auxiliary electrode used in this work was a carbon rod.

1.2.8 Factors affecting mass transport.

It is routine practice to use the 3 electrode cell configuration in modern electrochemical techniques. Electrochemists are generally concerned in areas which involve mass transport or electrode kinetics, since either or both limit current. There are three forms of mass transport. These are

- (1) Migration - which is the transport of ions through an electric potential gradient. To minimise migration the solution contains a high concentration of an inert electrolyte, called the supporting electrolyte. This ensures a nearly constant electric potential throughout the solution
- (2) Convection - which is the transport of ions or molecules by mechanical motion of the solution. Convection may occur either through gravity operating on a density gradient or through stirring of the solution or motion of the electrode. Convection may be minimised by maintaining a controlled temperature or using a rotating disc electrode.
- (3) Diffusion - which is the transport of ions or molecules through a chemical potential gradient. In stagnant solutions with excess electrolyte, the predominant form of mass transport is diffusion.

1.2.9 Electrochemical Cells

As mentioned earlier the cell current passed between the working and auxiliary electrodes. Ideally the reference electrode is placed in a salt bridge and is connected to the solution via a luggin capillary whose tip is placed near the working electrode. This is done to minimise the error associated with the iR_s potential drop observed. The optimum distance of the tip of the luggin capillary from the working electrode is $2d$, where d is the outside diameter of the capillary tip [12].

As temperature control is necessary, cells are normally surrounded by a water jacket. This allows the circulation of thermostatted water around the cell and allows convection to be minimised. The presence of oxygen in the cell can cause problems due to unwanted oxide formation or the occurrence of oxygen reduction of cathodic potentials [18]. Oxygen present may also react with electrochemically generated intermediates at the working electrode. Some of these reaction may be useful. As an example, metalloporphyrins have been used

to catalyse the reduction of oxygen to water [24]. Electrochemically generated superoxide ion, obtained by the cathodic reduction of oxygen, has been used to decompose polychlorinated organic molecules [2].

To minimise oxygen interference, degassing of the solution is necessary. Usually degassing is achieved by bubbling oxygen-free argon, helium or nitrogen through the solution. Nitrogen is generally used for reasons of cost. There are a number of problems associated with the use of nitrogen. As nitrogen is lighter than air it must be left flowing over the solution during analysis to maintain an oxygen-free atmosphere. Argon, being heavier than air, forms a blanket over the solution while degassing. Helium is the most ideal gas for degassing, but it is expensive. The electrochemical cell used in this work was a single compartment 3 electrode cell, fitted with a water jacket. A nitrogen inlet was used for degassing the solutions. A luggin capillary was not used. The cell configuration is shown in figure 1.5. The cell configurations used for spectroelectrochemical and bulk electrolysis experiments will be discussed in the appropriate chapters.

1.2.10. Solvents

There is no single solvent which is ideal for all electrochemical work. The choice is often dictated by the solubility and reactivity of the materials to be studied. In organic and organometallic work, strongly basic anions or radical anions are often produced which are rapidly protonated by solvents like water or alcohols. Water is an impurity in many solvents and may make solvent purification and drying an important consideration. Some important properties of solvents for electrochemical use include,

- (1) Liquid range - generally the greater the liquid range, the greater flexibility in experiments.
- (2) Vapour pressure - since oxygen may be present as a unwanted interferent, the system is usually degassed with N_2 or Argon. The purge gas may be

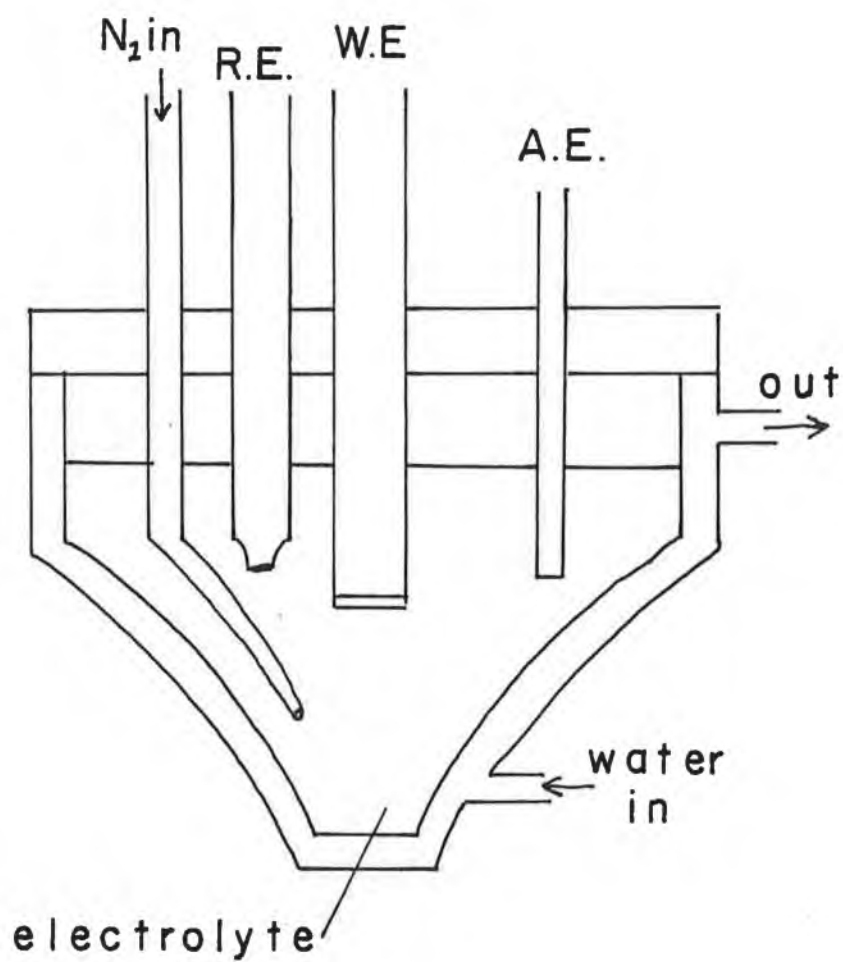


Figure 1.5 Cell Configuration used for electrochemical experiments.

presaturated with solvent. When the vapour pressure is high, it is often difficult to maintain a constant composition and temperature due to solvent evaporation.

(3) Solvent viscosity. Solvents of low viscosity will generally give electrolyte solutions with greater conductivities[25]. As diffusion is faster in such cases, diffusion controlled chemical reactions will therefore be faster. So an electrode process which is irreversible in a nonviscous solvent, because of a fast following chemical reaction may become reversible in a more viscous medium[25].

(4). Dielectric constant. To obtain conducting electrolyte solutions, the dielectric constant of the solvent should be high. The value of the dielectric constant of the solvent dictates the dissociative power of the solvent towards ionic compounds that provide the ions in solution to carry the charge. In solutions of low dielectric constant, solution iRs drop is usually a very serious problem since ions are not fully dissociated. Water has a dielectric constant of 78.4 at room temperature[26]. It has generally been accepted that a dielectric constant greater than 15 is required for dissociative dissolution of an ionic solute. A table of solvent properties for the solvents used in this work is given in Table 1.1[2].

The dielectric constants of solvents such as tetrahydrofuran (THF), can be raised to values sufficient for dissociative dissolution by the addition of water. All aqueous solutions used in this work were prepared using ultra pure water with a resistivity of 16-18 megaohms cm.

1.2.11 Supporting electrolyte

Voltammetry and related electrochemical techniques require an excess of

Solvent	Liquid Range($^{\circ}\text{C}$)	Vapour Pressure(kpa)	Dielectric Constant	Viscosity ($10^{-3}\text{kg m}^{-1}\text{s}^{-1}$)
Water	0 - 100	3.2	78.4	0.89
Dimethylsulphoxide (DMSO)	19 - 189	0.1	46.7	2.0
N,N Dimethylformamide (DMF)	-60-153	0.3	36.7	2.0
Acetonitrile	-44 - 82	11.8	37.5	0.34
Tetrahydrofuran	-108 - 66	26.3	7.6	0.46

Table 1. 1 Solvent properties of solvents use in this work at 20 $^{\circ}\text{C}$

inert electrolyte to make solutions conducting and to reduce the thickness of the electrode double-layer, hence minimising migration effects. In aqueous solutions KCl and HCl are commonly used. In non-aqueous work LiClO_4 is commonly used. The electrolyte used must be electrochemically inert over the potential range of interest. It should not react with the species of interest or with the solvent used. The presence of electrolyte ions adsorbed on the electrode surface or in the double-layer may greatly affect the kinetics of the electron transfer. The ability of commonly used ions to adsorb onto the electrode surface increases in the following order [28]



In this work the supporting electrolyte concentration was typically 0.1 mol dm^{-3} .

1.1.12. Potentiostats

An instrument known as a potentiostat is used to control the potential between the working and reference electrodes. A common potentiostat design based on an operational amplifier is shown in figure 1.6 [25]. The function of the reference electrode in the two electrode system is divided in two. A true reference electrode is used as a source of constant potential, and an auxiliary electrode is used as a sink for all faradaic current. A voltage follower is attached to the reference electrode so that very little current is drawn in this part of the circuit. A control potential, equal and opposite to the desired potential of the reference electrode, is added to the actual reference electrode potential and the sum applied to the inverting input of the operational amplifier. The positive input is at ground potential as is the working electrode. It is this addition of input potentials which permits the generation of complex waveforms. The working electrode feeds a current follower, CF, whose output is proportional to the current flowing in the cell, ie. the CF measures current flowing. Two different potentiostats were used in

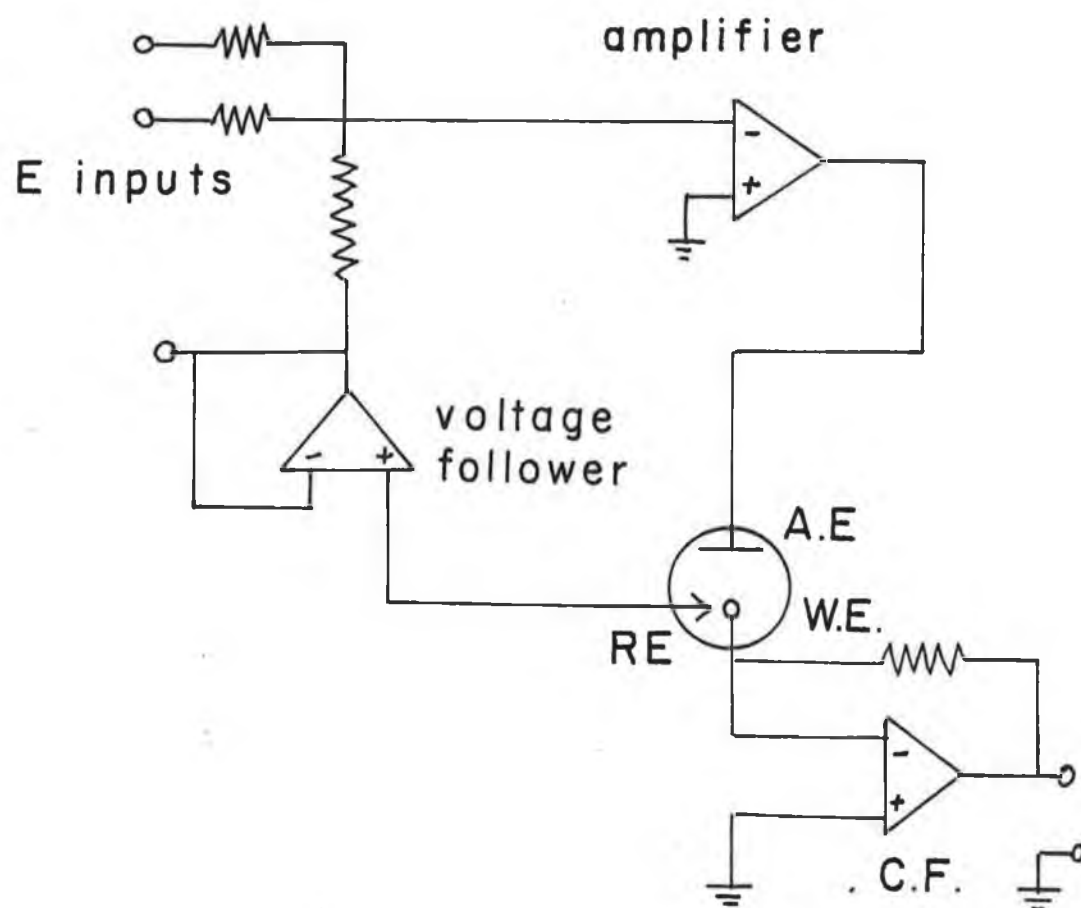


Figure 1.6 Schematic representation of potentiostat circuit for control of a three-electrode cell configuration.

this work. A Sycopel Scientific potentiostat, model DP301, with an inbuilt waveform generator was used. Also a H.B. Thompson potentiostat linked to a H.B. Thompson precision "16 bit" ramp generator model DRG16 was used.

1.3 ELECTROCHEMICAL TECHNIQUES

1.3.1 Cyclic Voltammetry

Cyclic voltammetry is an extension of linear sweep voltammetry. If the potential is changed linearly with time a current-potential curve is produced. The resulting curve is called a linear sweep voltammogram. The potential is changed linearly by applying a potential ramp as a function of time to the working electrode. In cyclic voltammetry the voltage is cycled between two potential limits. The triangular potential waveform is applied to the cell so that the working electrode potential is swept linearly past the formal potential of a couple and then back again. For a solution of oxidized form, O, the potential is swept linearly past E^{01} in accordance with equation 1.4. On the forward scan, the current response is due to O being reduced to R. On the reverse scan the R molecules near the electrode are reoxidized to O and an anodic peak results. The resulting set of peaks is called a cyclic voltammogram, as can be seen in figure 1.7. Much of the mathematics derived for linear sweep voltammetry can be applied to cyclic voltammetry. The use of this theory in conjunction with experimental results enables the determination of kinetic parameters, principally k^0 , the standard rate constant [29].

Generation of a triangular waveform is done as follows; At the initial potential, E_1 , no current flows. The potential is then swept at a rate, v , called the scan rate, to some potential E_2 , E_2 is termed the switching potential. At E_2 the sweep is reversed and the potential is swept back in the direction of E_1 , at a scan rate v , as shown in figure 1.7. It is normally impractical to use standard redox potentials for electrochemistry experiments. Standard potentials refer to standard

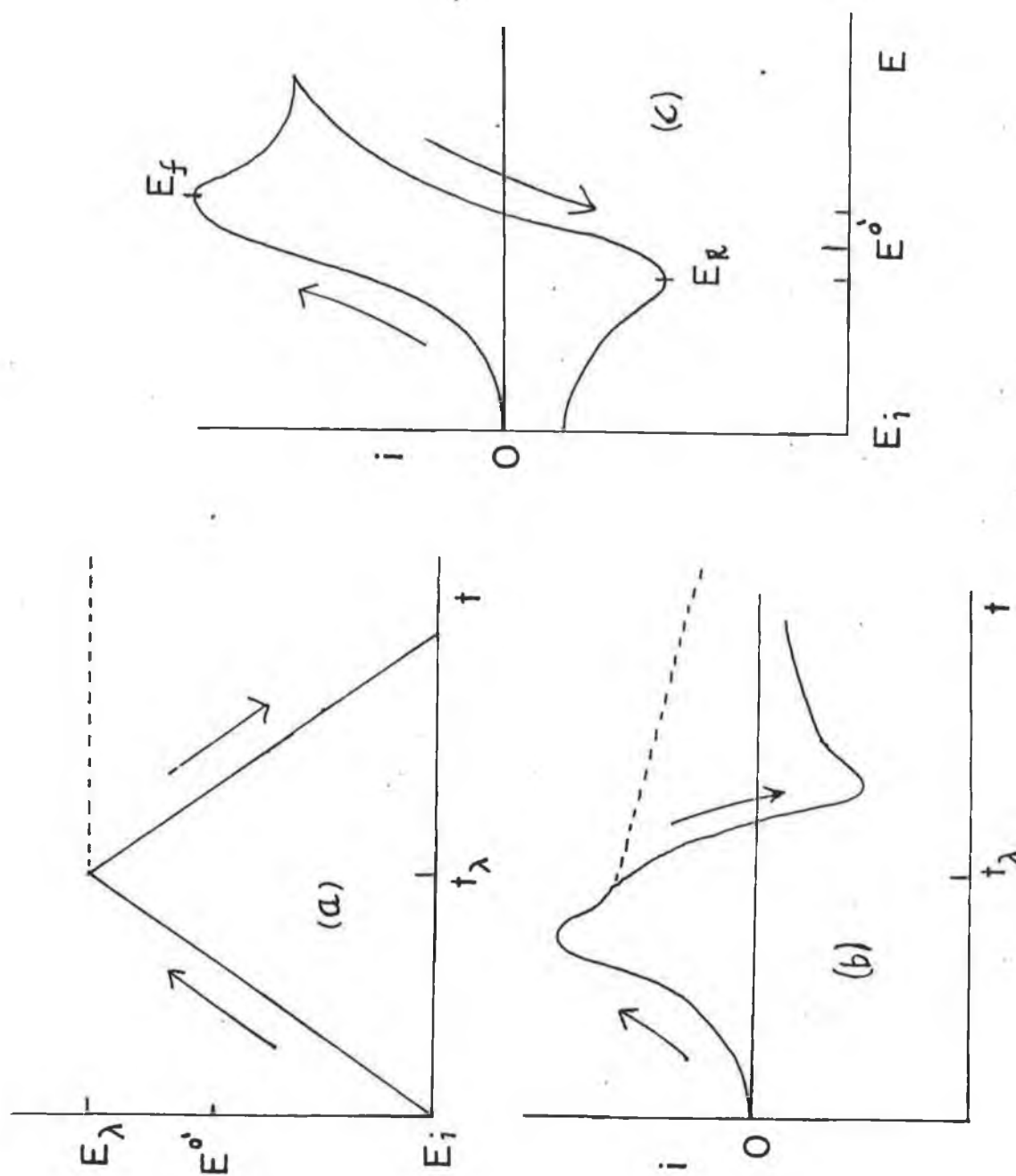


Figure 1.7 Cyclic Voltammetry representation.
 (a) Applied potential waveform for cyclic voltammetry.
 (b) Resulting cyclic voltammogram as a function of time.
 (c) Resulting cyclic voltammogram as a function of potential.

states, which, for solution species are hypothetical 1 molar ideal solutions of both O and R. The measurement of standard potentials involves the determination of activity coefficients. To avoid this problem it is normal to use formal potential, E_f . The formal potential is defined as the potential of the half-cell when the concentration quotient of the Nernst equation is equal to one, when concentration and nature of electrolyte is quoted [30]. Alternatively, if a general cell is considered the half-reaction at the right hand electrode is



The Nernst equation is therefore

$$E = E^0 + \frac{RT}{nF} \ln \left[\frac{O^{v_o}}{R^{v_R}} \right] \quad 1.11$$

which is an expression for the potential of the O/R electrode versus the Normal Hydrogen electrode, as a function of the activities of O and R. It also defines the concentration dependence of the emf of the reaction [31]. So the formal potential, E_f , is measured potential of the half-cell versus NHE when,

- (1) the species O and R are present such that the ratio $[O] / [R]$ is one
- (2) other specified substances, e.g background electrolyte, in the medium, are present in known concentrations.

When E_f lies between E_1 and E_2 , then as the potential approaches E_f , electron transfer begins. Reduction of the couple occurs as potential is scanned from E_1 to E_2 . Once reduction begins the diffusion layer starts to extend out into the solution. This means the reactant has a greater distance to travel. The increased diffusion layer thickness results in a peak arising in the cyclic voltammogram, as shown in figure 1.7(b). After E_2 , as the potential approaches E_f , oxidation of the product occurs and the diffusion layer is depleted.

There has been much work carried out developing the theory of the application of a triangular potential waveform to solution species which exhibit reversible electrochemistry [32 - 34].

A number of parameters can be measured to glean information from cyclic voltammetry experiments. The peak separation, ΔE_p in mV, is useful parameter for characterising systems. For reversible systems the peak separation is approximately $58/n$ mV at 25°C , where n is the number of electrons transferred. Uncompensated resistance in the cell may lead to problems when applying this type of test. Varying the scan rate has been shown to have no effect on the peak potential for a reversible system.. Peak current is, however, found to change with varying scan rate. The equation relating peak current, i_p , to scan rate, v , for a reduction process using linear sweep voltammetry has been developed by Randles and Sevcik [32.33]

$$i_p = -0.4463 nAF \left| \frac{nF}{RT} \right| C^* D^{1/2} v^{1/2} \quad 1.12$$

where all the other terms have their usual meaning. It should be noted that the reoxidation peak current cannot be measured from the baseline. The reason for this is that the reduction peak is assumed to begin from a potential where no current flows. So all peak current measurements must be made from the zero-current axis. Nicholson has developed an equation which allows the direct determination of the anodic peak current [35]

$$\frac{i_{pa}}{i_{pc}} = \frac{(i_{pa})_o}{(i_{pa})} + \frac{0.85 (i_{sp})_o}{i_{pc}} + 0.086 \quad 1.13$$

where i_{pa} , i_{pc} , $(i_{pa})_o$ and $(i_{sp})_o$ are the anodic peak current, cathodic peak current, the uncorrected anodic peak current and the uncorrected current at the switching potential, respectively, as shown in figure 1.7. (c). For a perfectly reversible system the ratio of anodic and cathodic peak current should be 1, provided the switching potential is greater than $35/n$ mV past the reduction peak potential [36]. For reversible systems, the rate of electron transfer between analyte and the

electrode is fast. In such systems the rate of electron transfer is greater than the rate of mass transport. As the rate of electron transfer becomes more sluggish, the electrochemistry becomes what is termed quasi-reversible. Here scan rate becomes extremely important. At fast scan rates the kinetics become apparent in the cyclic voltammogram [37]. At slower scan rates more time is allowed for the analyte to reach the electrode. Quasi-reversible electrochemical peaks are broader due to a slower rate of change in concentration at the electrode due to slower kinetics. The concentration gradient at the electrode is very scan rate dependant. The peak current increases with the square root of scan rate but is not proportional to it. The ratio of anodic and cathodic peak currents for quasi-reversible systems should be 1 [3].

In a totally irreversible system the reverse peak is absent. This absence of reverse peak may also be due to a following chemical reaction. Care should therefore be taken with analysis of such systems. The relationship between peak current and scan rate for a truly irreversible system is given by [35]

$$i_p = (2.99 \times 10^5) n (\alpha n_a) AC^* D^{1/2} v^{1/2} \quad 1.14$$

where α is the transfer coefficient, n is the number of electrons involved in the overall process and n_a is the number of electrons involved in the rate determining step. Other parameters have their usual meanings.

E_p has been shown to be a function of scan rate, shifting in a negative direction by $30/n_a$ mV at 25°C for a reduction for a tenfold increase in scan rate [35].

In more complex systems there may be more than one set of peaks present in the cyclic voltammogram. Analysis of such systems is usually performed by varying the initial, switching and final potentials. This may yield information about possible subsequent reactions and the relationship between the peaks in the voltammogram. The relationship between scan rate and peak current can yield information about adsorption, diffusion and/or complex mechanisms.

Cyclic voltammetry is generally used for preliminary electrochemical

characterisation of a system. Basic information, such as the potential regions of electrochemical activity of a system and the reversibility of a system can be obtained. The technique can be used to analyse surface-bound species. In this type of situation the irreversible adsorption or the confinement of some species to the electrode surface has to be considered.

1.3.2. Rotating disk electrode experiments

As mentioned earlier, diffusion of the analyte towards the electrode surface is made difficult when the potential is scanned past the equilibrium potential due to increased diffusion layer thickness. The diffusion layer thickness can be maintained at a constant value by forced convection of analyte in solution by rotating the electrode. A slow scan rate must be maintained in order to allow formation of sufficient product to achieve a steady state, typically 2mV/s. One of the few convective electrode systems for which the hydrodynamic and convective - diffusion equations have been solved rigorously for the steady-state, is the rotating disk electrode, (RDE) [38]. This type of electrode is relatively simple to construct. It generally consists of a disk of the electrode material embedded in a rod of insulating material. Throughout this work electrodes of platinum or glassy carbon embedded in Teflon were used. The rod is attached to a motor directly by a chuck or by a flexible rotating shaft and rotated at a certain frequency, f , (revolutions per minute). The parameter of interest is the angular velocity, $\omega(\text{sec}^{-1})$, where $\omega = 2\pi f/60$. The schematic construction a typical R.D.E. is shown in figure 1.8. Due to the onset of turbulence, a rotation rate of 1000 s^{-1} is the maximum used for an electrode of radius 0.1 cm [38]. At low rotation rates the scan rate must be very low, as the diffusion thickness increases the rotation rate is lowered. A schematic representation of the solution flow due to forced convection at a R.D.E. is shown in figure 1.8(b). As the electrode rotates, adjacent solution is pulled along by viscous drag and thrown away from the axis of rotation by the centrifugal force. The expelled solution is replaced by flow normal to the

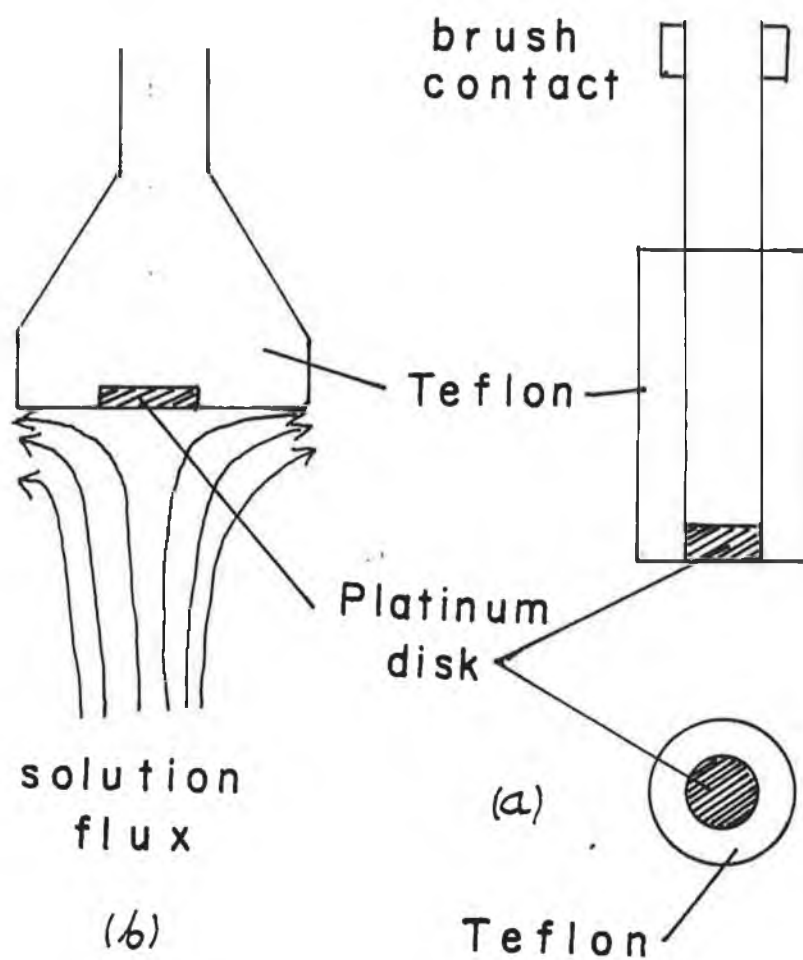


Figure 1.8 Rotating Disc representation.
 (a) Schematic representation of rotating disc electrode.
 (b) Representation of solution flow at a rotating disc electrode.

electrode surface. The rotating disc thus acts as a pump which moves solution up from below and then out away from the electrode.

The signal obtained is of the form shown in figure 1.9. It is a wave rather than a peak. Ficks law for a rotating disc electrode can be solved analytically for such a system and the following equation relates the limiting current, i_L , to the rotation rate for an oxidation process [39]

$$i_L = 0.62 n F A D^{2/3} \nu^{-1/6} C^* \omega^{1/2} \quad 1.15$$

where C^* is the bulk concentration in mol cm^{-3} , ν is the kinematic viscosity, and, ω is the rotation rate in radians per second. Equation 1.15 is termed the Levich equation. A plot of i_L versus $\omega^{1/2}$ should be linear, if the system is under mass transport control. If electron transfer kinetics are slow, then at high rotation rates the flux of material to the electrode surface is enhanced. This yields a lower current than expected by the Levich equation. Where slow electron transfer occurs the Levich equation is modified to take kinetics into account. Then the following equation is obtained [38]

$$\frac{1}{i} = \frac{1}{n F A k_f C^*} + \frac{1.61 \nu^{1/6}}{n F A C^* D^{1/2}} \cdot \frac{1}{\omega^{1/2}} \quad 1.16$$

k_f is the rate constant for the forward reaction. All other parameters have the same meaning as in the Levich equation. A plot of $1/i$ vs $1/\omega^{1/2}$ should be linear with a slope that is independant of potential, but the intercept is very dependant on potential because of the presence of k_f

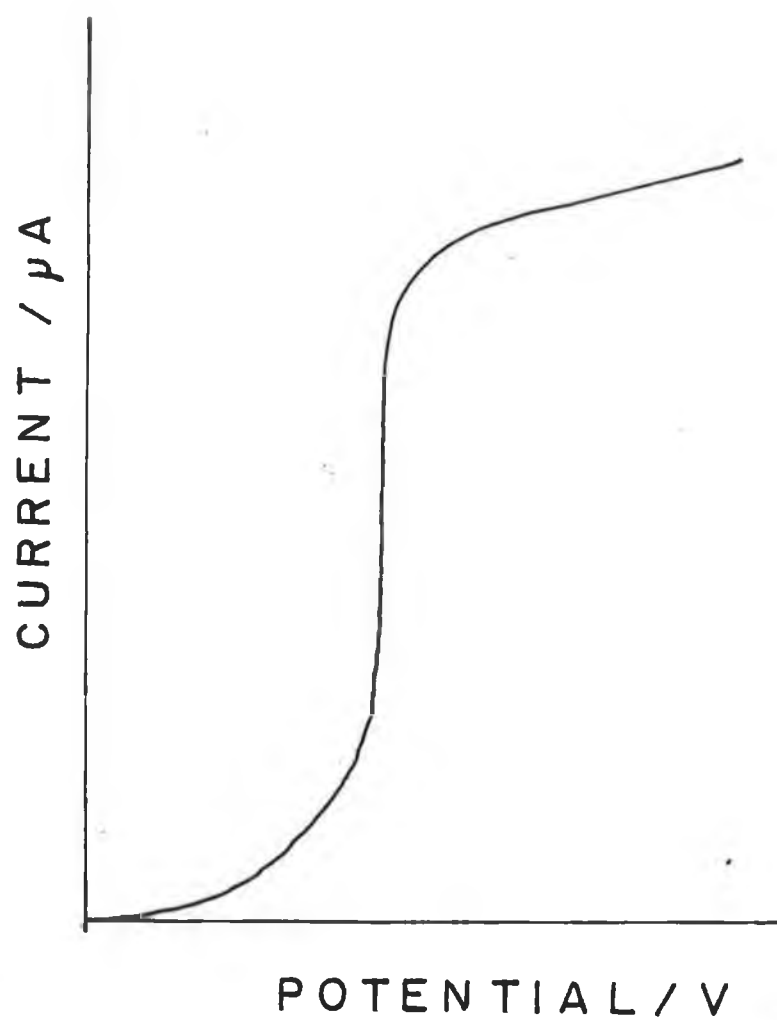


Figure 1.9 Rotating Disc electrode voltammogram for an oxidation process. i_L is the limiting current in the region of mass transport control.

1.4 CONDUCTING POLYMERS: GENERAL INTRODUCTION

1.4.1. Polymer modified electrodes

Applications of polymer modified electrodes has been in the areas of electrocatalysis, preconcentration of analyte, membrane barriers, electroreleasing layers and for the creation of microstructures [40]. Practical modification of the electrode surface has been achieved in a number of ways, including casting or spin-coating techniques [41, 42]. In both cases a solution of the polymer is applied dropwise onto a stationary or rotating electrode and allowed to dry.

Electrocatalysis involves electron transfer mediation by an immobilized catalyst between the electrode and the analyte in solution results in faster electron transfer at lower potentials [29]. Preconcentration involves the use of a molecular film that has a partition effect for an analyte. This leads to a higher concentration of analyte near the electrode surface, leading to an increased signal for the analyte [43]. Membrane barriers are coatings that are designed to keep out interfering species. Electroreleasing involves the expulsion of species from a coating on the electrode surface by changing the oxidation state of the film or some constituent within the film [44]. This allows a controlled dosage of a reagent of interest into the solution phase. Microstructures may take the form of miniature electrodes coated with polymer films. These electrodes may also be used for *in vivo* analysis, such as Nafion coated carbon fiber electrodes.

A problem which is often encountered when a catalyst is electrostatically bound in a polymer matrix is that the catalyst can slowly leach out over a period of time due to the weak electrostatic interaction between the catalyst and the polymer. The problem is further complicated by the presence of background electrolyte in the solution. Bipolar polymer systems have been suggested, where an outer protective layer is applied, to overcome this problem [45]. In this work platinum was deposited in an polypyrrole matrix. Platinum

has previously been deposited in Nafion, poly (4 - vinylpyridine) and polypyrrole [46 - 48]. Electrochemical deposition is commonly employed to cast layers onto electrode surfaces. One of the most studied of all conducting polymers, polypyrrole was employed in this work and will be discussed in the next section.

1.4.2 Polypyrrole

Polypyrrole has been formed chemically by the action of hydrogen peroxide on pyrrole and was reported to form a black powder termed pyrrole black [49]. Dall'Olio first reported, in 1968, the formation of polypyrrole by the electrochemical oxidation of pyrrole to form a conducting polymer film on a platinum electrode in an aqueous solution containing sulphuric acid [50]. This resulted in a brittle film with a conductivity at 25° of $8 \Omega^{-1}\text{cm}^{-1}$. In 1979 Diaz, et al, reported the generation of continuous layers of polypyrrole by the oxidation of pyrrole in acetonitrile, containing 1% water, using tetrabutylammonium tetrafluoroborate as background electrolyte [51]. Since then a large amount of interest has been shown in the properties of polypyrrole. It has been formed in many solutions and the properties of the resulting polymer have been shown to be very dependant on the method of preparation [52,53].

The actual electrochemical oxidation reaction is complex and irreversible in aqueous and non-aqueous media. In aqueous media the potential at which polymerisation begins is around 0.65V with reference to SCE [54], although this can be lower. The positive potential limit has been found to influence the redox behaviour of the conducting polymer. If the applied potential is greater than the peak potential for monomer oxidation, an irreversible loss of activity occurs and a gradual loss of conductivity is observed within the layer. If the applied potential is kept below the peak potential for the monomer oxidation, the polymer film remains active for further oxidation in later scans [54].

The proposed mechanism for the electrochemical formation of polypyrrole is shown in figure 1.10. This involves the generation of a radical cation by

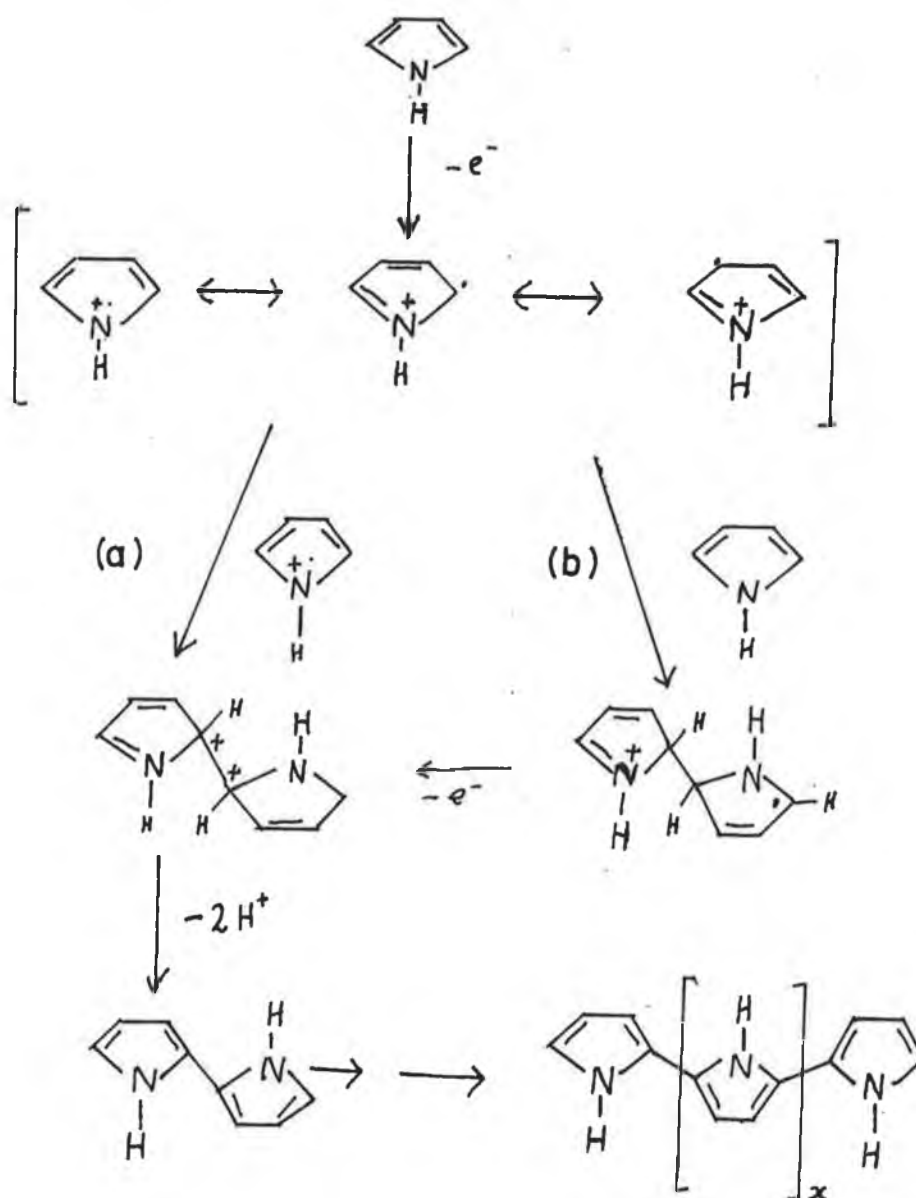


Figure 1.10 Proposed mechanism for the oxidative polymerisation of pyrrole. Route (a) represents the radical-radical coupling step while (b) represents the radical-monomer coupling route.

oxidizing pyrrole, followed by polymerisation via an electrochemical-chemical-electrochemical, ECE, mechanism [55]. The mechanism of growth of polypyrrole films on electrodes is discussed in the next section. The growth of the polymer has been shown to occur primarily by nucleation. The initial stages of nucleation in this case often involve the formation of a nucleus of the new phase as the first step. The nucleus arises as a result of the formation of ad-atoms on the electrode surface. Surface diffusion of neighbouring ad-atoms results in the formation of small clusters which form growth centres. Such systems are treated theoretically by modelling the growth of centres which are assumed to have a definite geometry [56]. The types of geometry used for modelling nucleation are spheres and hemi-spheres. In the case of conducting polymers the formation of the nucleus may either involve the adsorption of the radical cation or the precipitation of the polymer onto the electrode surface once it attains a molecular weight where it is no longer soluble in the solvent. This may explain the very marked differences in electrochemistry observed between films formed in polar and non-polar solvents [57]. When polypyrrole is electrochemically formed, it is formed in the oxidized, PPy^{+1} , state. The electronically conductive form of PPy is a polycation, therefore charge-balancing anions are present in the polymer phase. It is also accepted that excess electrolyte is also incorporated into the polymer phase [5]. In the conducting form the polymer has been shown to consist of one delocalized cationic centre per three or four pyrrole rings [58]. The presence of this delocalised positive centre leads to vacancies in the p-electron network allowing conductivity along the polymer chains. The electronic structure of polypyrrole will be discussed in chapter 2. When the polycationic form is reduced the neutral polymer is form PPy^0 . The neutral form of the polymer is generally unstable and easily reoxidized to PPy^{++} [59]. The oxidized polymer is reasonably stable in air and in many solvents but decomposes in basic solutions and halogens [58, 59]. When the solution has been degassed the film may be cycled between the oxidized and reduced forms, resulting in the removal and insertion of electrons in the pi-electron network. The redox

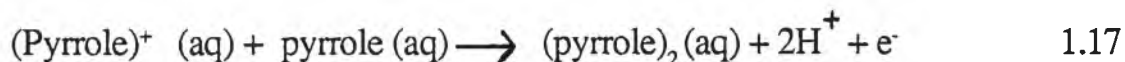
behaviour may also be accompanied by ion exchange between the polymer and the bulk solution. This occurs because of the loss of positive charges from the polymer backbone on reduction and their subsequent regeneration upon oxidation. So, in neutral form, ie. after reduction, the counterions are expelled into solution. In chapter 2, the effect of counterion on polymer electrochemistry will be examined. The ion exchange which occurs upon cycling of the film between conducting and insulating phases is dependant upon the size of counterion in the film and in solution. It is unlikely that large anions within the polymer will be ejected upon reduction and it is more likely that cations from solutions will be incorporated into the polymer incorporated into the polymer film. Reoxidation have leads to these cations being ejected [60].

The attraction of using polypyrrole films for the modification of electrode surfaces include their ease of fabrication, high conductivity and their redox behaviour. It has been observed that platinum particles, embedded in polymer systems, not only retain their high activity much longer than a bare platinum electrode but the platinum particles are embeded in a three-dimensional array within the polymer matrix [61]. The characteristics of the resulting polymer could be tailored to prevent adsorption of species which might interfere with efficient electron transfer at these particles. It has been suggested that polypyrrole film in platinum electrodes are porous to solvent and electrolyte and that this accounts for the reversible behaviour of some redox couples at modified electrodes [62.63].

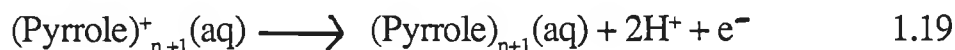
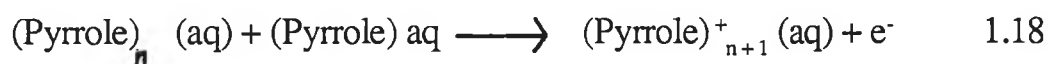
1.4.3. Mechanism of growth of polypyrrole films on electrodes.

The mechanism can be considered to consist of a number of steps;

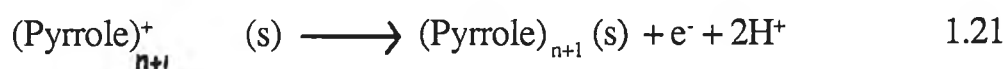
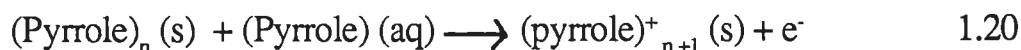
- (1) The reaction of polypyrrole monomers in solution: The anodic oxidation of pyrrole involves the transfer of one electron to the electrode to form the radical cation species. This is the rate determining step. The radical cation than reacts with a neutral pyrrole, transferring a second electron and losing two protons to form bipyrrrole.



- (2) Reaction of pyrrole oligomers in solution - Further oxidation of bipyrrrole and reaction with a pyrrole unit produces the trimer. Continued growth of polypyrrole chains occurs by their stepwise oxidation with reaction with pyrrole units, to form radical cations, followed by fast electron transfer and the loss of two protons.



- (3) Reaction of polypyrrole at the electrode - as time progresses, eventually polypyrrole chains that surpass the solubility limit form, causing a supersaturation at the electrode/solution interface. This is the driving force for the nucleation of polypyrrole on the electrode surface. Once established, it is likely that the film continues to grow according to the succession of steps outlined above.



Where (s) denotes the electrode surface.

The model described above ignores the following point; as the concentration of pyrrole monomers near the electrode surface decreases and becomes comparable to that of the oligomers formed, reactions between polymeric radical cations and neutral oligomers may become more frequent.

1.4.4. Charge transport through conducting polymers

The design and understanding of well-defined conducting structures of nanometer dimensions is one of the most challenging goals of contemporary solid state science. Fundamental studies of the electronic structure and conducting mechanism of conducting polymers would benefit greatly from such studies. Ultimately this could lead to the reduction in size of electronic circuitry to molecular dimensions. The electrical conductivity of polypyrrole films is quite sensitive to the incorporated counteranion. It is not yet established whether this effect is due to an electronic interaction between the polypyrrole chain and the anions or to differences in morphology as a result of growth from different electrolyte solutions. Some workers have found evidence that the anions may be fairly mobile within the film [64]. Models for electronic conduction will be discussed in chapter 2.

1.5 ELECTROCHEMICAL MEDIATION

Fouling or poisoning of the electrode surface is a common occurrence, especially in biological fluids, primarily due to adsorption. This generally leads to a decrease in electrocatalytic behaviour at the electrode surface, where strong adsorption occurs, or inefficient electron transfer from analyte to the electrode surface where there is weak adsorption. Modification of the electrode surface, with, for example, cellulose acetate, may be used to prevent adsorption from biological fluids. Figure 1.11 shows a schematic diagram depicting a mediation process. The mediator M_O is reduced at the electrode surface to M_R , a mediator

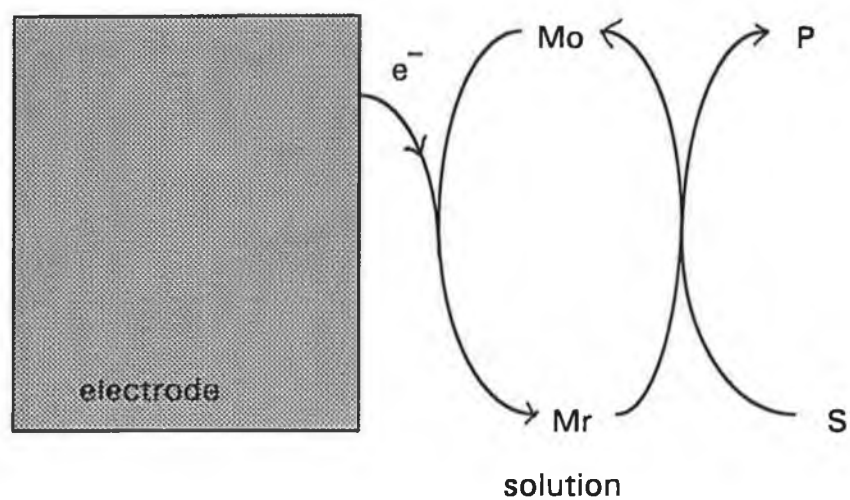
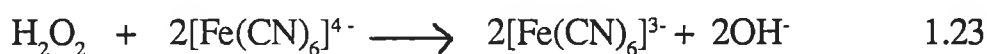


Figure 1.11 Schematic representation of a mediation process.

Mo represents the oxidized form of the mediator, M_r the reduced form, S the substrate in solutions and P is the product of the reduction of S .

which is chosen because of its catalytic properties. The substrate, S, in solution, interacts with the mediator M_R producing the product P, by reduction in bulk solution may be



where it is simpler to look at the reduction of $[\text{Fe}(\text{CN})_6]^{3-}$ at the electrode than H_2O_2 [65]. In the latter case an example is the incorporation of $[\text{Ru}(\text{bpy})_3]^{3+}$ in a Poly (4 - vinylpyridine) layer on an electrode surface which can mediate the oxidation of Fe^{++} [66 - 68].



As can be seen from reaction 1.25 the Ru^{2+} complex is regenerated facilitating increased catalytic activity. In this work both forms of catalysis were employed. Pt. particles incorporated in a conducting polymer matrix coated onto various substrate electrodes and used to reduce O_2 to superoxide. The O_2^- was then used to decompose C - halogen bonds. Bulk solution catalysis was also employed where an organometallic complex was solubilised in aqueous micellar systems. Again this method was used to decompose chlorinated organic molecules. These systems will be discussed in chapters 3 and 4.

1.6 REFERENCES

- [1] S.C.I. Symposium, Electrochemical Techniques for a cleaner environment, London, April 1990.
- [2] J.L. Roberts and D.T. Sawyer, J. Am Chem Soc. 1981, **103**, 712 - 714
- [3] J.F. Rusling, Chun-Nian Shi and S.L. Suib, J. Electroanal. Chem., 1988, **245**, 331 - 337
- [4] G.N. Kamau and J.F. Rusling, J. Electroanal. Chem., (1988) **240**, 217 - 226
- [5] Nuifei Hu and J.F. Rusling, Anal Chem. 1991, **63**, 2163 - 2168
- [6] T.F. Connors and J.F. Rusling, J. Electrochem. Soc., (1983) **130**, 1120.
- [7] G.H. Eduljee, Chemistry in Britain, March 1988, pp 242 - 244
- [8] R.B. Pojasek, Ed, Toxic and Hazardous Waste Disposal, Ann Arbour, Mich., 1979 Vol. 1 pp 105
- [9] G. H. Eduljee, Chemistry in Britain, December 1988, pp 1223 - 1226
- [10] G. F. Bennett and K. P. Olmstead, Chemistry in Britain, February 1992, pp. 133 - 136
- [11] R.W. Harvey, et al, ibid, 1989, **23** (1)51
- [12] A.J. Bard and L.R. Faulkner, Electrochemical Methods, Fundamentals and Applications, Wiley, New York, 1980, Chapter 1.
- [13] A. J. Bard and L. R. Faulkner, Electrochemical Methods, Fundamentals and Applications, Wiley, New York, 1980, pp103.
- [14] P.H. Rieger, Electrochemistry, Prentice Hall International, Englewood Cliffs, (1987), pp 70 - 80
- [15] P.H. Rieger, Electrochemistry, Prentice Hall International, Englewood Cliffs, 1987) pp.33
- [16] A.M. Couper, D. Pletcher and F.C. Walsh, Chem. Rev., 1990, **90**, 837 - 865
- [17] J.F. Cassidy, W. Breen, A. McGee, T. Mc Cormac and M.E.G. Lyons, J. Electroanal, Chem., **333** (1992), 313.

- [18] D.T. Sawyer and J.L. Roberts Jr. Experimental Electrochemistry for Chemists, Wiley, New York, 1974, pp 60 - 74, 170 - 171
- [19] L. Meites, Polarographic Techniques, 2nd Ed, Wiley, New York, 1965
- [20] A. McGee, Final year project, BSc. (Applied Science), 1990, Dublin Institute of Technology.
- [21] V.J. Jennings, T.E. Forster, J. Williams, Analyst, (1970) **95**, 718
- [22] G. Cauquis, D. Serve, J. Electroanal Chem., (1972) **34**, 1
- [23] P.H. Rieger, Electrochemistry, Prentice Hall International, Englewood Cliffs, (1987), pp37
- [24] O. Ikeda, T. Kojima, H. Tomura, J. Electroanal, Chem. (1986), **200**, 323
- [25] P.H. Rieger, Electrochemistry, Prentice Hall International Englewood Cliffs, (1987), pp. 190 - 199.
- [26] D.T. Sawyer, J.L. Roberts Jr, Experimental Electrochemistry for Chemists, Wiley, New York, 1974, pp. 204 - 205
- [27] P.H.. Rieger, Electrochemistry, Prentice Hall International, Englewood Cliffs, (1987), pp. 461
- [28] W. Breen, PhD Thesis, University of Dublin, 1991. pp. 52
- [29] Southampton Electrochemistry Group, Instrumental Methods in Electrochemistry, Ellis Harwood, Chichester, 1985, pp. 178 - 250
- [30] P.H. Rieger, Electrochemistry, Prentice Hall International, Englewood Cliffs, (1987), pp. 21
- [31] A.J. Bard and L.R. Faulkner, Electrochemical Methods, Fundamentals and Applications, Wiley, New York, 980, pp. 51
- [32] J.E.B. Randles, Trans Faraday Soc., (1948), **44**, 327
- [33] A. Sevcik, Collect, Czech, Chem. Commun., (1948), **13**, 349.
- [34] R.S. Nicholson, I. Shain, Anal. Chem., (1964) **36**, 704
- [35] R.S. Nicholson, Anal Chem., (1965), **37**, 1351
- [36] A.J. Bard, L.R. Faulkner, Electrochemical Methods, Fundamentals and Applications, Wiley, New York, (1980), pp. 228

- [37] H. Matsuba, Y. Ayabe, *Z Electrochem.*, (1955). **59**, 494
- [38] A.J. Bard and L.A. Faulkner, *Electrochemical Methods, Fundamentals and Applications*, Wiley, New York (1980) pp. 280 - 289
- [39] B.G. Levich, *Acta, Physiochimica, URSS*, (1942) **17**, 257.
- [40] R.W. Murray, A.G. Ewing, R.A. Durst, *Anal. Chem.*, (1987), **59**, 379A
- [41] J. Wang, P. Tuzki, *J. Electrochem. Soc.*, (1987) **134**, 586.
- [42] R. Lange, K. Doblhofer, *J. Electroanal. Chem.*, (1987) **216** 214
- [43] J.F. Cassidy, K. Tokuda, *J. Electroanal. Chem.* (1990) **285**, 287
- [44] L.L. Miller, Q.X. Zhou, *Macromolecules*, (1987), **20**. 1594.
- [45] D. Belanger, *J. Electroanal. Chem.* (1988) **251**, 55
- [46] K. Itaya, H. Takahashi, I. Uchida, *J. Electroanal. Chem.*, (1986) **208**, 373
- [47] K.M. Kost, D.E. Bartak, B. Kazee, T. Kuwana, *Anal. Chem.*, (1990) **62**, 151
- [48] S. Holdcroft, B.L. Funt, *J. Electroanal. Chem.*, (1988) 240 89
- [49] A. Angelo, *Gazz. Chim. Ital.*, (1916), **46**, 279
- [50] A. Dall'Olio, 7, *Duscola, Varracca, V. Bocchi, C.R. Hebd. Seances Acad. Sci Ser. C*, (1969), **267**, 433
- [51] A.F. Diaz, K.K. Kanazawa, G.P. Gardini, *J. Chem. Soc., Chem Commun.*, (1979) 635
- [52] P. Pfluger, M.Krounbi, G.B. Street, *J. Chem. Phys.*, 78.(6) Part 1.
- [53] L.F. Warren, D.P. Anderson, *J. Electrochem. Soc.*, 1987, **134**. 101
- [54] S. Asavapiriyantort, G.K. Chandler, G.A. Gunawardena, D. Pletcher, *J. Electroanal. Chem.*, (1984) **177**, 229
- [55] B.R. Scharifher, E. Garcia-Pastoria and W. Marino, *J. Electroanal. Chem.*, (1991) **300**, 85 - 88
- [56] Southampton Electrochemistry Group, *Instrumental Methods in Electrochemistry*, Ellis Harwood, Chichester, 1985 pp. 283 - 316
- [57] J.M. Ko, H.W. Rhee, S.M. Park, Y. Kim, *J. Electrochem. Soc.*, (1990), **137**, 905
- [58] A.F. Diaz, *Chem. Scr.*, (1981) **17**, 145.

- [59] G.B. Street, T.C. Clarke, R.H. Geiss, V.V. Lee, A. Nazzal, P. Pfluger, J.C. Scott, J. Phys. Colloq., C3, (1983) 5993.
- [60] Q.X. Zhou, C.J. Koloski, L.L. Miller, J. Electroanal. Chem., (1987), **233**, 283
- [61] A. Kowal, K. Doblhofer, S. Krause, G. Weinberg, J. Applied Electrochemistry, (1987), **17**, 1246 - 1253
- [62] R.A. Bull, F. Fan, A.J. Bard, J. Electrochem Soc., (1982) **129**, 1009
- [63] T.A. Skotheim, S.W. Feldberg, M.B. Armand, J. Phys. Colloq., C3, (1983), 615
- [64] L.S. Curtin, G.C. Komplin and W.J. Pietro, J. Phys Chem. 1988, **92**, 12 - 13
- [65] C. Clinton, Dip in App. Sci. Final year project, D.I.T. 1992
- [66] J.M. Clear, J.M. Kelly, L.M. O'Connell, J.G. Vos, Chem. Res. M (1981) 3039
- [67] S.M. Geraty, D.W.M. Arrigan, J.G. Vos in M. Smyth and J.G. Vos (Ed), Electrochemistry, Sensors and Analysis, Elsevier, Amsterdam, 1986, p303
- [68] J.F. Cassidy, J.G. Vos, J. Electroanal. Chem., (1987) **218**, 341

2. CHARACTERISATION OF POLYPYRROLE LAYERS

2.1 INTRODUCTION

There has been considerable interest shown in recent years in organic conducting polymers because of their potential for engineered electrical applications due to their low density, air and water stability, high conductivity and ease of fabrication [1]. The polymers may be formed by chemically or electrochemically polymerising the monomer. The polymer layers thus formed are molecular composites containing a cationic polymer with approximately one positive charge per three or four monomer units and accompanying “dopant” anions for the maintenance of charge neutrality [1 - 4]. The idealized structure of polypyrrole doped with perchlorate anion is shown in figure 2.1(a). The physical properties, quality and morphology of electrochemically generated polypyrrole films are very dependant on the deposition conditions, including the background electrolyte, solvent, deposition potential and the counterion present [1,5,6]. Warren and coworkers noted three different morphologies when polypyrrole was deposited anodically onto a gold electrode from 0.1M BF_4^- solutions when the solvents were acetonitrile/water mixtures. The three morphologies observed were termed “crystalline”, “nodular” and “spongy” [6]. This work also suggests that the greater the amount of water present in solution, the greater the degree of crystallinity observed in the polymer film. Ko et al [5], compared the electrochemical characteristics, conductivities and morphologies of PPy films prepared in aqueous and non-aqueous, (acetonitrile), solutions. Films formed in acetonitrile were found to be superior to these prepared in aqueous solutions in terms of their electron transfer

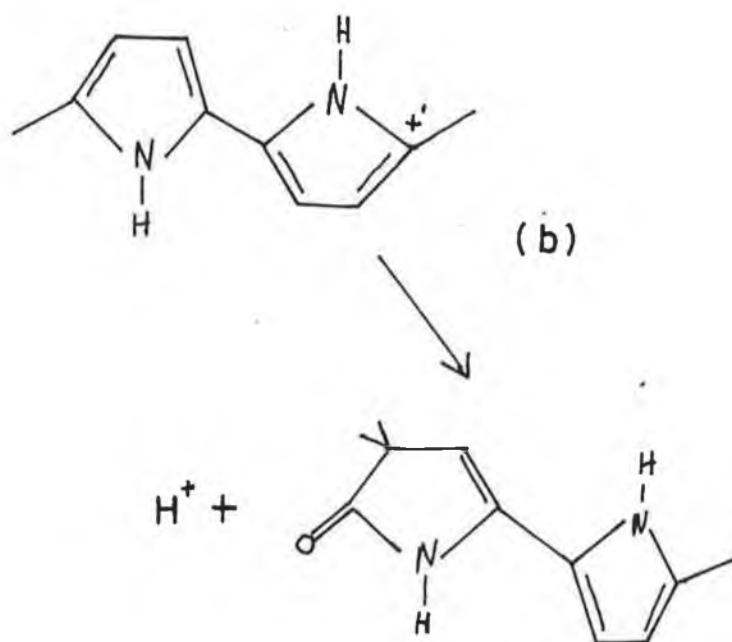
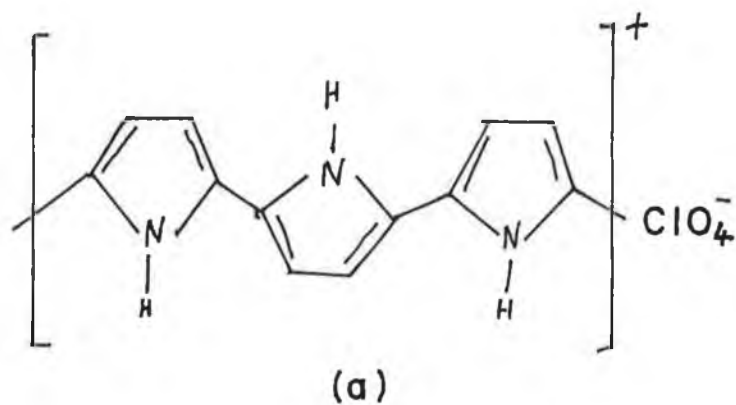


Figure 2.1 Structure of polypyrrole
 (a) Idealized structure of polypyrrole perchlorate
 (b) The radical cation being attacked by water to give electrochemically inactive products

characteristics and conductivities. The films prepared in water exhibited a greater porosity than their counterparts in acetonitrile. There is also evidence to suggest that when working in aqueous media some electroactive sites are lost during the doping process, as indicated by the smaller reverse currents observed during the cathodic scan [6]. This is reasonable as the radical cation generated by oxidizing pyrrole may be attacked by water to give undesirable, electrochemically inactive products according to the reaction shown in figure 2.1 (b).

It is much more preferable to use aqueous solutions as this solvent offers a greater variety of supporting electrolyte anion systems. Some of the anions that have been used within electrochemically generated PPy layers include inorganic anions such as Cl^- , NO_3^- , HSO_4^- , ClO_4^- and $[\text{Fe}(\text{CN})_6]^{4-}$, and organic anions such as dodecyl sulphate (SDS), dodecylbenzenesulphonate, (DBS), and polystyrenesulphonate [6 - 8]. As mentioned earlier, the effect of anion and its subsequent reaction with solvent has a direct effect on the morphology of the film. This prompted Warren and others to carry out a study on the effects of anions upon the order of the polymer film [1,6]. Among the anions studied were a number of organic sulphonates, some of which were surfactants containing long organic chains. From S.E.M. studies Breen observed a compact uniform structure for PPy^+DBS^- films [8], unlike the nodular morphology of PPy^+Cl^- . The differing electrochemistry of these two layers is thought to be due to the differing nucleation and growth behaviour of both polymers [8]. The electrical conductivity is another parameter which is also very sensitive to the counter ion [3]. It is not known whether the effect is due to an electronic interaction between the polypyrrole chain and the anion or the differences in morphology due to polymer growth from different electrolyte solutions. Excess electrolyte is incorporated into the polymer phase from pores Martin, et al, [2], carried out a study to determine what percentage of the ionic charge is carried by the excess electrolyte and what fraction is carried by the counterions. It was found that the conductivity of charge-balancing counterions was small and therefore it was stated that for solution electrolyte concentrations greater than 0.05 mol dm^{-3} , ionic

conduction within the film was accomplished almost exclusively by excess electrolyte [2,9]. Low conductivity of charge-balancing anions, compared to the excess electrolyte, was attributed to low concentration or low mobility of the anions. The low mobility was attributed to strong electrostatic attractions to the fixed cationic sites of the polymer chain. When the concentration of electrolyte is 0.2 mol dm^{-3} , the concentration of excess electrolyte in the polymer phase is approximately the same as the concentration of charge-balancing anions in the polymer phase [9]

Polypyrrole is formed in the oxidized state, PPy^{+1} . It can be reduced to the neutral, insulating, state, PPy^0 . Shimidzu and workers found the subsequent redox behaviour to be very anion dependant [10]. Warren believed these differences to be greatly influenced by swelling/hydration of the film [6]. Work carried out here and elsewhere [3], give evidence to suggest that upon reduction there is expulsion of the counterion and shrinkage of the film. The reoxidation and subsequent anion insertion after this initial reduction would be greatly influenced by swelling of the film. It is generally believed that charge neutrality is maintained by cation movement [8, 10], particularly when the counterion is a large anion such as DBS^- which would be sterically hindered from expulsion and so cation movement is much easier in these cases. It has been observed that there are peculiar relationships between peak current, i_p and scan rate, v , with increased size of anion [8,10]. These differences were attributed to either restructuring of the polymer film or differences in morphology.

The perchlorate anion is commonly used as a counterion for electrochemically grown polypyrrole films as these films have a high degree of uniformity and reproducibility [3]. By Auger analysis [3], a uniform concentration of ClO_4^- was observed throughout the film. It was suggested that this may be due to the fact that the relatively small ClO_4^- ion may be quite mobile within the film. The electropolymerisation of pyrrole to produce polypyrrole films and their subsequent electroactive behaviour represents a unique combination of electrochemical processes. The electroactive behaviour is unique as it is an

example of a redox reaction which is accomplished by a change in the electrical properties of the film from an insulator to a conductor. The reduced form of polypyrrole is a neutral, insulating, hydrophobic organic polymer, whereas the oxidized form is a conductive polyelectrolyte which contains a high cationic charge density. In this work cyclic voltammetry was used to examine the effect of forming polypyrrole films with incorporated anions of varying sizes. Different solvent systems were also used. The subsequent electrochemistry of these layers was examined in background electrolyte solutions containing a counterion of different size.

2.2 THEORY

2.2.1. Electronic spectroscopy of conducting polymers

By applying an appropriate potential to an electrode coated with a conducting polymer layer, it is possible to reduce the layer to a neutral form or oxidize the layer to a conducting form. Most kinetic studies have been based on the assumption that kinetics are controlled by the diffusion of dopant ions through the layer or electron hopping along or between strands of polymer [11]. The in-situ measurement of absorption spectra of layers coated on transparent electrodes as a function of applied potential is known as spectroelectrochemistry. The most interesting phenomenon which can be observed when using this technique is the electrochromic properties of the film with changes in doping. Similar spectral changes have been reported with changes in doping from a number of different groups [11,12]. The typical changes in the absorption spectrum obvious for oxidized and neutral layer are shown in figure 2.2 [13]. The neutral yellow form displays a maximum at about 400nm, while the fully-oxidized blue/black form shows a broad absorption with a maximum around 900nm [13]. The optical properties of a conducting polymer are important to the understanding of the basic electronic structure of the polymer. The charge on the polymer is believed to be

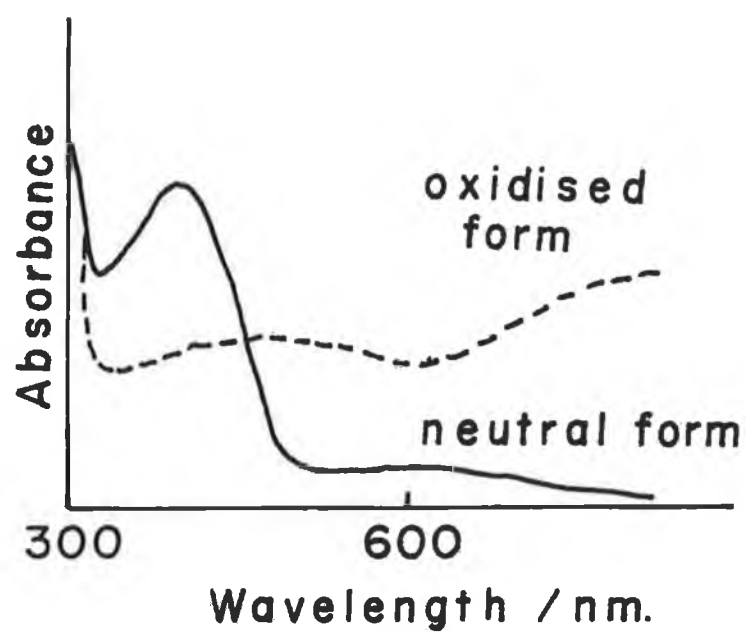


Figure 2.2 Typical changes in the absorption spectrum of polypyrrole for oxidized and neutral layers.

mobile along the conjugation of the π - backbone of the polymer. The amount of π - conjugation in the polymer determines the colour and electronic spectra. Thus UV-Vis spectroscopy is a powerful probe for characterizing the electronic processes that occurs in the polymer in the undoped, doped and during doping states. Patil and coworkers [12], reviewed optical and physical properties of a number of conducting polymers including polyacetylene, polypyrrole and polythiophene as a function of doping.

The three bands shown in figure 2.2 have been assigned as follows [11]. The A band has been assigned to the π - π^* transition of conjugated cationic segments. In a polymer, the interaction of a polymer unit cell with its neighbours leads to the formation of broad electronic bands, characteristic of oxidized forms (B,C,) but not of a neutral form (A). Bands B and C take the form of defect, polarons or bipolarons localised in the electronic structure [4,13,14]. It has been shown by Waller and Compton [15] that the mobilities of these two types of defects are approximately equal and thus both contribute to the electronic conductivity in a strand. A schematic diagram of the predicted electronic structure of a conducting polymer in its neutral state, as well as states containing polarons and bipolarons is shown in figure 2.3 [4]. Oxidation of the neutral polymer, which corresponds to π - type doping, as occurs in polypyrrole, leads first to the formation of cation radical sites which correspond to polaron states in the gap [14], since polarons are considered cation and bipolarons as a dication “defect” in the polymer strand. The lowest polaron level is termed the bonding cation level (BCL), while the upper level is called antibonding cation level (ACL). For higher levels of doping the removal of a second charge creates another cation radical site which can combine with a similar site to form a dication. The bonding and antibonding levels associated with the dication, are the bonding dication level, (BDL) and the antibonding dication level, (ADL), which can enlarge to two bands for high dopings. Under particular conditions these two bands constitute a bipolaron state [14]. Murao and Suzuki [16], found that polaron states are initially predominant upon doping but are subsequently transformed to the bipolaron state by the self-quenching reaction

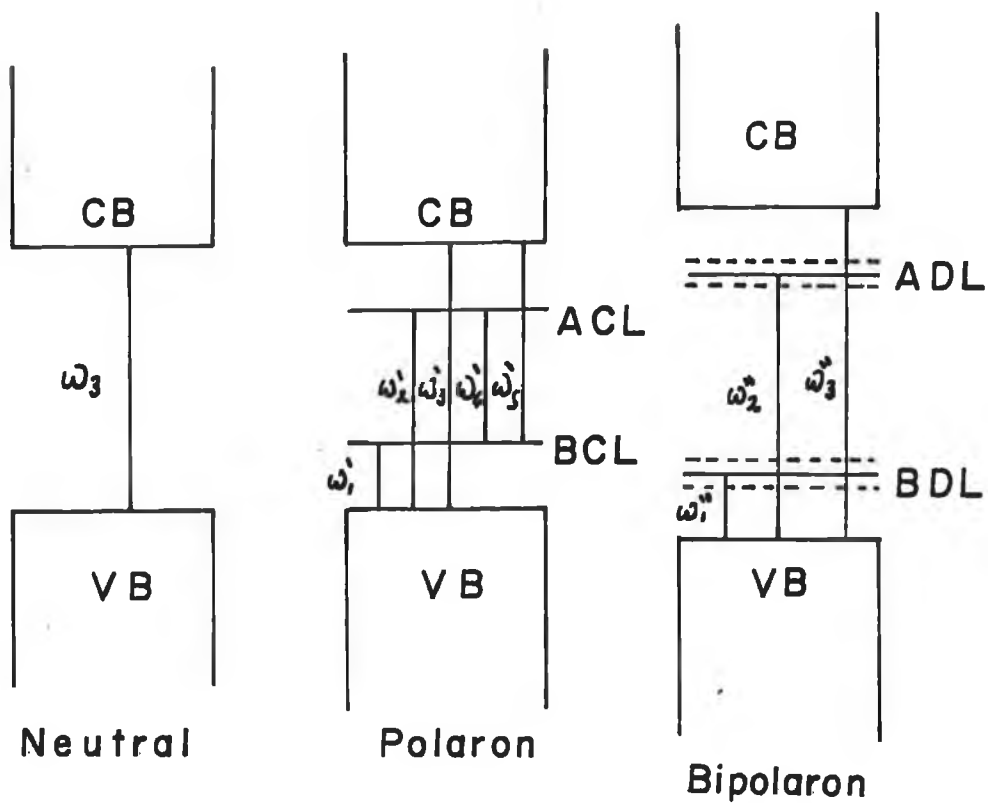
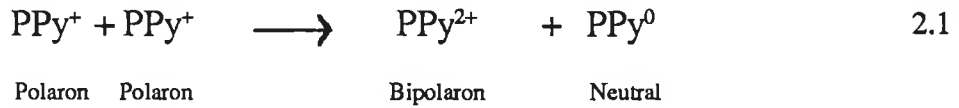


Figure 2.3 Schematic diagram of the band structure of polypyrrole in its neutral, polaron and bipolaron states showing expected electronic transitions.



where PPy^0 = neutral, PPy^+ = cation, PPy^{2+} = dication. This occurs because one bipolaron is more thermodynamically stable than two polarons. Kaufman, et al [17], showed that the energy levels for the bipolaron and polaron midgap states are close enough that for the sake of this analysis $\omega_1'' = \omega_1''$ and $\omega_2' = \omega_2''$. As the formation of the polaron involves the removal of one electron from the valence band, VB, then it can also be assumed that $\omega_3 = \omega_3'$. At high doping levels the bipolaron energy states overlap into bands of their own, causing ω_1'' to increase. The electronic transitions for polypyrrole will occur at [4];

$$\omega_1' \approx 0.5 \text{ eV} \rightarrow 245\text{nm}$$

$$\omega_2' \approx 2.3 \text{ eV} \rightarrow 540\text{nm}$$

$$\omega_3' \approx \omega_3'' \approx 3.2\text{eV} \rightarrow 390\text{nm}$$

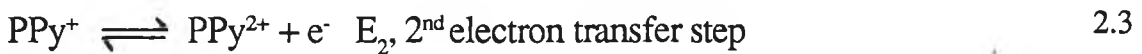
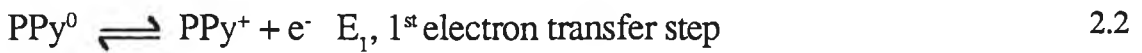
$$\omega_4' \approx 1.8 \text{ eV} \rightarrow 690\text{nm}$$

$$\omega_3'' \approx 3.6 \text{ eV} \rightarrow 345\text{nm}$$

$$\omega_5' \approx 2.3 \text{ eV} \rightarrow 540\text{nm}$$

There have been reports of other values for some of these transitions [11,14,18]. Genies and Pernaut [14] distinguished only three absorption areas in the visible region. These consisted of the transitions ω_3 , ω_2^1 and ω_4^1 .

The electrochemical interpretation of polypyrrole can be represented as follows



This is the same as equation 2.1

In polypyrrole films three different species are seen to exist [19]. These species are described by the “monomer unit” model. The three species are neutral monomers, slightly oxidized monomers (polarons) and fully oxidized monomers (bipolarons). The observed optical absorptions are possible by intramolecular or intermolecular transitions by these species. The broadness of the band observed at B in figure 2.2 is attributed to these transitions and their overlap [19].

There has been much discussion concerning the cyclic voltammetry of conducting polymers. The question of what fraction of the observed total current is capacitive relative to the faradaic current arises. Experimental data suggests that the redox chemistry of polypyrrole can be divided into three regions [2],

- (1) At a low potential regime where the polymer is an electronic insulator. The oxidation of this reduced form of polypyrrole appears to depend on the diffusion of anions into the layer [9, 20].
- (2) At a high potential regime where polypyrrole is conducting. Both oxidation and reduction appear to be capacitive in this region.
- (3) At intermediate potentials where the polymer is conducting and where a peak current occurs due to layer oxidation.

Faradaic current involves charge transfer across an interface while capacitive current involves charge storage at an interface. If the insulating form of polypyrrole is considered, the interface of most importance is the electrode/polymer interface. Such interfaces are analogous to electrode/electroactive solution interfaces. Conventional faradaic electron transfer occurs across such an interface [21]. Charge is also stored at such an interface. Oxidation of the insulating form of polypyrrole is analogous to the oxidation of a redox polymer [21]. The completely oxidized, conductive form of polypyrrole is highly porous [2]. The “pore space” is filled with electrolyte phase similar to the external electrolyte. The important interface in this case is the interface between the molecular wire and the electrolyte incorporated into the polymer pore space. This can be seen from examining figure 2.4. Charge is not transported across the

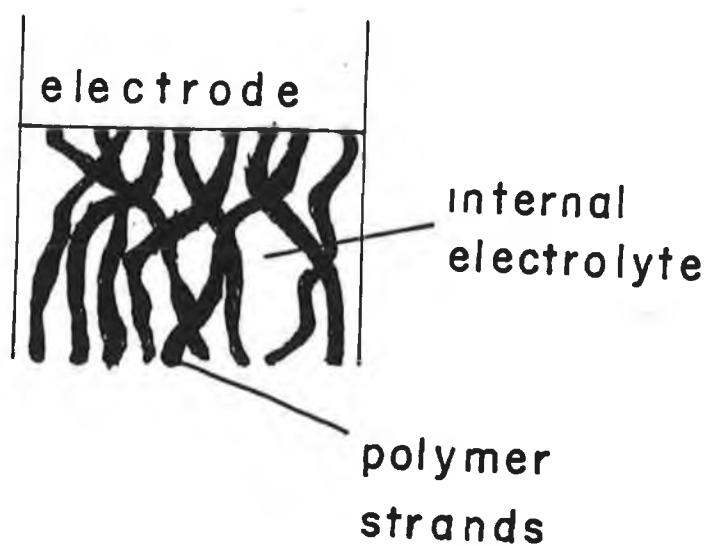


Figure 2.4 Simple heuristic model for the morphology of completely oxidized polypyrrole on an electrode surface. Based on reference [2]

molecular wire/internal electrolyte interface, but is, instead, “pulled out” of the molecular wire. A counterion from the internal electrolyte phase is bound at the surface of the wire. Therefore, in this region, the process resembles a purely capacitive process, Cai and Martin [2] felt that in the intermediate potential regime both insulating and conductive regions exist within the film. They felt that both faradaic and capacitive mechanisms were at work here. The advantage of this model is that it shows no clear dividing line between anions moving toward the molecular wire for faradaic or capacitive reasons. Kalaji and Peter [22] analysed the small-amplitude periodic transmittance of polyaniline films and concluded that the a.c. response of the film is dominated by faradaic processes. They were unable to solve the discrepancy between a.c and cyclic voltammetry capacitance values. They believe that the capacitive current observed is not truly capacitive but is some “pseudo-capacitance”.

In this work spectroelectrochemical analysis of polypyrrole films formed from aqueous electrolytes and run in a different electrolyte was carried out. It was expected that this work, coupled with cyclic voltammetry, would shed some further insights into the structure and redox behaviour of polypyrrole.

2.2.2. Optical Spectroelectrochemistry

Recent years have seen much interest in studying electrode processes by experiments that involve more than the usual electrochemical variables of current, charge and potential. Some of the reasons for this work have been to provide ways for collating information about electrochemical systems that could not be gathered by purely electrochemical means. Other efforts have been driven by interest in using stimuli such as photons to influence electrode reactions.

The simplest spectroelectrochemical experiment is to direct a light beam through a transparent electrode and to measure absorbance changes resulting from the species produced or consumed in the electrode process. The main prerequisite of such a system is an optically transparent electrode (OTE). These OTE's may be

thin films of a semiconductor e.g. doped SnO_2 or In_2O_3 or a thin layer metal, e.g. Au or Pt, deposited on a glass, quartz or plastic substrate. Alternatively such cells may be constructed with electrodes of fine wire mesh minigrids with several hundred wires per centimeter [23]. The optically transparent electrodes used in this work were Indium doped Tin Oxide, (ITO), electrodes.

Transmission experiments may involve the study of absorbance versus time as the electrode potential is stepped or scanned, or may involve wavelength scans to provide spectra of electrogenerated species. The measurement of absorbance is analogous to that of charge. The method of transmission experiments carried out in this work involves using a thin-layer system as shown in figure 2.5. In this system the working electrode is placed into a thin layer glass cuvette ($d = 4\text{mm}$), containing the electroactive species in solution. In this type of system cyclic voltammetry, bulk electrolysis and coulometry can be carried out in the normal way as well as providing a facility for obtaining absorption spectra of the solution species [23]. An advantage of this system is that the whole solution reaches equilibrium with the electrode potential in a few seconds. Spectral data can therefore be gathered on a static solution composition. In this work optical absorbance data was used to obtain absorbance versus wavelength measurements with varying potentials. This data was subsequently used to obtain Nernst plots and to estimate the bandgap energy, (ω_g), of neutral polypyrrole.

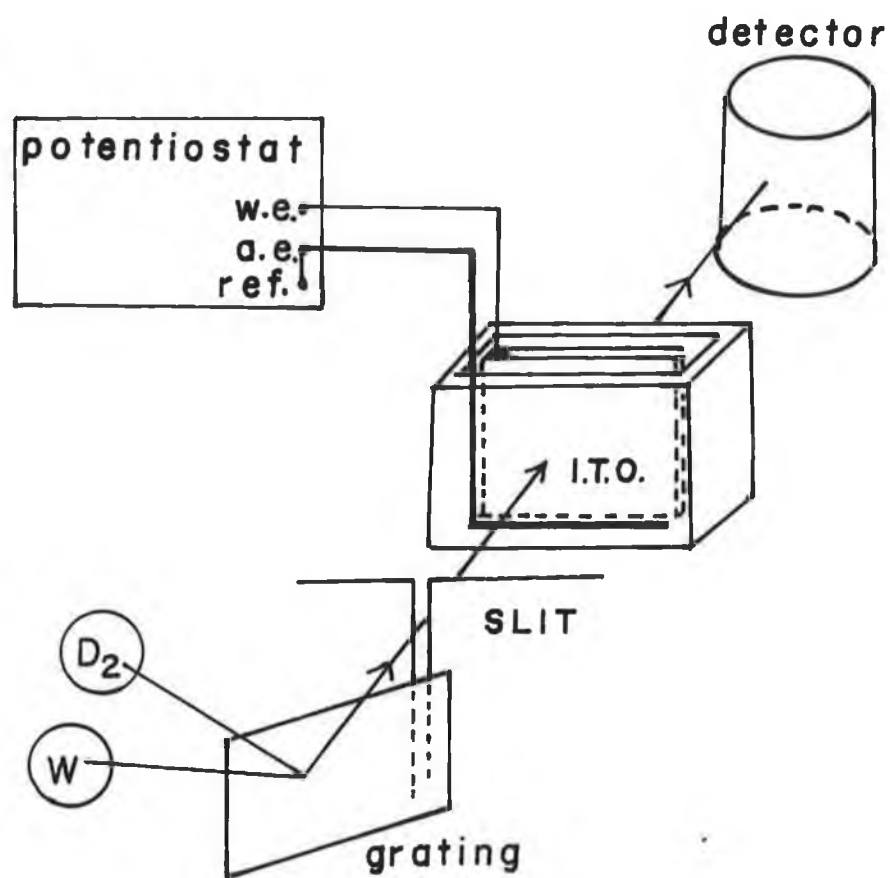


Figure 2.5 Schematic diagram of the thin layer system used for spectroelectrochemical studies.

2.3 EXPERIMENTAL

2.3.1. Instrumentation, cells electrodes and chemicals

A Metrohm, three electrode, single compartment cell was employed for all electrochemical experiments. A platinum disc, sealed in Teflon, with an exposed surface area of 0.071 cm^2 was used as a working electrode. A carbon rod was employed as an auxiliary electrode, while all potentials quoted were with respect to a calomel electrode containing saturated NaCl Solution. The electrode surface was pretreated prior to polymer deposition by polishing with $0.3 \mu\text{m}$ alumina slurry on felt.

Cyclic voltammetry, potential control and charge and current measurement was performed using a Sycopel potentiostat, model DP301, which was linked to a J.J. Lloyd PL3 chart recorder.

Sodium Dodecylbenzenesulphonate (NaDBS) was technical grade. Pyrrole was distilled under nitrogen and stored in the dark prior to use. The pyrrole was found to remain stable for a period of 3 to 4 weeks if treated in this way. Water was distilled and deionised. Tetrahydrofuran (THF), was HPLC grade and was used as received. The temperature for all experiments was ambient ($20^{\circ}\pm 4^{\circ}\text{C}$), unless otherwise stated. All electrolyte concentrations were 0.1 mol dm^{-3} unless otherwise specified.

2.3.2 Polymer Layer formation

A freshly prepared solution of 0.1M pyrrole and 0.1M counterion was placed in the cell. The solution was degassed with oxygen-free nitrogen for approximately 5 minutes prior to the experiment. A blanket of nitrogen was maintained over the solution throughout the layer formation. In aqueous solution the potential was continuously scanned between the limits of 0.0V and 0.8V , at a scan rate of 100mV/s , until a charge of 20mC was passed. For the THF/water mixture equal

volumes of THF and water were mixed and allowed to reach equilibrium. For layer formation in the THF/water mixture, the potential was cycled between 0.0V and 1.45V at 100mV/s, until a charge of 20mC was obtained. The charge and layer thickness are related, ($24\text{mCcm}^{-2} = 0.1\mu\text{m}$) [24]. Therefore the thickness of layer observed throughout this work was 1.2 μm . The layer, when formed was always maintained at a potential positive of the redox reaction of the layer. Following formation, the layer was rinsed and allowed to dry in air prior to use, when dry the layer was transferred to a solution of background electrolyte in the same solvent. The reduction of the layer was then monitored by scanning the potential from 0.6V to -0.8V, at 25mV/s, continuously. Polymer preparation was also attempted in pure THF. This was found to be a very slow process and hence abandoned. As all layers were formed using the same charge, some comparison could be made between the various electrolytes within a particular solvent system.

2.3.3. UV - Vis Spectroelectrochemistry

Polymer layers were formed on ITO transparent electrodes in a manner described in the last section. After rinsing and subsequent drying, the polymerised ITO electrode was transferred to the cell as depicted in figure 2.5. All U.V. - Vis work was carried out in aqueous solution only. A two electrode system was used for spectroelectrochemical work. The ITO electrode was employed as a working electrode while a thin platinum wire served as an auxiliary electrode.

Potential control was performed using H.B. Thompson DR16 waveform generator and a H.B. Thompson potentiostat linked to a J.J Lloyd PL3 X - Y recorder. Absorbance studies were carried out using a Shimadzu UV - 160 spectrometer with 4 nm resolution. Again the temperature for all experiments was ambient.

2.4 RESULTS AND DISCUSSION

2.4.1 Cyclic voltammetry of polypyrrole layers

As mentioned earlier, polypyrrole layers formed in aqueous solution, exhibit a more porous structure than obtained when the layer is formed from an organic solvent, such as acetonitrile containing tetraethylammonium perchlorate as electrolyte [5]. There have been reports of layers obtained from aqueous solutions with porosity of up to 40% [2]. When long-chain alkyl sulphonates, such as DBS, are used as electrolyte in aqueous solutions, a greater degree of order is imparted onto the layer [1,2].

In this work polymer layers were studied in a number of different background electrolytes in one of two solvents. One of the solvents was water and the other was the previously mentioned, 50/50 by volume, mixture of water and tetrahydrofuran, called the THF/water mixture.

Figure 2.6 shows the voltammetric behaviour of a layer formed in aqueous $0.1 \text{ mol dm}^{-3} \text{ LiClO}_4$. Figure 2.7 shows a similar layer formed and run in same electrolyte as figure 2.6, but in this case the solvent was the THF/water mixture. The scan of most interest here is the first scan in both cases. Figure 2.6 shows only a very small current at potentials more positive than the polymer redox peak on the initial scan. The reduction peak is attributed to an influx of cations as reported previously [8,9,25], because of the relatively large size of the DBS^- ion. As the potential is continuously scanned between 0.6V and -0.8V the cathodic peak is seen to broaden and shift towards more positive potentials. This broadness and decrease in peak height may be associated with mobility of the Na^+ ion within the layer or irreversible swelling or shrinkage of the film upon oxidation and reduction. The sharpness of the initial cathodic peak may indicate a greater degree of order and equivalence of redox sites within the film. The cyclic voltammetry of the system is quite different on second and subsequent scans. If figure 2.6 is examined, there is virtually no "capacitive - like" current, usually seen

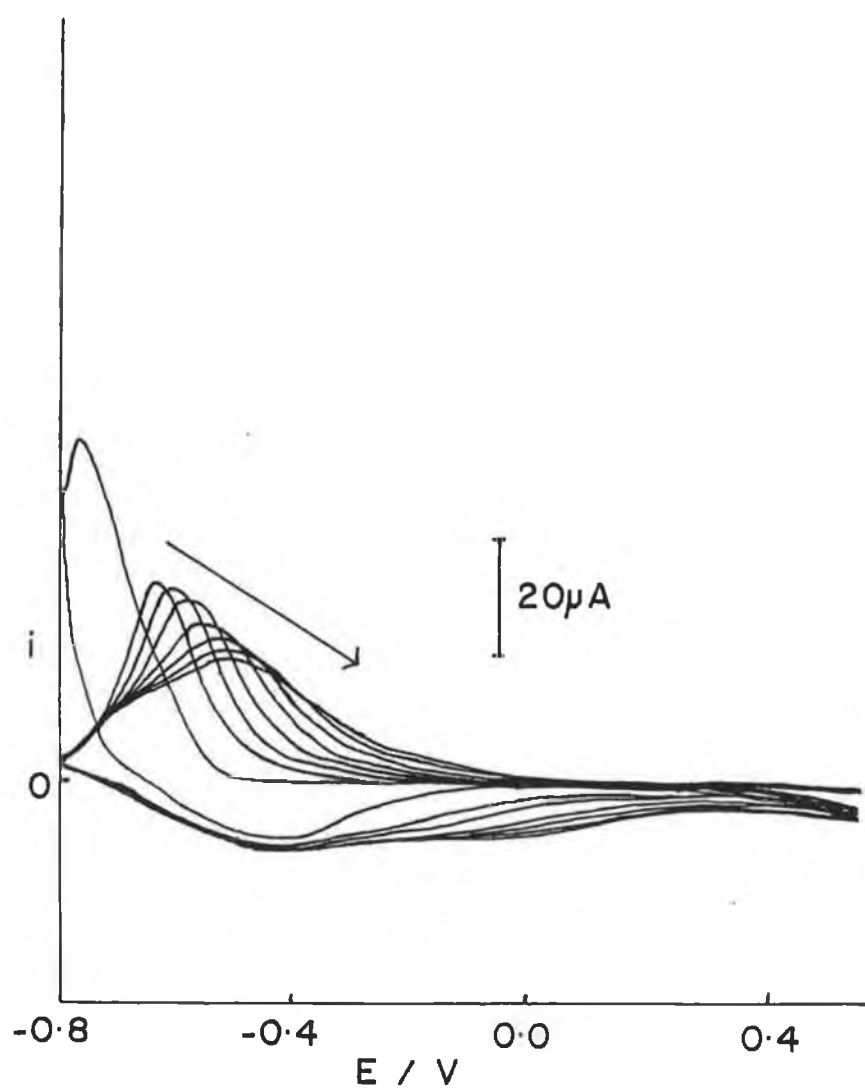


Figure 2.6 Cyclic voltammogram of a PPy DBS layer being continually cycled in 0.1M aqueous NaClO_4 solution.

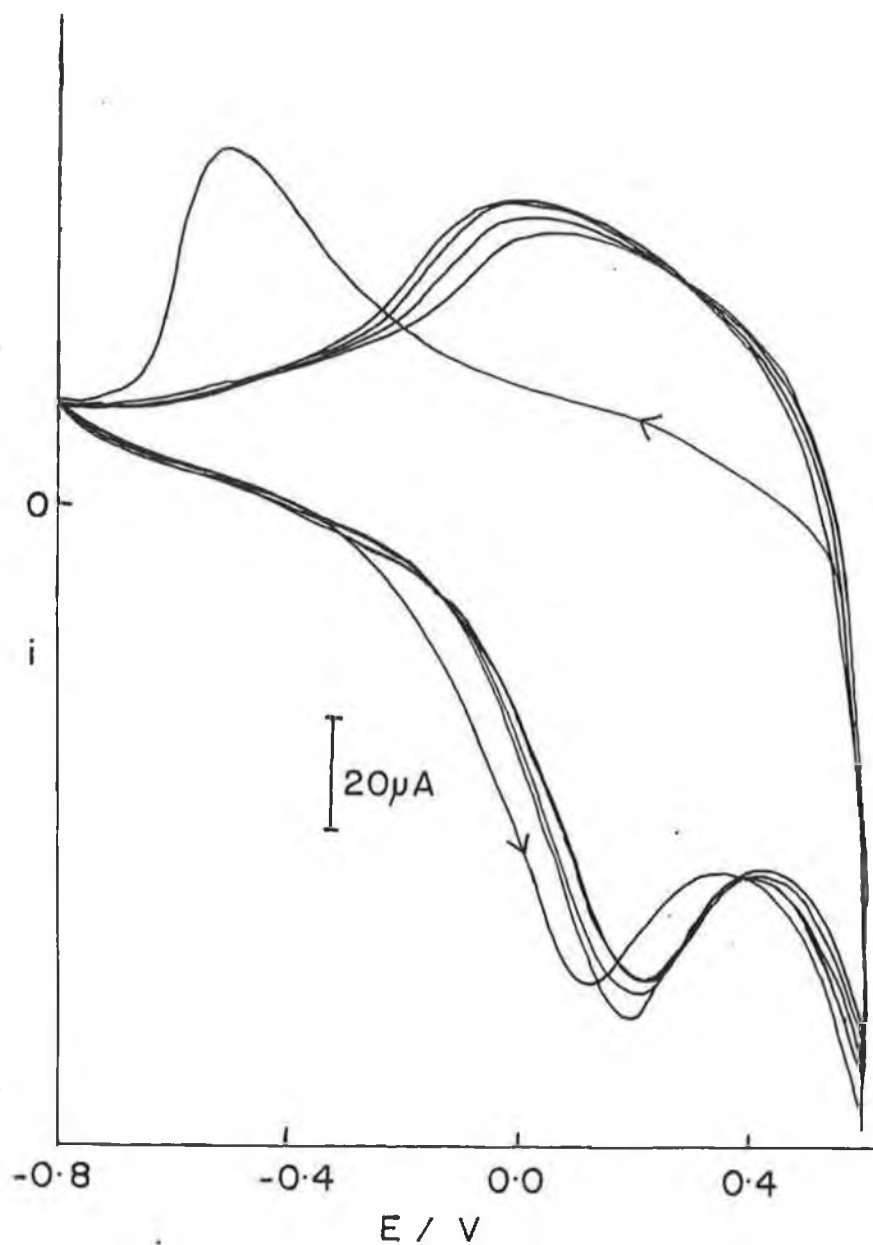


Figure 2.7 Cyclic voltammogram of PPyDBS layer being continually cycled in 0.1M NaClO₄ solution. In this case the solvent is the THF/water¹ mixture

for polypyrrole layers positive of the redox peak, upon cycling of the potential between 0.6V and -0.8V. This may be due to the fact that the layer is very compact, as suggested by S.E.M. studies [8], so there is no great exposure of surface area to electrolyte incorporated within the layer. If the current in this region was faradaic, the small amount of current observed here may be due to the fact that the DBS imparts some order into the layer. Therefore once the layer is oxidized there are no remaining unoxidized regions which would gradually become oxidized as the potential is scanned in a more positive direction.

When the layer is formed in DBS⁻ solution and run in ClO₄⁻ solution in the THF/water mixture, as shown in figure 2.7, there is a rapid exchange between DBS⁻ within the layer and ClO₄⁻ in solution. In the THF/water mixture the anion is seen to move. The cathodic peak at approximately -0.45V is characteristic of the DBS⁻ going out of the layer, while the anodic peak at approximately + 0.2V is due to ClO₄⁻ going into, and replacing the DBS⁻ within the layer. So once the DBS⁻ has been expelled from the layer the voltammetry is characteristic of polypyrrole perchlorate. The voltammetry of the second and subsequent scans in figure 2.7 is characteristic of a layer formed and run in ClO₄⁻ in the THF/water mixture.

When the layer is formed in aqueous NaDBS and run in aqueous NaDBS as shown in figure 2.8, a behaviour similar to that of figure 2.6 is observed. This would suggest that the DBS⁻ in solution has little effect on the voltammetry of the layer. It would appear that again the Na⁺ is exchanged into and out of the layer. This could be due to the small, mobile nature of the Na⁺ ion. In figure 2.8, at potentials more negative of the cathodic peak (- 0.72V), there is an underlying couple which appears to be steady-state in nature.

Figure 2.9 supports the idea of anion movement in layers formed in the THF/water mixture where the layer formed with DBS⁻ incorporated into the layer is reduced and reoxidized in NaDBBs. The formal potential of the layer has moved in this case compared to figure 2.7. Also, the cathodic peaks are more thin layer in appearance. They also decrease in magnitude and move towards more positive

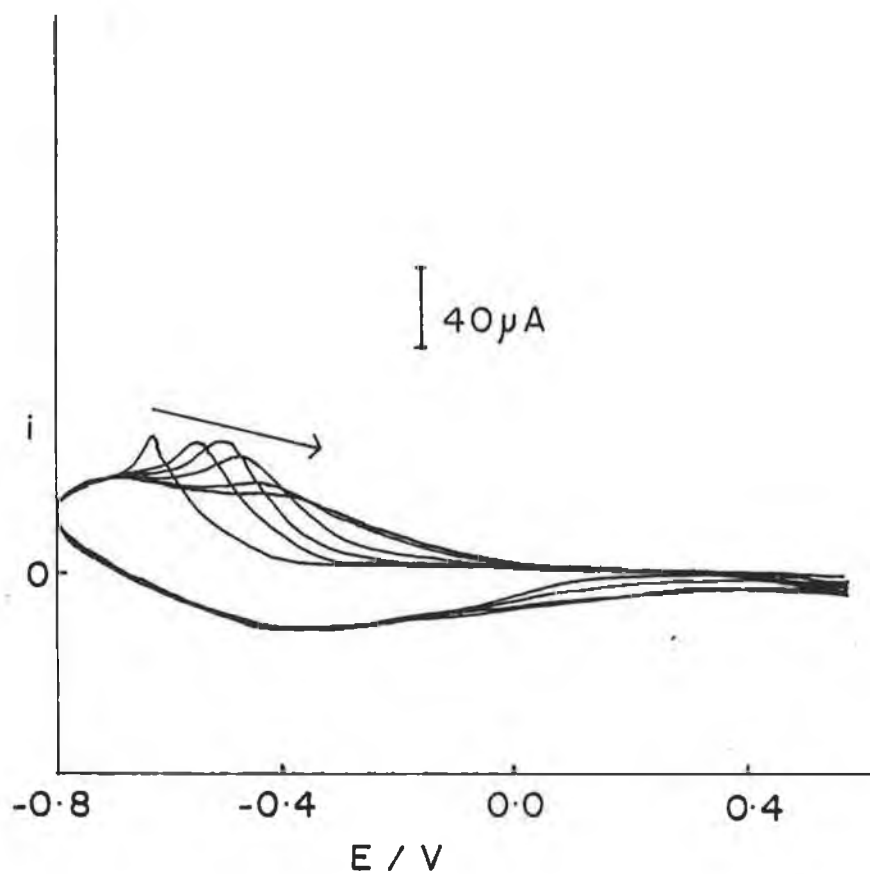


Figure 2.8 Cyclic voltammogram of a PPyDBS layer being continually cycled in aqueous 0.1M NaDBS solution

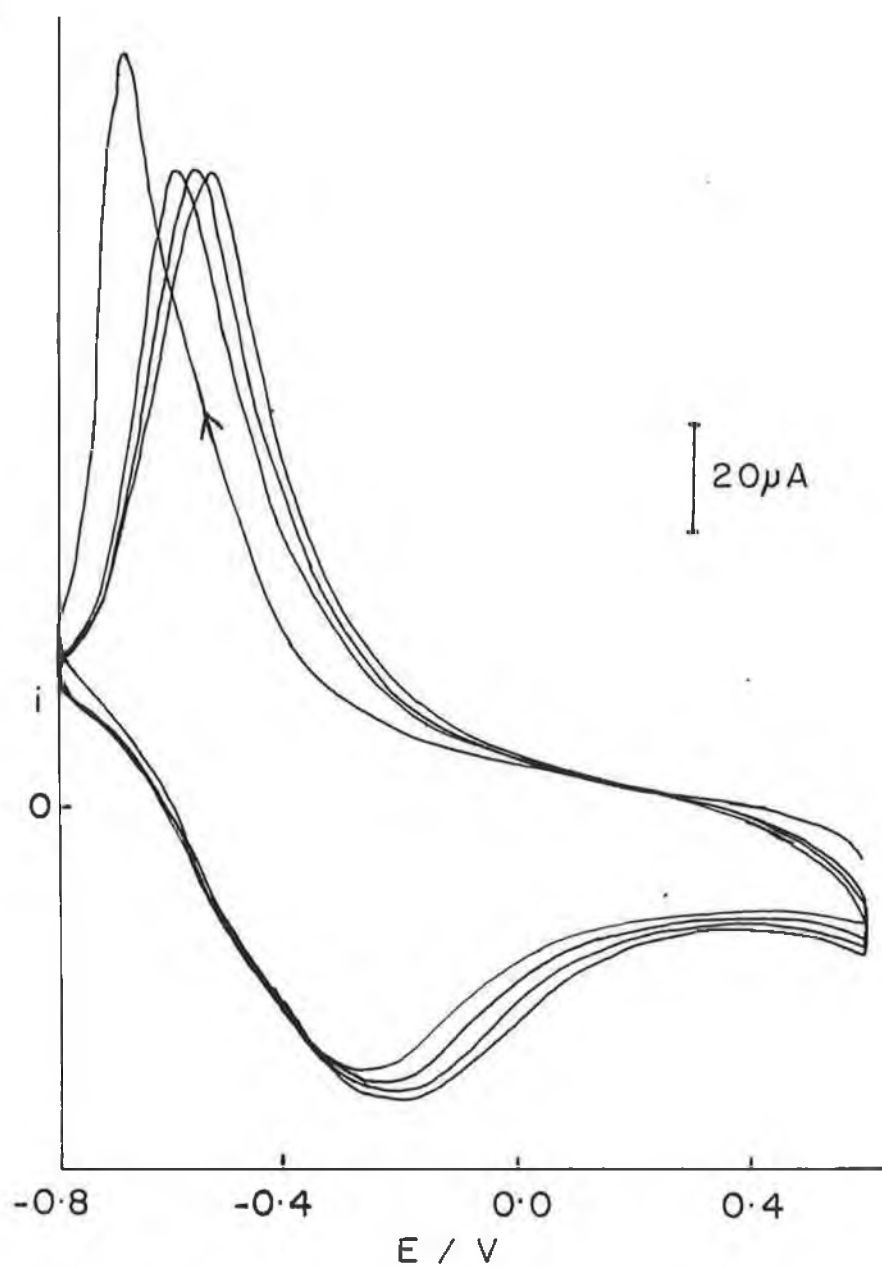
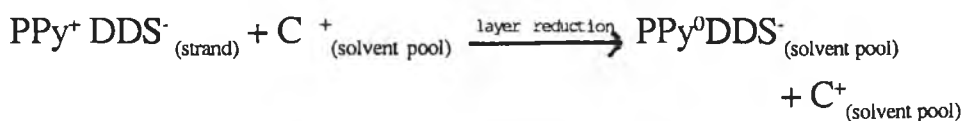


Figure 2.9 Cyclic voltammogram of a PPyDBS layer being continually cycled in 0.1M NaDBS. Solvent is the THF/water mixture.

potentials after a number of scans. This may be due to the fact that as the DBS⁻ ion is much larger than the ClO₄⁻ ion then it may be harder to expel and reincorporate into the layer. Only a small amount of the DBS⁻ may be expelled on each reduction while a lesser amount may be reincorporated on oxidation. Again, as in figure 2.6, 2.7, the compactness of the layer may hinder ion movement. Also the DBS⁻ is not as mobile as the ClO₄⁻ ion. By comparing figures 2.7 and 2.9 it can be seen that although the morphology of the original layer should be the same in both cases, the “capacitance-like” current at potentials more positive of the formal potential is more evident with smaller anions. Thus the counterion within the layer dictates the electrochemistry of the layer.

From figures 2.6 and 2.8, a set of peaks which appear as shoulders, can be seen at more negative potentials. To examine these peaks in greater detail, a layer was formed in aqueous DBS⁻ then cycled in aqueous NaBr. The cyclic voltammetry observed is shown in figure 2.10. From figures 2.6, 2.8 and 2.10 there appears to be two couples, one of whose voltammetry does not change, and another which changes gradually as scanning continues. Thus it was felt, in the case of figures 2.6, 2.8 and 2.10, that the cation is the mobile species.

To investigate this proposal further, a similar layer was formed in aqueous DBS⁻ and cycled in aqueous TEABr, figure 2.11. As can be seen the voltammetric behaviour is totally different. The peak positions remain in a constant position while gradually increasing in height with continued scanning. This gradual increase in peak height can be explained by a slow entering of TEA⁺ into the layer. The peak to peak separation is greater in figure 2.11 than in figure 2.10. This can be attributed to the fact that the TEA⁺ slows down the kinetics of the following process



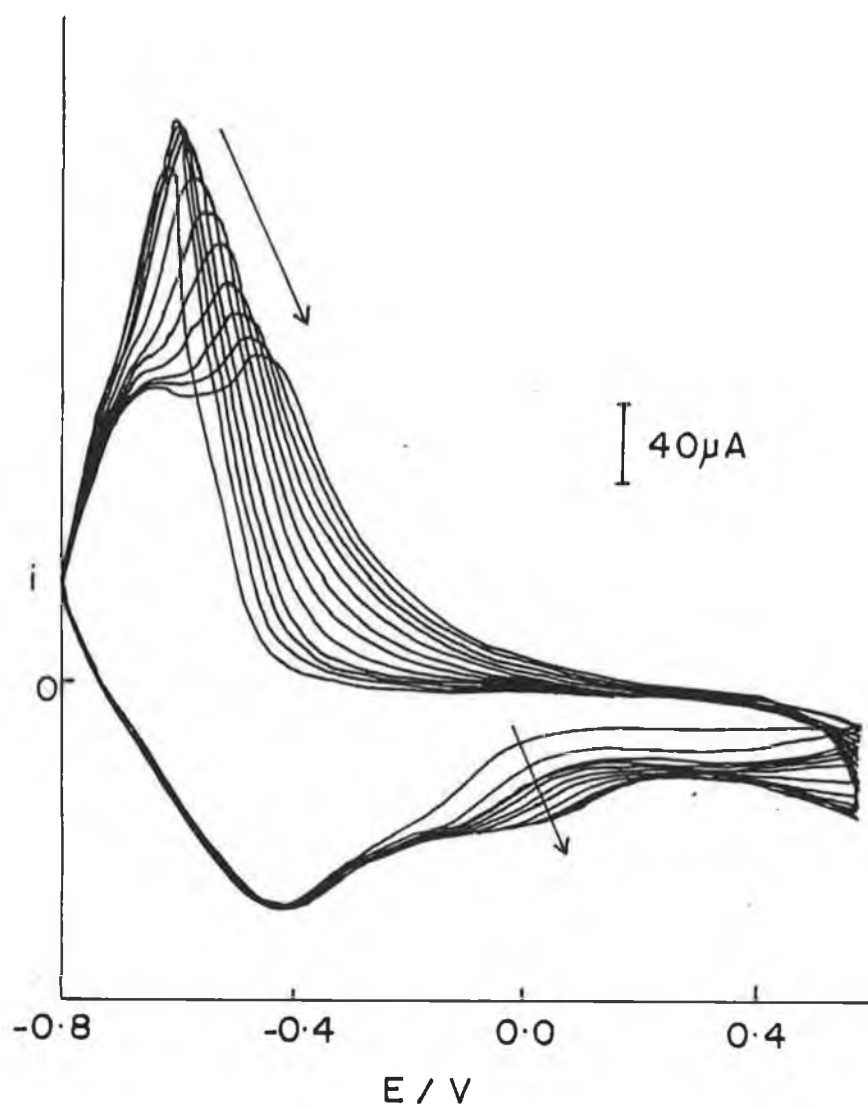


Figure 2.10 Cyclic voltammogram of a PPyDBS layer being continually cycled in aqueous 0.1M NaBr

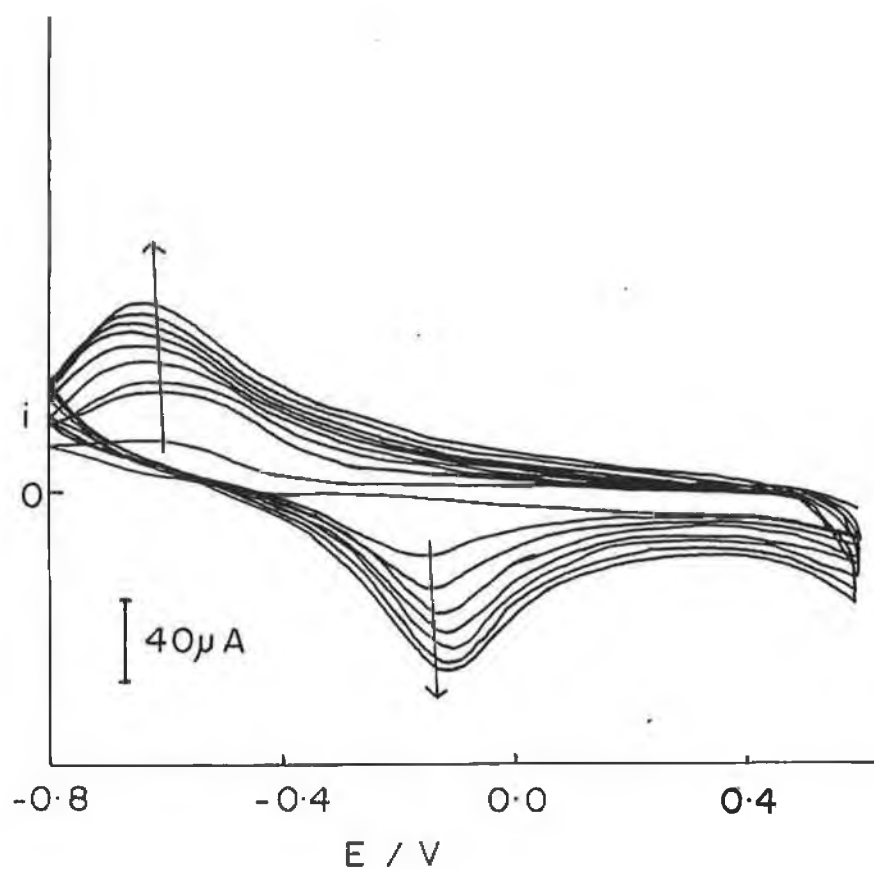


Figure 2.11 Cyclic voltammogram of a PPyDBS being continually cycled in aqueous 0.1M TEABr solution

This equation is afterwards referred to as process I. The slow kinetics of the process when TEA⁺ is used must be due to the relative size of the TEA⁺ cation. Perhaps the TEA⁺ is sterically hindered from entering the layer. Also worthy of note in figure 2.11 is that there is no gradual shift in peak potentials, characteristic of smaller “inorganic” cations. The process characteristic of “steady-state” behaviour for the inorganic cation along with the organic cation may be represented as



This is termed process II.

When the layer was formed in aqueous TEABr was run in aqueous NaBr classical voltammetric behaviour consisting of a large “double-layer” charging component was seen, characteristic of PPy⁺ Cl⁻ [8] and PPy⁺ ClO₄⁻. The voltammograms obtained were broad exhibiting large capacitance - like currents at potentials positive of the redox potential of the layer. When the converse is studied, ie. the layer is formed in aqueous NaBr and cycled in aqueous TEABr, a similar type of voltammogram is obtained but the cathodic and anodic peaks decrease with time. In these cases it appeared that perhaps both the cation and anion have some effect. This layer also exhibits the large “charging” current at positive potentials. To investigate this further a layer was formed in aqueous TEABr (large cation), and cycled in aqueous NaDBS (large anion). The cyclic voltammetry of this layer can be seen in figure 2.12. Here the Br is lost and DBS⁻ is too large to enter into the layer.

However if the layer was formed in 0.1 M NaClO₄ and run in DBS⁻, as shown in figure 2.13, the signal due to DBS can increase and reach a steady state after the initial scan. It appears that ClO₄⁻ is expelled and there is some incorporation of DBS⁻ into the layer. The behaviour of the layer is similar to that

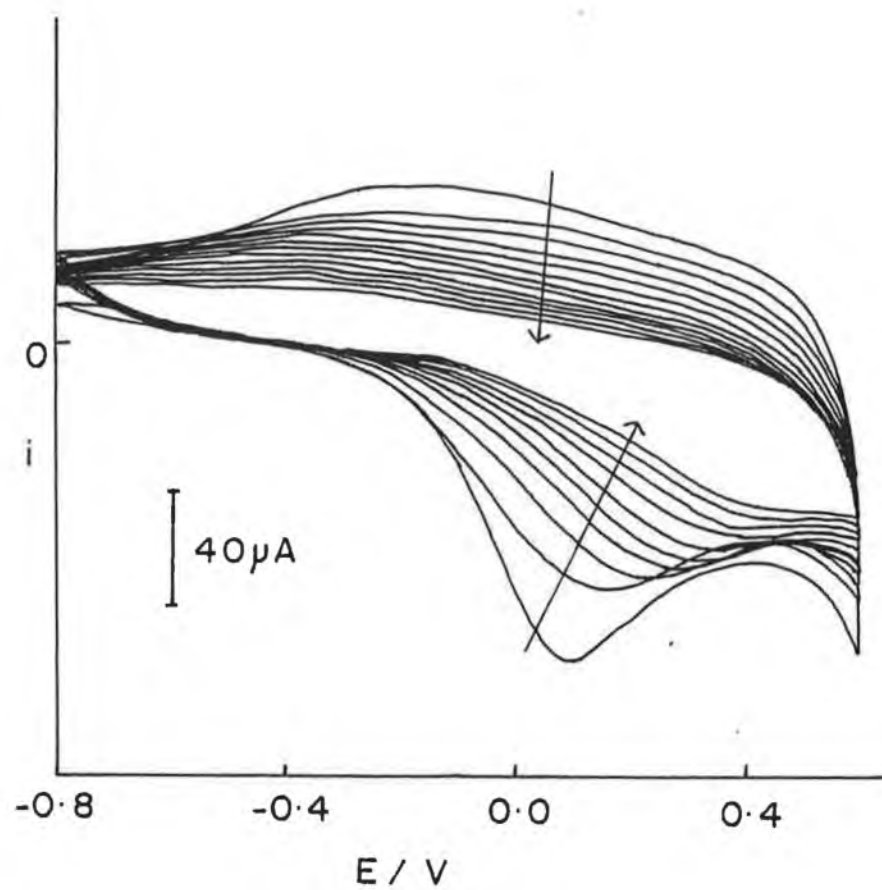


Figure 2.12 Cyclic voltammogram of layer formed in aqueous 0.1M TEABr solution and cycled in aqueous 0.1M NaDBS solution.

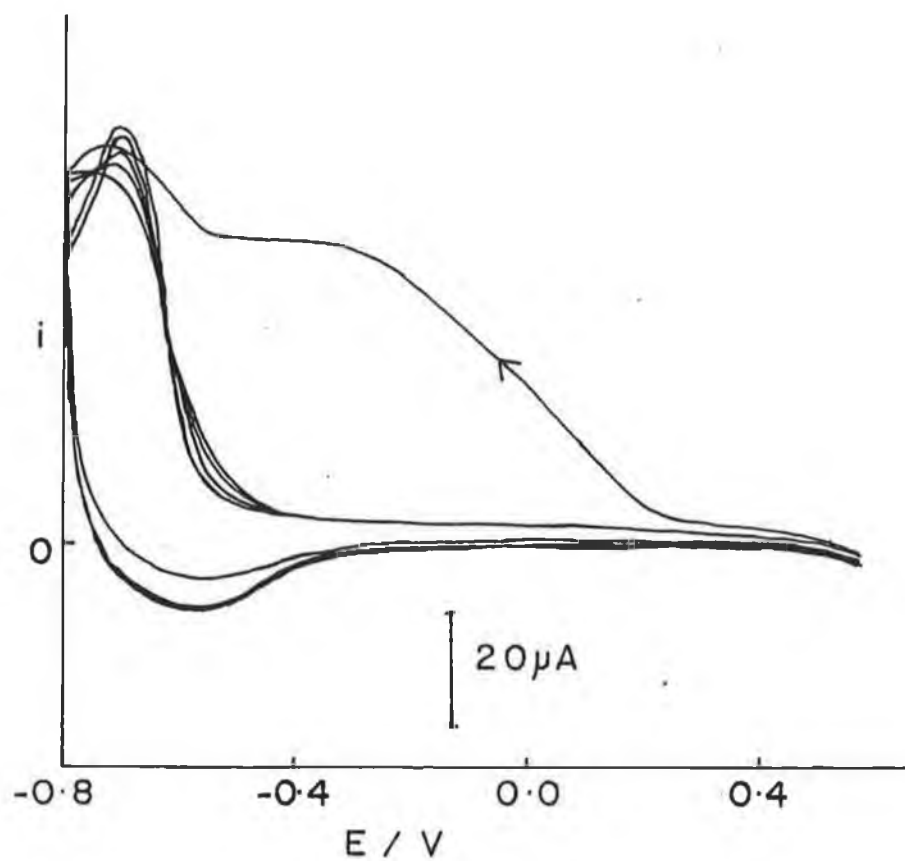


Figure 2.13 Cyclic voltammogram of $PPyClO_4$ layer cycled in 0.1M (aqueous) NaDBS solution.

shown in figure 2.10, indicating process II, from equation 2.6, is occurring. So unlike the $\text{PPy}^+ \text{Br}^-$ case, some DBS^- appears to be able to get into the larger pores of the $\text{PPy}^+ \text{ClO}_4^-$. It would be noted that the charge under the second and subsequent scans of the voltammogram is considerably less than for the initial scan indicating partial incorporation of DBS^- . If the layer from figure 2.13 is transferred back to a solution of ClO_4^- , the ClO_4^- is exchanged back into the layer. This can be seen in figure 2.14. The voltammogram shows behaviour resembling the layers formed in NaBr and TEABr and run in TEABr and NaBr respectively. It seems that not all the DBS^- is lost in suggesting that some irreversible incorporation has occurred. Figures 2.12 and 2.14 are interesting in that the large double-layer charging current, characteristic of ClO_4^- , (similar to that observed by Breen [8]), and that seen in BF_4^- , disappears when the DBS^- is introduced, and reappears when the layer is rerun in ClO_4^- . This type of behaviour would suggest that the voltammetric behaviour of the layer is not solely due to the morphology of the polymer layer but is also due to the nature of the anion/cation within the layer.

The morphology of PPyClO_4 layers is similar to that observed for PPyCl [8]. So the results obtained here would suggest that although a layer with morphology characteristic of ClO_4^- anion was originally formed (this was porous and cauliflower-like), the voltammetry changes considerably when the DBS^- is exchanged into the layer. This may be due to adsorption of DBS^- . Also noteworthy is the presence of an isopotential point in figure 2.14. This is characteristic of a one step equilibrium process. From figure 2.13 it appears that the steady-state components in figures 2.6, 2.8 and 2.10 are due to process I, while the time-dependent components are due to cation insertion, i.e. process (II). Figure 2.13 does suggest that even in aqueous solution, DBS^- may be exchanged into a layer if the layer is sufficiently porous.

The charge associated with the oxidation and reduction of the layers containing larger anions is less than that for smaller anions, indicating that it may not be possible to move anions easily from the strand, as would be required

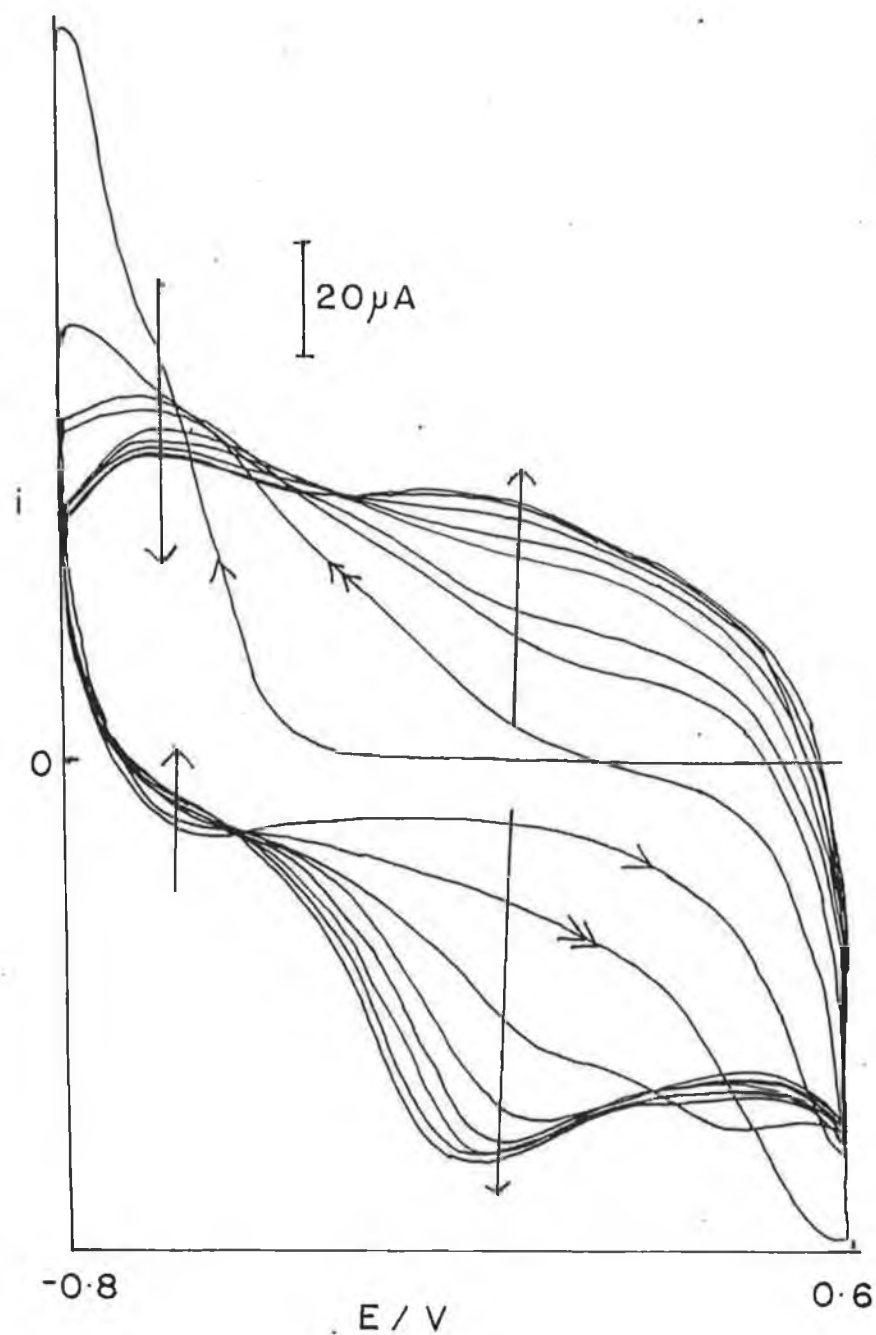


Figure 2.14 Voltammetry of layer formed in aqueous 0.1M NaDBS solution and then finally reduced in aqueous 0.1M $NaClO_4$.

for strand reduction. The fact that the larger anions are less mobile than the smaller ones would also contribute to this.

2.4.2 U.V - Vis Spectroelectrochemistry of Polypyrrole layers

The optical absorption spectrum of a polypyrrole layer formed in aqueous NaClO_4 on a ITO electrode and reduced in aqueous ClO_4^- is shown in figure 2.15 (a). The subsequent reoxidation of this layer is shown in figure 2.15(b). The neutral form shows a broad peak at approximately 500nm. This peak corresponds to the ω_3 transition, ie. valence band to conduction band transition. The wavelength at which this transition occurs, is in a region close to that reported by other laboratories [4,7,13,], though their results are not reproducible. Also of interest here is the fact that upon reoxidizing the neutral polymer, the optical spectrum is seen to change slightly, indicating that the system is not fully reversible. Perhaps this irreversibility may be due to the fact that the potential limits may be so relatively high or low, that some irreversible oxidation or reduction of polymer occurs.

If a polypyrrole layer is formed in aqueous NaDDS and subsequently reduced in aqueous DDS^- solution (figure 2.16 (b)), the spectrum obtained are different to those in perchlorate. A relatively well defined peak is observed at around 450 nm, while the peak beginning to appear at wavelengths greater than 850nm is similar to that reported by Zotti and Schiavon [13]. The difference in this spectrum compared to that observed in the ClO_4^- case is, the peak of maximum absorption for the DBS layer was different to the perchlorate layer for neutral layers. The reason why NaDDS was used in this study was that it was thought that when such a layer is reduced the anion does not leave as shown in the voltammetric studies.

The ITO electrodes used in this work were of a cross-reactional area of approximately 6cm^2 . It would be unfeasible to think that a homogenous layer of polymer would be obtained on the electrode. As a matter of fact, the coated ITO

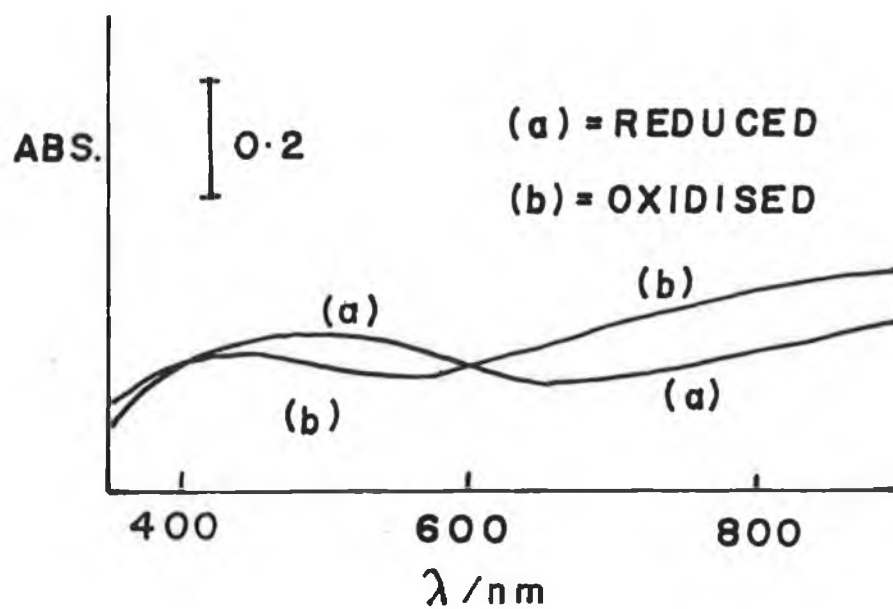


Figure 2.15(a) Optical absorption spectrum of polypyrrole layer formed in aqueous 0.1M NaClO_4 on an ITO electrode and reduced in aqueous 0.1M ClO_4^- . The subsequent reoxidation is shown in figure 2.15(b).

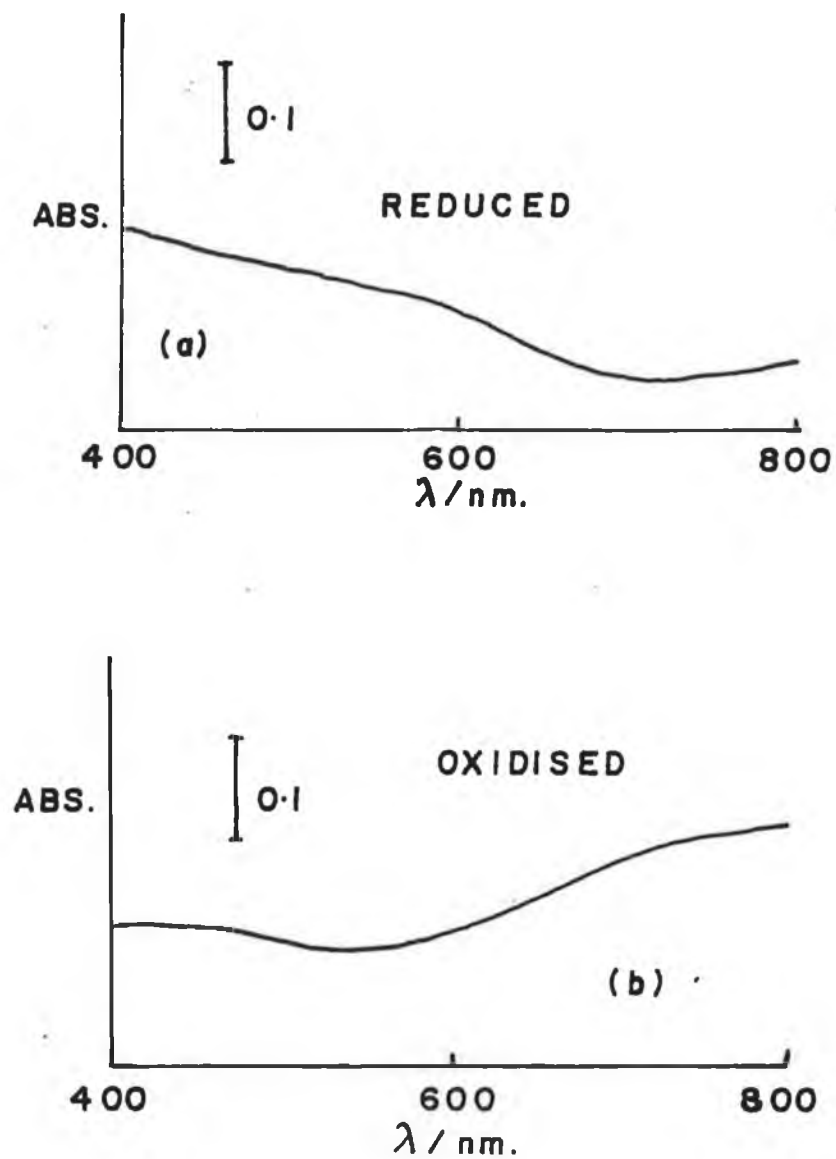


Figure 2.16 Optical absorption spectra of PPy formed in aqueous NaDDS solution
(a) is the spectrum of the reduction while
(b) is the spectrum due to reoxidation

electrodes showed visibly differing regions of polymer covering. For this reason it is not really feasible to draw quantitative comparisons between one spectrum and the next one. If, as was shown in the last section, the incorporated anion has an effect on the subsequent electrochemistry of some polypyrrole layers, how would the optical spectra be changed by, for example, forming the polymer with a “large” incorporated anion, such as dodecyl sulphate, DDS^- , and then reducing the layer in a “smaller” anion i.e. ClO_4^- .

The absorption spectrum of a layer formed in an aqueous DDS^- solution and the reduced in aqueous NaClO_4 is shown in figure 2.17. The reduced, neutral, form shows a well-defined peak at approximately 420nm corresponding to ω_3 , the VB to CB band energy transition. The overall spectrum is much more like the spectra observed by previous workers from PPyClO_4 layers in acetonitrile [11,13]. The spectrum of polypyrrole formed in DDS and reduced in NaClO_4 in aqueous solution is quite different compared to either of the previous spectra. This may be due to the fact that when a layer is formed in DDS and reduced DDS that there is not as great an amount of Na^+ available as in a solution of 0.1M NaClO_4 . Certainly there is a dramatic qualitative change in spectrum for the reduced form where, in 0.1 M NaClO_4 . There is a maximum at 420nm.

The variations in absorbance at 400nm and 800nm for each of the three systems, with changing potential are given in figures 2.18, 2.19 and 2.20 respectively. The absorbance were measured in going from the neutral to the oxidized form. For this work, only the variations in absorbance at 800 and 400nm with changing potential were analysed. The curves for all three systems were relatively similar. In all cases studied the variation in absorbance with potential at 400nm is less pronounced than the corresponding absorbance change with potential at 800nm. This can be attributed to the fact that the transitions at 800nm are not well defined and there may be some overlap of more than one transition [19]. Change in absorbance is related to charge injection into the layer. The apparent “extinction coefficient” associated with the reduced form of the layer is much smaller than the oxidized form. It can be seen from figures 2.18 and 2.20 that for the 400nm

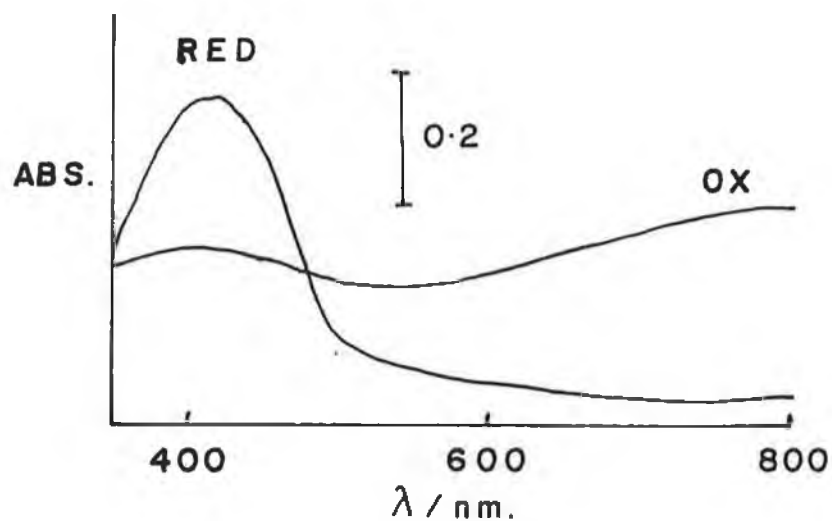


Figure 2.17 The absorption spectrum of a layer formed with DDS^- as counterion and subsequently reduced and reoxidized in NaClO_4

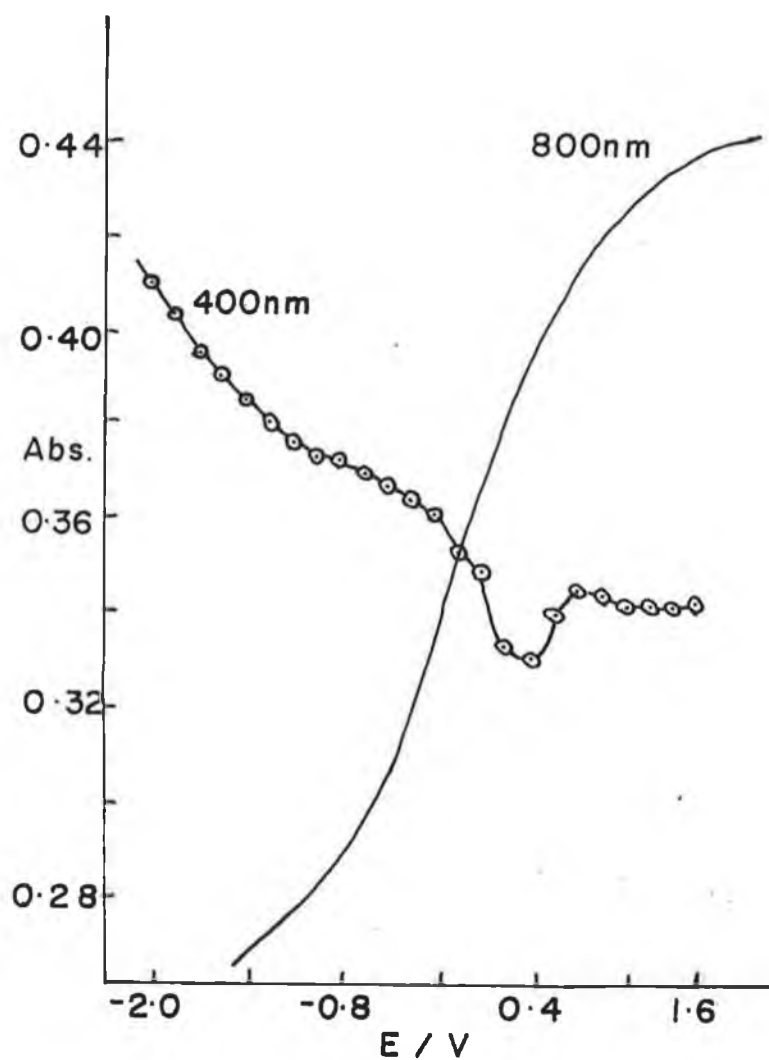


Figure 2.18 Plot of variation in absorbance with potential for layer formed with ClO_4^- as counterion, run in 0.1M NaClO_4 solution.

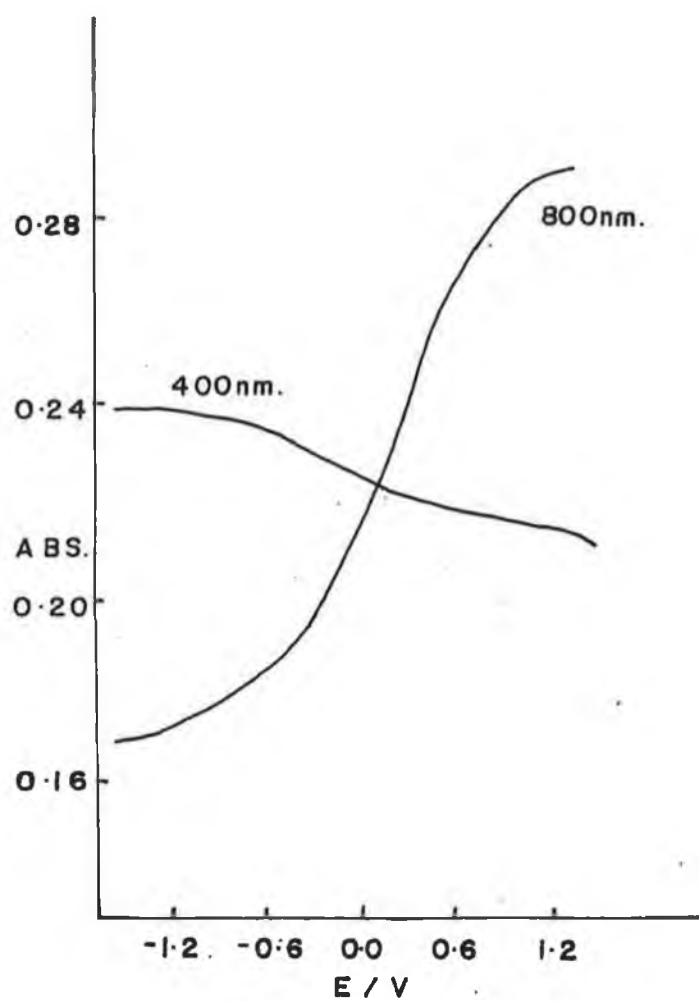


Figure 2.19 Plot of variation in absorbance with potential for layer formed with DDS^- as counterion run in 0.1M NaDDS solution.

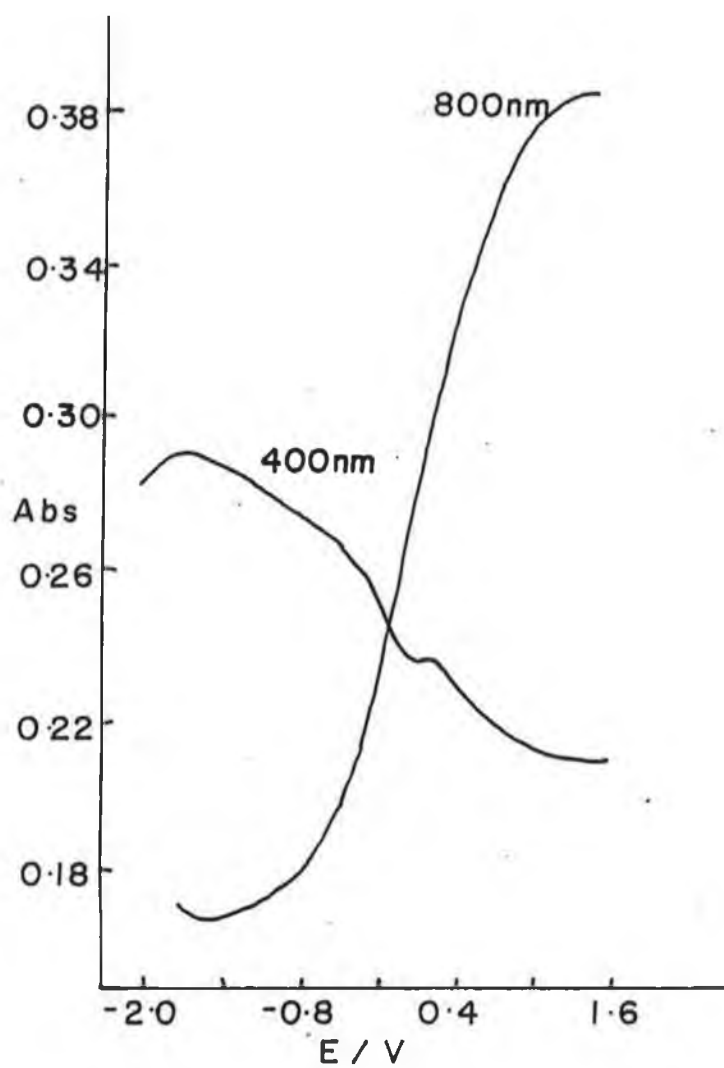


Figure 2.20 Plot of variation in absorbance with potential for layer formed with DDS^- as counterion run in 0.1M NaClO_4 solution.

plot there is a curious dip in the middle. This dip may be due to interference due to B-band shown in figure 2.2, This corresponds to the $\pi - \pi$ transition of conjugated cationic segments. This is a very broad band and it is logical to assume that this band may in some way interfere with the absorbance at 400nm. These figures show that the behaviour of a layer which has an anion exchanging in and out of the layer, as the “dip” is only seen in layer that were run in ClO_4^- , which is similar to the behaviour of the PPyDDS layer where cation exchange occurred.

If a plot of the change in absorbance with change in mean potential, dA/dE , is plotted against mean potential, a curve which is related to a cyclic voltammogram is obtained. This curve is depicted in figure 2.21(a) and is the spectroscopic analog of a cyclic voltammogram (figure 2.21 (b)). The C.V., if plotted on the same axis, can help to yield information as to what fraction of the total current is faradaic and what is due to double-layer charging. This was carried out only for the polypyrrole layer formed in aqueous NaDDS and reduced in aqueous NaClO_4 . The graph of current versus potential is representative of the total current, while the dA/dE versus E^1 curve shows only the faradaic component of current. As can be seen from the superimposition of the two curves, there must be a large double-layer charging component as the current is seen to be rising after the dA/dE vs E^1 peak, yet there is no further oxidation of material beyond this point. As can be seen from figure 2.21(b), the voltammetry of the polypyrrole is very different from that observed when using a conventional three electrode system. The ITO electrode is by no means ideal as quantitative information is not accessible.

2.4.3 Nernst model of polypyrrole system

Previous workers have utilized the Nernst equation to analyse spectroelectrochemical behaviour of polypyrrole films [19]. The formal potentials and “n-values”, (the apparent number of electrons transferred during the redox reaction), can be obtained using this method. As shown in the absorption spectra

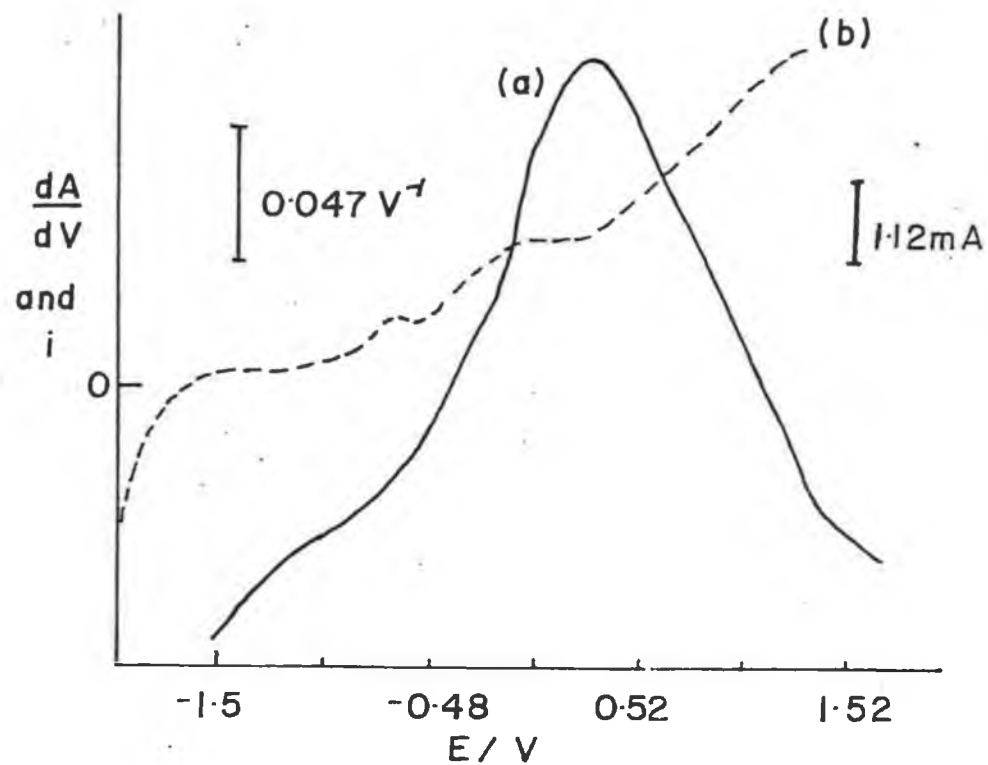


Figure 2.21 Plot of dA/dE versus mean potential
 (a) Superimposed onto this is a plot of change in current with potential
 (b) The polymer layer used for this plot was formed in aqueous NaDDS and reduced in aqueous $NaClO_4$

earlier some of the spectra do not show simple isosbestic points, so the redox reactions in the polymer film cannot be represented by simple one-step equilibrium reactions among the neutral monomers, slightly oxidized, (polarons), and full oxidized, (bipolarons), layers.

The following assumptions are necessary to apply the Nernst equation to the data [19],

- (1) the overlapping of absorption spectra are neglected,
- (2) only three species, neutral monomers, slightly oxidized monomers (polarons) and fully oxidized monomers (bipolarons), exist in the film at a given potential and
- (3) only two reactions occur (a) between neutral monomers (Polarons) and (b) between slightly oxidized monomers (polarons) and fully oxidized ones (bipolarons).

The “monomer unit” model is used here. This treats the redox reaction of the PPy films in terms of the pyrrole monomer unit. This work assumes that the absorption at approximately 400nm is due to the $\pi - \pi^*$ transition of the neutral pyrrole monomers [4,19]. 800nm was taken as the wavelength at which the broad band due to the fully oxidized monomers existed.

The absorption data is treated according to the Nernst equation, assuming Beers law, At 400nm the equation is

$$E = E_1^{01} + (0.059/n_1) \log ([Py^+] / [Py^0]) =$$

$$E_1^{01} + (0.059/n_1) \log \{ (\Delta Abs)_{max} - \Delta Abs) / \Delta Abs \} \quad 2.7$$

At 800nm the equation is

$$E = E_2^{01} + (0.059/n_2) \log ([Py^{+n}] / [Py^+]) =$$

$$E_2^{01} + (0.059/n_2) \log \{ \Delta Abs / (\Delta Abs)_{max} - \Delta Abs) \} \quad 2.8$$

Layer formed in NaDDS. Run in NaDDS solution		
<u>Wavelegth:</u>	<u>Potential. (V)</u>	<u>Electrons trasferred</u>
400nm	$E_1^{01} = -.425V$	$n_1 = 0.043$
800nm	$E_2^{01} = 0.155V$	$n_2 = 0.095$
Layer formed in NaDDS. Run in NaClO ₄ solution		
400nm	$E_1^{01} = +0.163$	$n_1 = 0.064$
800nm	$E_2^{01} = +0.05V$	$n_2 = 0.088$
Layer formed in NaClO ₄ Run in NaClO ₄ solution		
400nm	$E_1^{01} = -0.300V$	$n_1 = 0.046$
800nm	$E_2^{01} = 0.296V$	$n_2 = 0.062$

Table 2;1 Data obtained from applying the Nernst equation to the spectroscopic data

where E is the potential applied to the electrode, E_1^{01} , E_2^{01} are the formal electrode potentials, n_1 and n_2 are the number of electrons transferred and Py^0 , Py^+ , Py^{+n} correspond to the neutral monomer, slightly oxidized monomer and the fully oxidized monomer respectively. The ΔAbs ' are the absorbance changes relative to the fully oxidized spectrum at 400nm and that relative to the fully reduced spectrum at 800nm. The $(\Delta Abs)_{max}$ is the maximum absorbance change between fully oxidized and fully reduced states. The contributions of counterions are omitted for convenience. As observed by Ameniya and co-workers, the plots obtained are not linear [19], but linear regions are obtained in certain potential regions. The Nernst plots for the three systems studied in this work are shown in figures 2.22 to 2.27. Something worthy of note here is the fact that in the case of the polypyrrole layers formed in 0.1M NaDDS and run in ClO_4^- solution, the Nernst plots, at both wavelengths are linear. Table 2.1 lists the data obtained from these graphs.

In table 2.1 the values of n_1 and n_2 are much smaller than 1, which has been observed previously [19]. For layers formed and run in the same electrolyte, the E_1^{01} value is less positive than E_2^{01} . This implies that there is a two step electron transfer with 500mV between the two values. Uncharacteristically, for a layer formed in NaDDS and run in $NaClO_4$ the situation is dramatically different, in that E_2^{01} is slightly negative of E_1^{01} . Thus, this implies that once polarons are formed there is a rapid further oxidation to bipolarons as shown in equation 2.1. This is a result which requires further work. These results are complicated by the addition of an extra potential term (an excess chemical potential) to equations 2.7 and 2.8, which serves to make the values of E_1^{01} , E_2^{01} somewhat invalid [19]. That the theory is valid is verified by the good linearity obtained in figures 2.22 to 2.27.

2.4.4 Bandgap Energy estimation for polypyrrole

The final use of optical data obtained in this work was to attempt to make an estimation of the bandgap energy of neutral polypyrrole, ie. transition ω_3 in

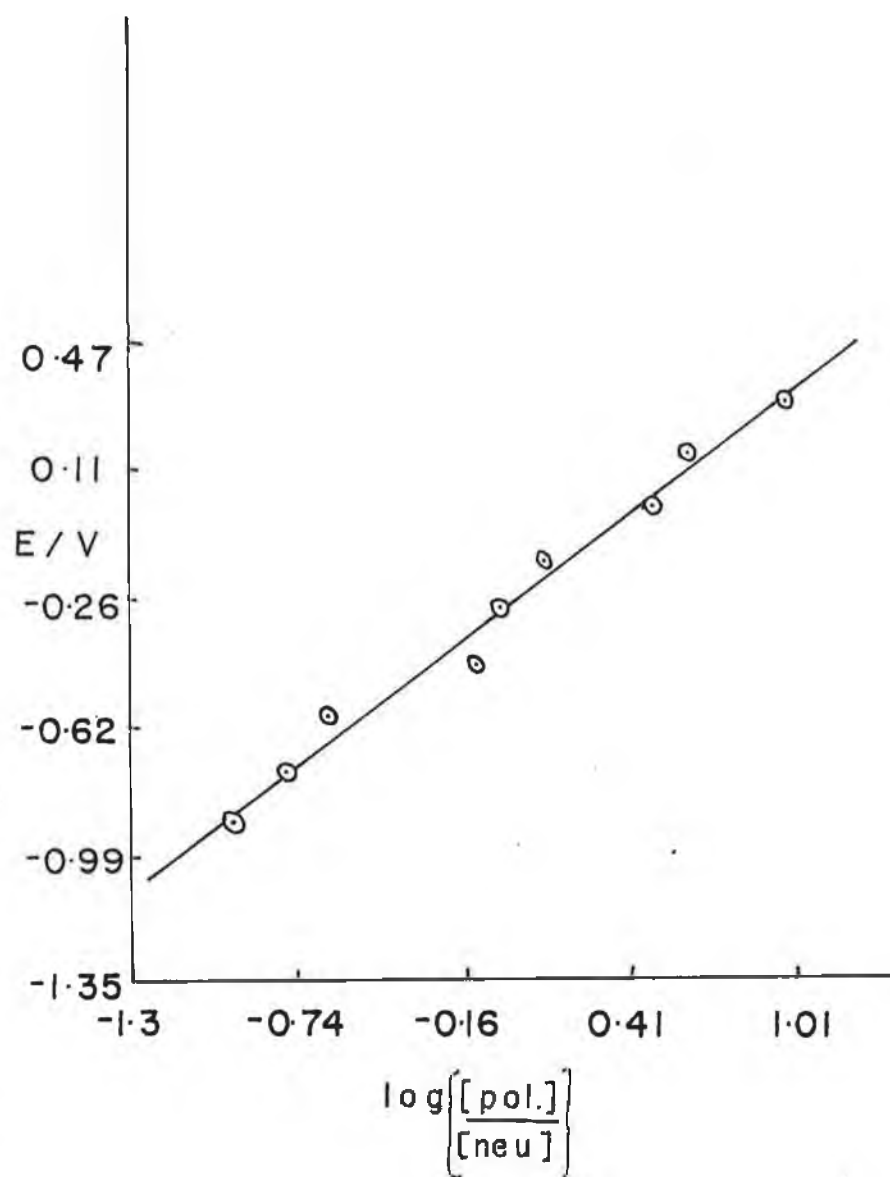


Figure 2.22 Nernst plot calculated from the absorbance at 400 for a polypyrrole layer formed in 0.1M NaClO₄ and run in 0.1 M NaClO₄.

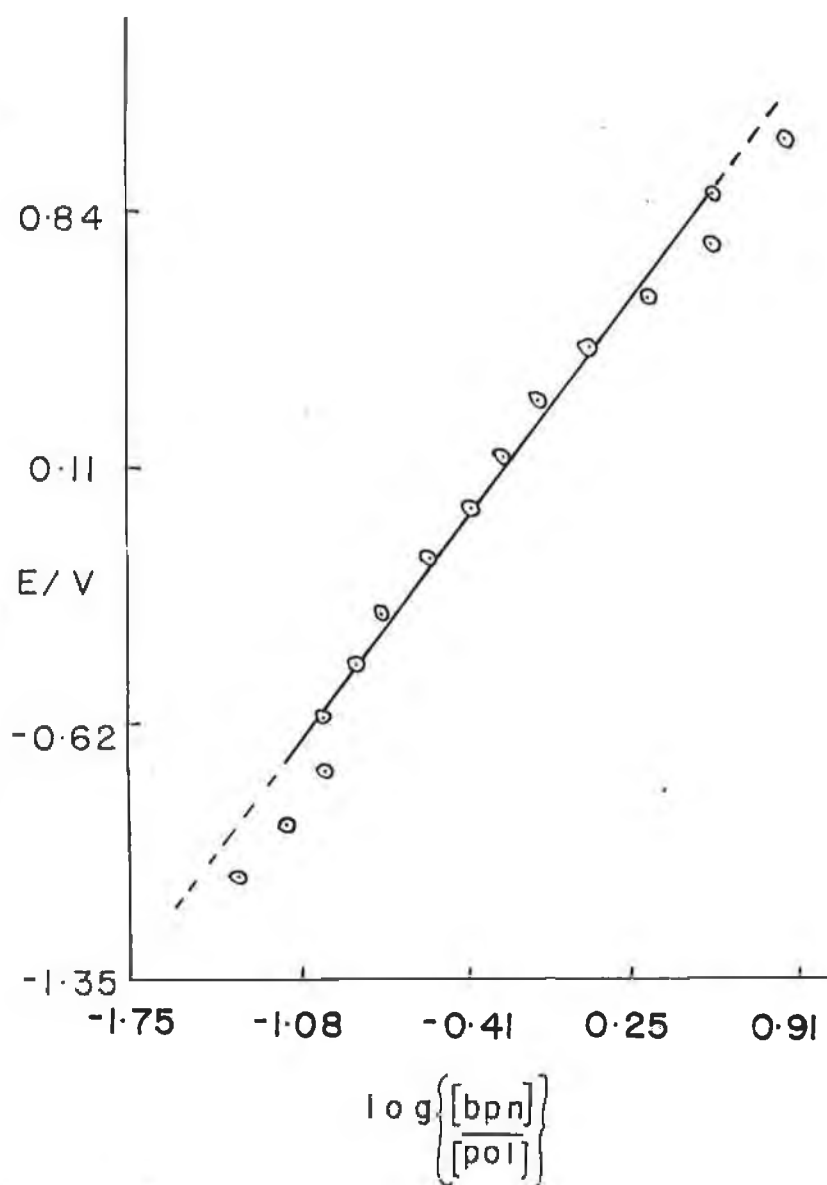


Figure 2.23 Nernst plot calculated from the absorbance at 800 nm for a polypyrrole layer formed in 0.1M NaClO₄ and run in 0.1 M NaClO₄.

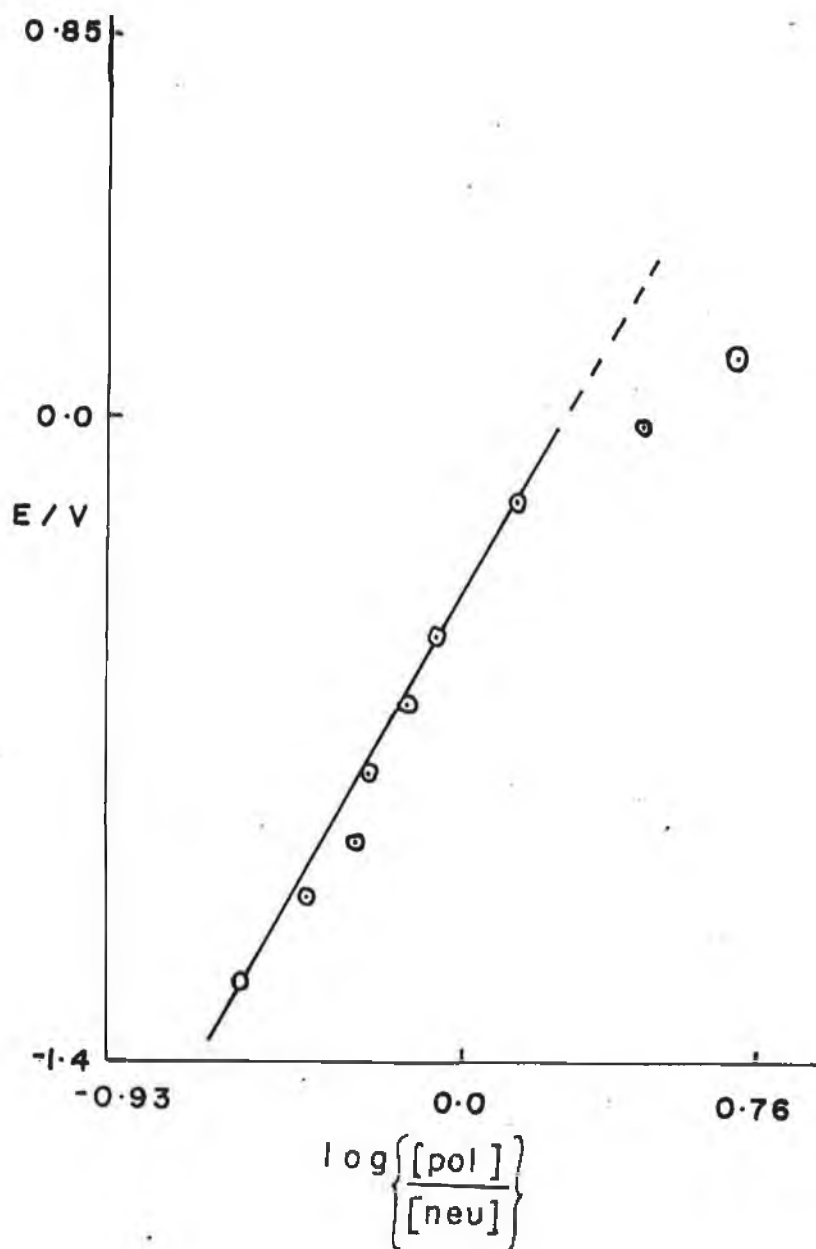


Figure 2.24 Nernst plot calculated from the absorbance at 400 nm for a polypyrrole layer formed in 0.1M NaDDS and run in 0.1 M NaDDS

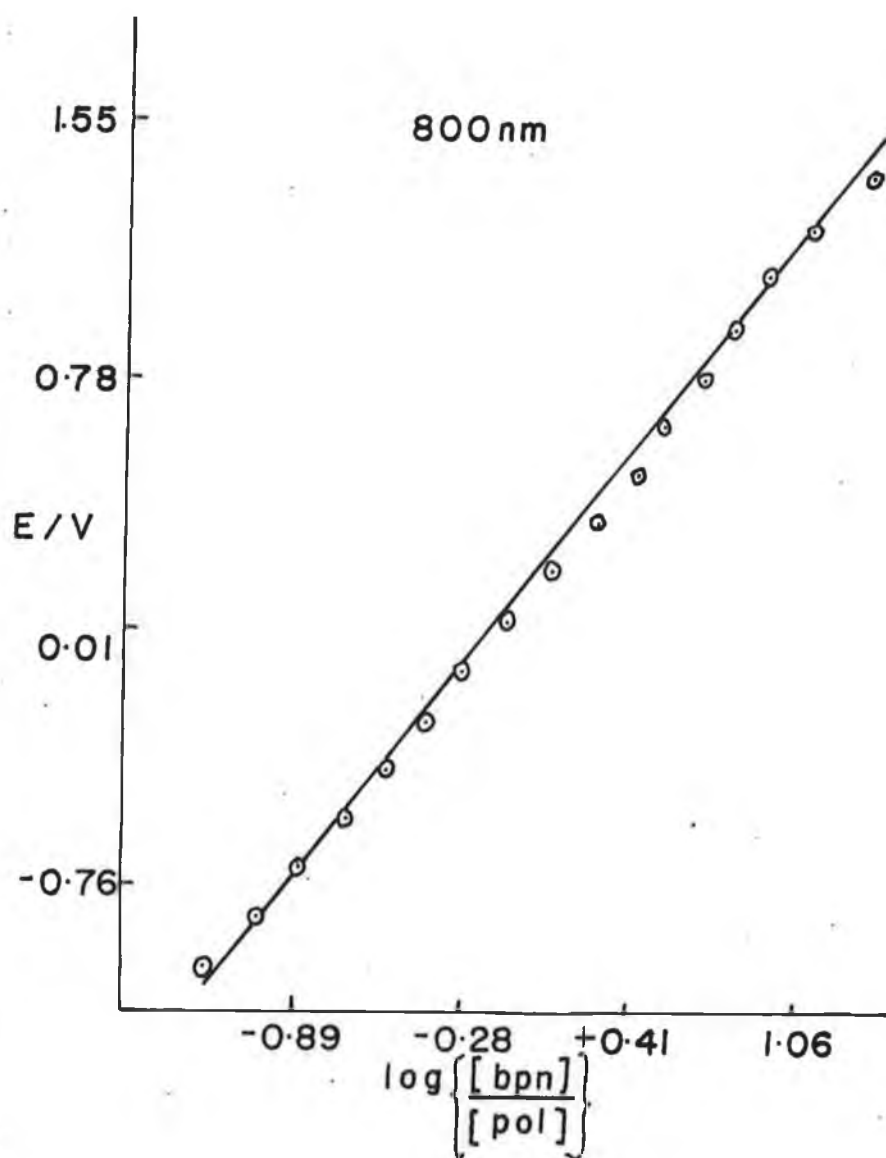


Figure 2.25 Nernst plot calculated from the absorbance at 800 nm for a polypyrrole layer formed in 0.1M NaDDS and run in 0.1 M NaDDS.

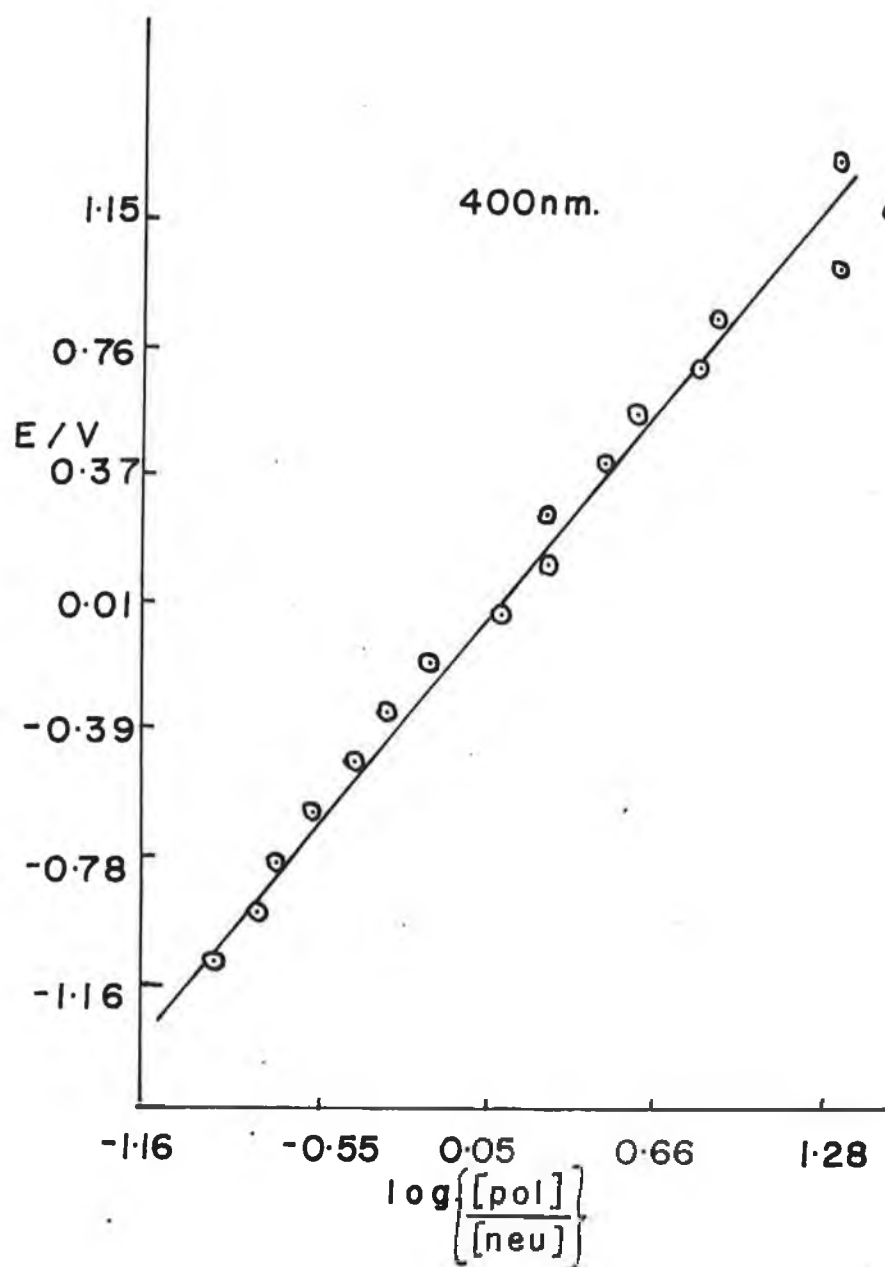


Figure 2.26 Nernst plot calculated from the absorbance at 400 nm for a polypyrrole layer formed in 0.1M NaDDS and run in 0.1 M NaClO₄.

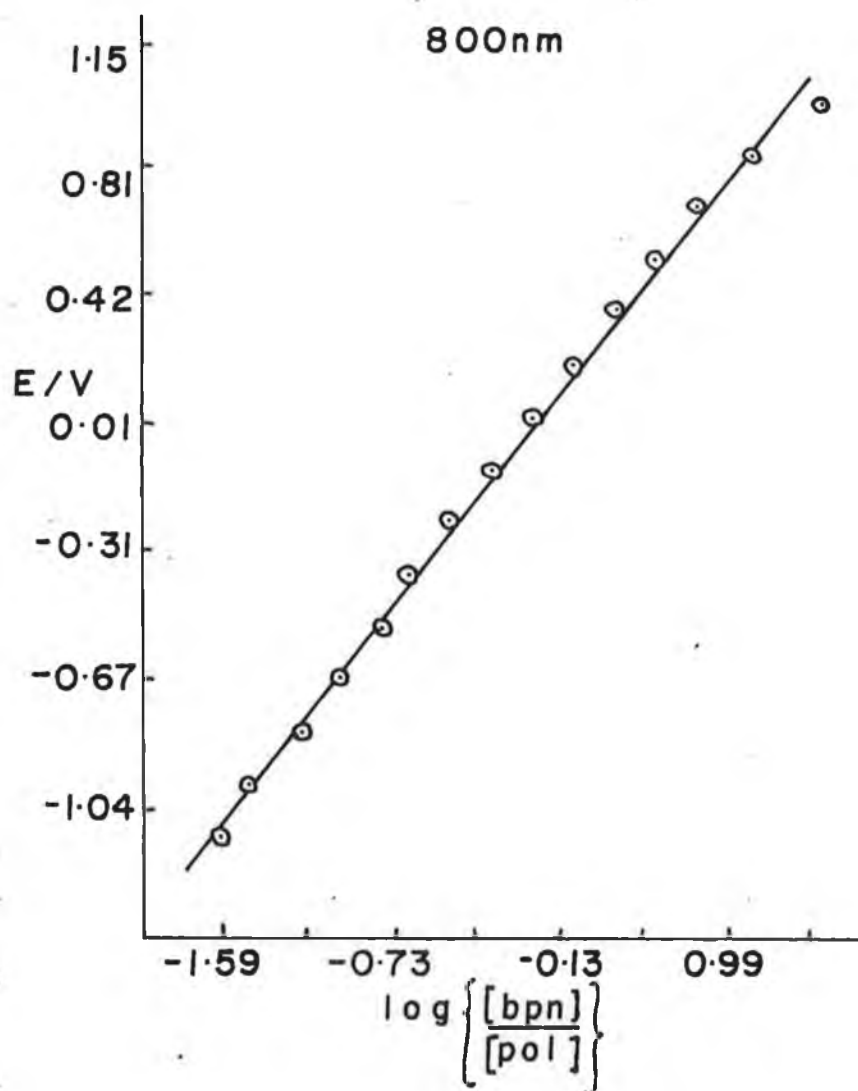


Figure 2.27 Nernst plot calculated from the absorbance at 800 nm for a polypyrrole layer formed in 0.1M NaDDS and run in 0.1 M NaClO₄.

figure 2.2. The method used is simple graphical method, as used by Josowicz and Blackwood [4]. The system studied in this work was the polymer layer formed in aqueous 0.1M NaDDS and reduced in aqueous 0.1M NaClO₄, as these spectra were the most reproducible and showed a sharp peak at around 400nm, corresponding to ω_3 .

If the energy bands are assumed to be parabolic, the absorption coefficient, α , is related to the photon energy by [26].

$$(\alpha h\nu)^{2/n} = B(h\nu - E_g) \quad 2.9$$

where h is Plancks constant, ν is the frequency of the incident radiation, E_g is the bandgap energy and B is some constant, n is a parameter which takes the value of 2 for direct transitions and 4 for indirect transitions. Note that the wavelength, λ , is related to ν by the following

$$\nu = c/\lambda \quad 2.11$$

here c is the velocity of light. So using the section of the spectra immediately to the right of the 400nm peak and plotting the relative absorption intensity times $h\nu$, all raised to the power of 2 (direct) or 1/2 (indirect) versus $h\nu$ can yield an estimation of the bandgap energy of neutral polypyrrole. The straight line graph corresponding to $n = 1$, is shown in figure 2.28. This shows that indeed ω_3 is a direct transition. From the intercept on the abscissa a value for the bandgap energy of 2.76 eV was obtained. This value was lower than that observed by Bredas [26], but very similar to that observed by Josowicz [4]. This difference may partly be due to band tailing caused by the amorphous structure of polypyrrole or perhaps the change in anion may have had some effect on the bandgap energy.

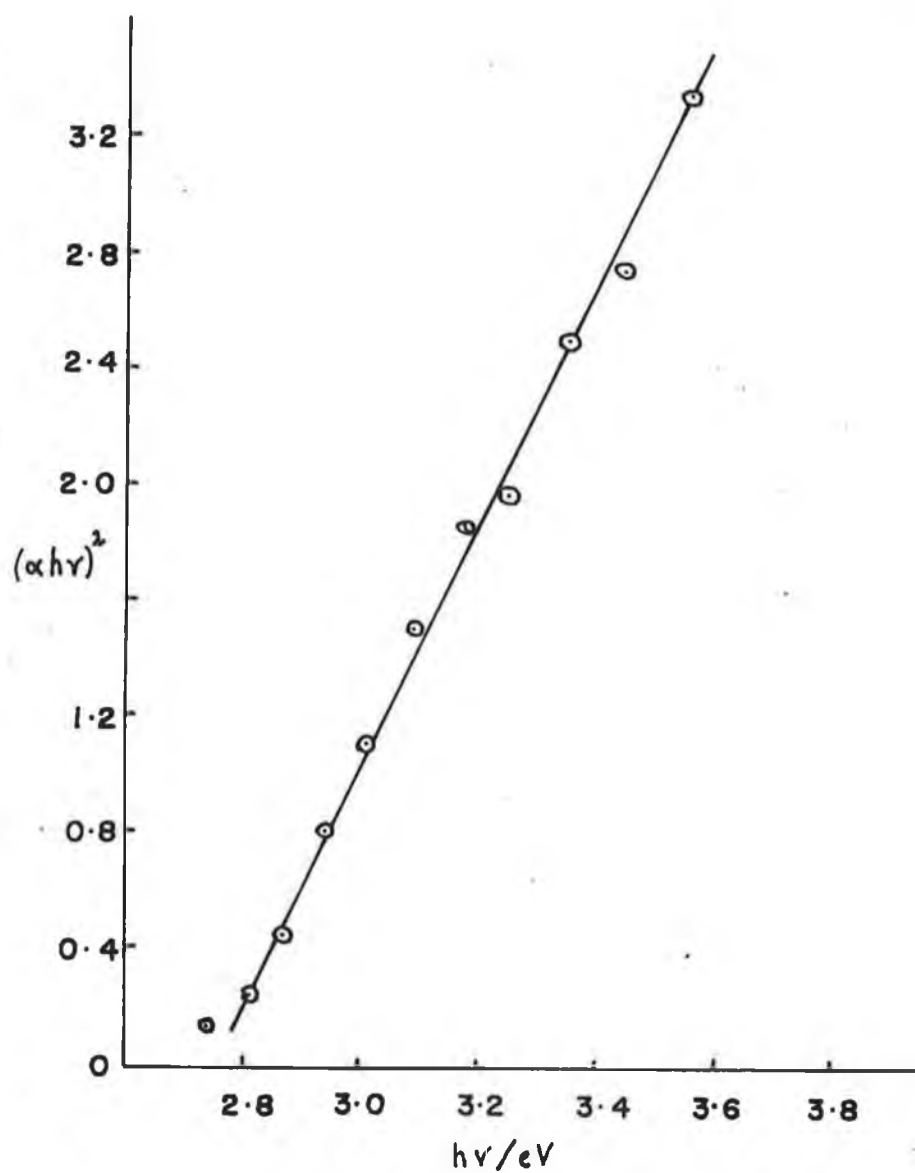


Figure 2.28 Plot of $(\alpha h\nu)^2$ vs $h\nu$ for a layer formed in 0.1 M NaDDS and run in 0.1 M NaClO₄ at an ITO in order to determine the bandgap energy.

2.4 CONCLUSIONS

In aqueous solutions, with polypyrrole layers, some interesting voltammetry is observed; There is very little "charging current" at potentials more positive than the redox potential of the polymer, in the case of PPyDBS and PPyDDS. This lack of charging current makes the polymer more suitable for analytical determinations [25,28].

In some cases in aqueous solution, cations appear to enter the polymer matrix. These cations may enter the polymer matrix without their hydration spheres, possibly due to the hydrophobicity of the polypyrrole matrix when neutral. Although the cations appear to move into and out of the layer, it appears in the case of the THF/water mixture charge neutrality is maintained by anion movement. This may be rapid or may occur gradually.

When a layer is formed in aqueous solution of pyrrole and DBS⁻, the DBS⁻ is not exchanged with other anions when the layer is cycled in solutions of these anions. However, if the layer is formed in aqueous solutions of ClO₄⁻, there is some incorporation of DBS⁻, perhaps due to adsorption. When the layer is recycled in aqueous NaClO₄ the DBS⁻ is retained within the layer.

The morphologies of PPyClO₄ and PPyDBS are very different [8], but the difference in cyclic voltammetry of the layers is due to more than just differences in morphology.

Layers formed in large anions such as DDS⁻ and DDS⁻ were more compact and adherent than layers formed with counterions such as ClO₄⁻, BF₄⁻, Cl⁻ etc. The larger anions seem to, therefore, impart a greater degree of order into the layer.

In the case of layers formed in DBS⁻, DDS⁻ in the THF/water mixture, and run in a "small" anion the following was observed. Once the large anion has been expelled, the voltammetry is characteristic of the voltammetry of the small anion in the same mixture. This indicates that there is no reincorporation of the DBS⁻ or

DDS⁻ or with the morphology of PPy DBS and run in ClO₄⁻, will eventually have the cyclic voltammetry characteristic of PPyClO₄⁻ while retaining its initial morphology. Therefore the voltammetry of the layers is not solely a product of the morphology of the layer, but is dependant on the anion within the layer.

Where the morphology does appear to be important is where the layer may be so compact as to hinder ion movement.

The size of whichever species is mobile, either cation or anion, has an effect on the electrochemistry of the layer. The voltammetry of layers formed in aqueous TEABr (large cation) and run in NaDBS show a large double-layer charging component characteristic of that of ClO₄⁻ (small anion), which disappears when the DBS⁻ is introduced. This subsequently reappears with the introduction of some small anion, indicating the very important role that the cation or anion has. Finally, it should be worth mentioning that due to some of the results observed here, it appears that the double-layer charging current subsequent to the faradaic peak may be removed by changing the anion. Anion mobility is very important.

From spectroelectrochemical experiments the following conclusions have been drawn;

The optical data obtained when using a layer formed in an aqueous solution of DDS appears to be more reversible irrespective of the solution in which it is reduced, than does the spectra of layers formed from ClO₄⁻ solutions.

From absorbance versus potential curves a fairly large double-layer charging current is observed at high potentials. Here, again the anion in the layer appears to have some effect on the "amount" of this charging current seen.

The curve of dA/dE vs E¹ superimposed on the voltammogram, indicates that there is a large double-layer charging component as the current continues to rise even though there is no further oxidation of electroactive species beyond this point.

The layers formed can be analysed using the Nernst equation to obtain formal potentials and n-values. Unlike some previous workers [14], the Nernst plots obtained were fairly linear. Unusual formal potentials were obtained on

forming layers in one electrolyte and then running it in another.

Finally the bandgap energy was obtained using a relatively simple graphical method, yielding a bandgap energy consistent with that obtained by previous workers [4, 27]. The advantage of this method is that it is so simple. Now that the characterisation of the layers has been studied, the layers were used as a substrate to incorporate platinum particles. This is the subject of the next chapter.

2.6 REFERENCES

- [1] L.F. Warren, J.A. Walker, D.P. Anderson, C.J. Rhodes and L.J. Buckley, J. Electrochem. Soc., Aug. 1984, Vol. 136, no. 8
- [2] C.R. Martin and Zhiahua Cai, J. Electroanal. Chem., (1991), **300**, 35 - 50
- [3] L.S. Curtin, G.C. Komplin and W.J. Pietro, J. Phy. Chem. 1988, **92**, 12 - 13
- [4] D. Blackwood and M. Josowicz, J. Phys. Chem., 1991, **95**, 493 - 502
- [5] J.M. Ko, H.W. Rhee, S.M. Park and C.Y. Kim, J. Electrochem Soc. March 1990, Vol. 137, no. 3
- [6] L.F. Warren and D.P. Anderson, J. Electrochem Soc., 1987, Vol. 134, no. 1 101 - 105
- [7] J.M. Pernaut, R.C.D. Peres, V.F. Juliano and M.A. De Paoli, J. Electroanal. Chem., 1984, **274**, 225 - 233
- [8] W. Breen, PhD Thesis, University of Dublin, 1990.
- [9] R.M. Penner, L.S. Van Dyke, C.R. Martin, J. Phys. Chem., (1988), **92**, 5274
- [10] T. Shimidzu, A. Ohtani, T. Iyoda, K. Honda, J. Electroanal. Chem., 1987, **224**, 123 - 135
- [11] Y. Tezuka, K. Aoki and K. Shinazaki, Synthetic Metals, (1984), **30**, 369 - 379.
- [12] A.O. Patil, A.J. Heeger and F. Wudl, Chem. Rev., 1988, **88**, 183 - 200
- [13] G. Zotti and G. Schiavon, Synthetic Metals, 1989, **30**, 151 - 158
- [14] E.M. Genies and J.M. Pernaut, J. Electroanal. Chem., 1985, **191**, 111 - 126
- [15] A.M. Waller and R.G. Compton, J. Chem. Soc., Faraday Trans., I, 1989, **85**, 977
- [16] K. Marao and K. Suzuki, Bull Chem. Soc. Jpn., 1987, **60**, 2809 - 2816

- [17] J.H. Kaufman, N. Colaneri, J.C. Scott, K.K. Kanazawa and G.B. Street,
Mol Cryst. Liq Cryst., 1985, 118, 171
- [18] G.B. Street, Handbook of conducting polymers, Skotheim, T.A. Ed; Marcel
Dekker, New York, 1986, Vol 1 pp265
- [19] T. Amemiya, K. Hashimoto, A. Fujihima, K. Itoh, Electrochem. Soc., 1991,
Vol. 138, No. 10
- [20] R.M. Penner, C.R. Martin, J. Phys. Chem., 1989, **93**, 984.
- [21] C.E.D. Chidsey, R.W. Murray, Science (Washington D.C.) 1986, 231, 25
- [22] M. Kalaji and L.M. Peter, J. Chem. Soc., Faraday Trans., 1991, **87** (6),
853 - 860
- [23] A.J. Bard and L.R. Faulkner, Electrochemical Methods, Fundamentals and
Applications Wiley, New York, (1980)
- [24] A.F. Diaz, K.K. Kanazawa, G.P. Gardini, J. Chem. Soc., Faraday
Trans., 1991, **87**, 115.
- [25] M.E.G. Lyons, W. Breen, J.F. Cassidy, J. Chem. Soc., Faraday Trans., 1991,
87, 115.
- [26] Yu. V. Pleskov, Yu. Ya. Gurevick, Semiconductor
Photoelectrochemistry; Bartlett, P.N., Ed; (translated from Russian),
Plenum, New York, 1986
- [27] J.L. Bredas, Mol. Cryst., 1985, **118**, 49
- [28] M. E.G. Lyons, C.H. Lyons, D.E. McCormack, J.J. McCabe, W. Breen,
J.F. Cassidy, Anal. Proc. (1991) **28**, 104.

3. PLATINUM-CONTAINING POLYPYRROLE LAYERS FOR THE FORMATION OF SUPEROXIDE ION IN NONAQUEOUS MEDIA.

3.1 INTRODUCTION

3.1.1. Introduction

As mentioned in chapter 1 the aim of this work was to attempt to find an electrochemical method of decomposing highly chlorinated organic wastes. In this work, platinum-containing polypyrrole was used to generate superoxide which is capable of breaking the carbon-chlorine bond. There were a number of reasons for embedding platinum particles in polypyrrole rather than using a platinum electrode. The most obvious reason is that if a reactor or column cell is the ultimate result, then cost is a vital factor. It has also been shown that Pt. particles incorporated into membranes retain their high catalytic activity much longer than does platinised platinum [1,2,3]. For example, Belanger, et al [2], found that by incorporating platinum microparticles into a polypyrrole-glucose oxidase electrode the response of the electrode increased by up to 40%, while Gholamian reported that there is a catalytic effect which occurs specifically because of the polymer-metal interaction [4]. Therefore the increase in activity is not solely due to the increase expected due to the increased surface area of platinum available. The polymer backbone also appears to promote three-dimensional growth of spherical microparticles rather than the two-dimensional growth which has been observed [5].

The Pt. modified PPy electrodes, when constructed, were then to be used to catalyse O_2 reduction to the superoxide ion, in aprotic solvents. Sawyer and co-workers investigated the mechanism of decomposition of various chlorinated organic compounds, including CCl_4 and DDT using electrochemically generated superoxide ion [6]. His work suggests that the superoxide preferentially degrades the compounds of highest chlorine content. Some of the chemistry of the

superoxide ion will be discussed in the next section.

3.1.2. The chemistry of the superoxide ion.

Only a few cases of representative interest will be discussed here. The superoxide ion is very unstable in aqueous solutions, but is sufficiently stable in some non-aqueous solvents to be regarded as a useful reagent. The electrochemical reduction of O_2 to yield $O_2^{\bullet -}$ is well documented in solvents such as pyridine, DMF and DMSO [7].

The superoxide ion can undergo a wide range of reactions including acid-base equilibria, nucleophilic attack and redox reactions. In Sawyers work [6], the $O_2^{\bullet -}$ acts as a nucleophile in substitution reactions with the chlorinated substrates. There have been reports of O_2 reduction being carried out at metalloporphyrin - doped polypyrrole film electrodes in aqueous solution [8], while Kalu and White reported the degradation of polyhalogenated aromatic hydrocarbons using electrochemically generated $O_2^{\bullet -}$ [9]. A problem which can arise when using superoxide as a reagent, is that due to the large number of reactions undergone by superoxide, that there may be a number of competing reactions occurring. This will decrease the amount of $O_2^{\bullet -}$ in solution for chlorinated compound decomposition.

All experiments in this work were carried out in dimethyl sulphoxide (DMSO). The dissolved oxygen concentration in DMSO has been reported as being between 2.1 and 4.0 mM at 25°C [9,10].

3.2 EXPERIMENTAL

3.2.1. Electrodes, cells, instrumentation and chemicals.

A Metrohm, three electrode, single compartment cell was employed for all

electrochemical experiments. Disc electrodes, sealed in Teflon, of surface area 0.071 cm^2 were used for preliminary experiments. Stainless steel (18/8/Cr/Ni) was cut and electrically bonded to copper wire with silver epoxy and encapsulated in a glass tube with Araldite, exposing an electrode area of approximately 0.1 cm^2 . Electrodes were pretreated by polishing on 0.3 micron alumina slurry on felt.

A saturated calomel electrode was used as reference with respect to which all potentials are quoted. A carbon rod was used as an auxiliary electrode.

A Metrohm model 628-10 rotating disc electrode was employed for rotating disc electrode experiments. Cyclic voltammetry was carried out using a Thompson 16 bit sweep generator, model DRG 16, and a Thompson ministat coupled with a J.J. Lloyd chart recorder.

Pyrrole (Aldrich) was distilled under nitrogen and stored in the dark prior to use. Dimethyl sulphoxide (DMSO) was dried over activated molecular sieves prior to use. All other chemicals were used without further purification. The temperature for all experiments was ambient ($20^\circ \pm 4^\circ \text{C}$), unless otherwise stated. All electrolyte concentrations were 0.1 mol dm^{-3} unless otherwise stated.

3.2.2. Polymer Layer Formation

Polypyrrole films were prepared by placing a freshly prepared solution of aqueous 0.1 M pyrrole and 0.1 M KCl in a cell. The solution was then degassed with oxygen-free nitrogen for approximately 5 minutes prior the experiment. A blanket of nitrogen was maintained over the solution during the experiment. The potential was stepped from 0.4 V to 0.8 V . The potential was maintained at 0.8 V for varying periods of time, ranging from 2 minutes to 10 minutes, to form PPyCl. The electrode was then removed from solution and rinsed with deionised water. The PPyCl film was then reduced in 0.1 M KCl by scanning the potential from 0.4 V to -0.5 V . The potential was maintained at -0.5 V for 20 minutes. The electrode was then transferred to a 10 mM solution of potassium chloroplatinate in 0.1 M

KCl. The electrode was then held at a potential of 0.5V for 30 minutes in order to oxidize the layer and absorb the Pt(IV). The electrode was rinsed, and the potential scanned from 0.5V to -0.5V in 0.1M KCl solution. The final reduction was done at a very slow scan rate of 2mV/s in order to ensure full reduction of the Pt (IV) to Pt.

Both the time of deposition of polypyrrole and the time of deposition of platinum were varied in an attempt to optimize the layers. Finally the electrodes were characterized using cyclic voltammetry and rotating disc electrode experiments in a solution of DMSO containing 0.1M LiClO₄ as background electrolyte.

3.3 RESULTS AND DISCUSSION

3.3.1 Current-Time analysis of PPy/Pt layers

Initially polypyrrole deposition experiments were carried out on glassy carbon or platinum disc electrodes. The current-time transients for the formation of polypyrrole/platinum layers on a glassy carbon electrode are shown in figure 3.1(a) to 3.1(d). The amount of charge passed in each stage was estimated. The shape of the transient obtained for the growth of polypyrrole is similar to that observed previously [10]. The transient shown in figure 3.1(a) exhibits the following attributes as first analysed by Hillman [11]. The current-time transient begins by a rapid current increase followed by a fall to a minimum. The current then increases to either a peak or plateau. The initial rapid increase in current is thought not to be totally double-layer charging in nature. Hillman attributed the minimum in the current to be due to the transition between monolayer coverages and subsequent multi-layer coverages [11]. This implies that this time is characteristic of how long it takes the electrode to become covered in a monolayer of polypyrrole. The region where the current rises after the minimum represents the current due to a second nucleation and growth process on the original

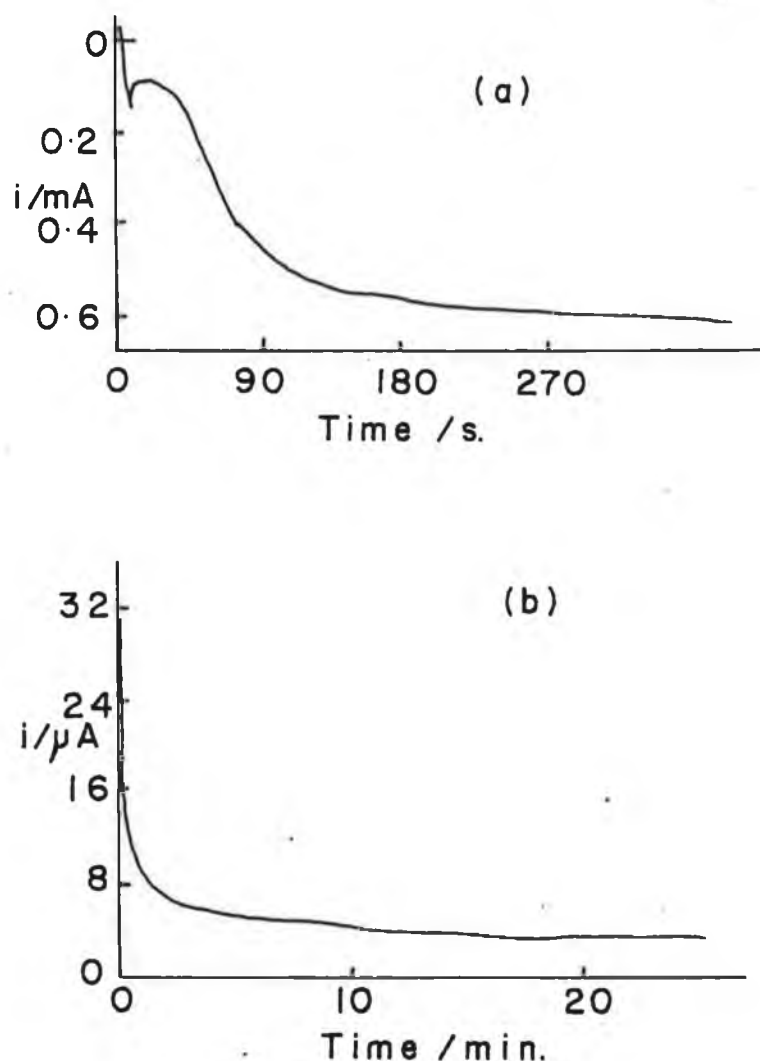


Figure 3.1

- Current-Time transients for the formation of PPy/Pt layers at a glassy carbon electrode.
- (a) Transient for oxidation of pyrrole in aqueous 0.1M KCl. Potential range was 0.4 to 0.8V
 - (b) Reduction of layer formed at (a) in 0.1 M KCl. Potential range 0.4 to -0.5 V. Potential maintained at - 0.5 for 20 minutes.
 - (c) Transient obtained when layer from (b) was held at 0.5 V for 30 minutes in a solution of 10mM potassium chloroplatinate in 0.1M KCl.
 - (d) Transient obtained when the layer from (c) was reduced from 0.05V to -0.5V at 2mVs^{-1} in 0.1 MKCl to ensure full reduction of Pt (IV) to Pt.

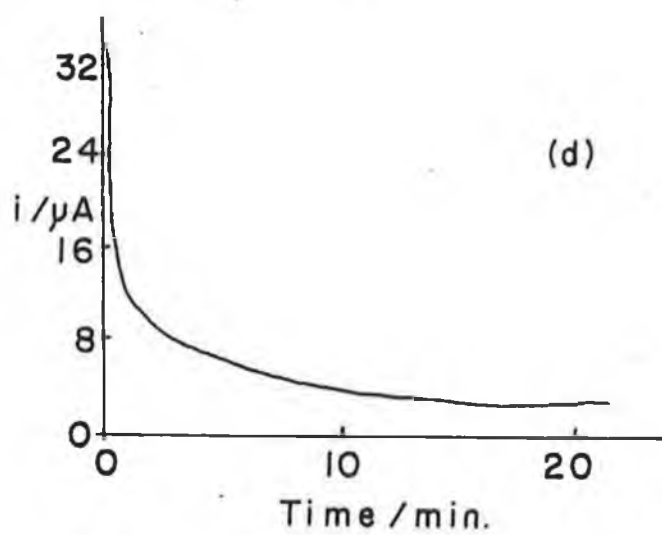
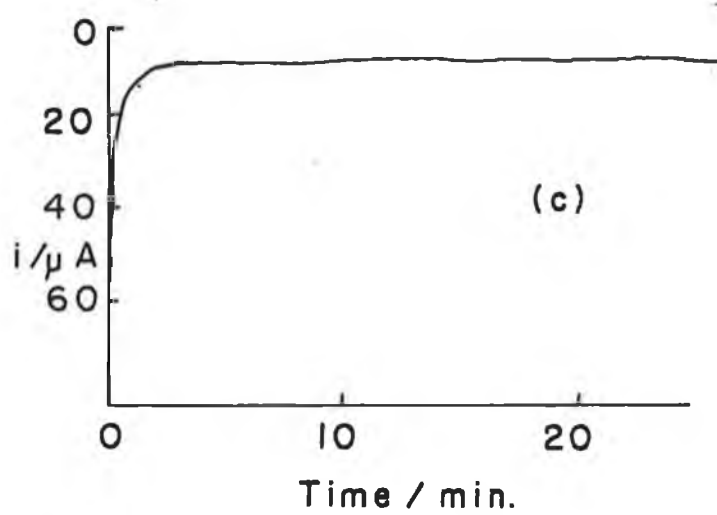


Figure 3.1 (continued)

monolayer[10]. All of the monolayer may not have necessarily formed before this second process begins [11]. At potentials of less than 0.9V the polymer growth has been found to be a two-dimensional growth with successive nucleation [11]. As mentioned in the experimental section the layer was formed (figure 3.1 (a)), reduced in Cl^- (figure 3.1.(b)), to expel Cl^- . The layer was then reoxidized in a solution of PtCl_6^{2-} (figure 3.1.(c)), and finally reduced to reduce the Pt. particles, (figure 3.1(d)). Figure 3.1 (d) represents the charge required to reduce the layer and also to reduce the Pt(IV) incorporated into the layer. The difference in charge between figure 3.1(a) and 3.(d), approximately 480mC, represents a Pt. loading of 1.75×10^{-8} moles cm^{-2} .

It can be seen that the processes in figures 3.1 (b,c,d) do not readily reach completion and that there is a steady state current even over periods as long as 20 minutes. This may reflect a reticulated structure within which charge travels slowly and in which there is only a gradual passage of current over long time periods. It is expected that the polypyrrole is reduced to passivating PPy^0 , where it is expected that the polypyrrole will become inactive and act solely as a supporting matrix for the platinum particles. It is open to question how the charge passes unless the Pt. particles are in contact or the layer is flexible. In the fourth step it is necessary for all the platinum to be in the layer as Pt^0 . After these initial experiments to test the viability of formation of such composite PPy/Pt . layers, their effectiveness for superoxide ion formation was tested using cyclic voltammetry.

3.3.2 Cyclic Voltammetry of PPy/Pt modified electrodes.

Early work carried out on the reduction of oxygen in nonaqueous media was carried out at solid platinum electrodes [6]. This work involved putting the composite layer onto various substrate electrodes. This was done to see if the layers could be deposited, and if O_2 reduction could be carried out using the incorporated platinum particles.

Figure 3.2 shows a cyclic voltammogram of oxygen reduction at a bare glassy carbon electrode in 0.1 M LiClO₄ in DMSO. The voltammogram shows quasi reversible behaviour with a peak to peak separation of around 740 mV at a scan rate of 100 mVs⁻¹. When a polypyrrole layer was deposited it appeared that O₂ reduction occurred at the underlying glassy carbon as well as at the platinum particles.

Figure 3.3 shows the cyclic voltammogram for oxygen reduction at bare platinum. The dotted line indicates the behaviour observed when the solution is degassed with nitrogen. The reoxidation peak in the case of platinum has more thin layer character than that of the corresponding peak for the carbon electrode. There is no flattening out of the voltammetry between the limits -0.6V to -0.3V as is observed in the case of glassy carbon, as can be seen in figure 3.2.

The voltammetry of oxygen reduction at a PPy/Pt layer is shown in Figure 3.4(a). The behaviour is similar to that observed at a bare platinum electrode. Figure 3.4 (b) shows the voltammetry observed when 1.00 cm³ of CCl₄ is added to the cell, of volume 50 cm³. The behaviour is similar to that seen by Sawyer and Roberts[6]. The cathodic peak is seen to be enhanced, indicating an intermediate step which generates O₂^{•-} while the diminished, in this case non-existent, oxidation peak, indicates that the O₂^{•-} generated, is removed by reaction with CCl₄. The complete reaction is



Even partial decomposition of the CCl₄ will regenerate oxygen which

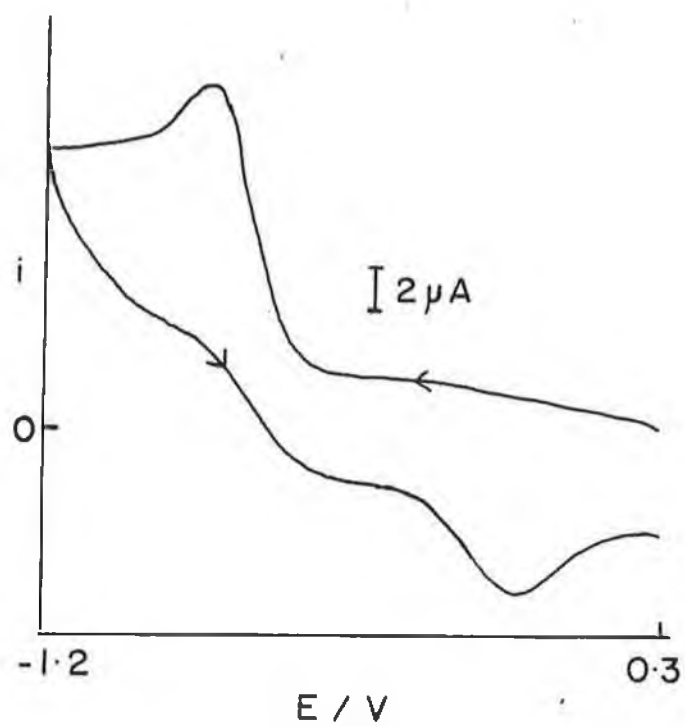


Figure 3.2 Cyclic voltammogram of O_2 reduction at a bare glassy carbon electrode in 0.1 M LiClO_4 in DMSO. $50 \text{ mVs}^{-1} = v$

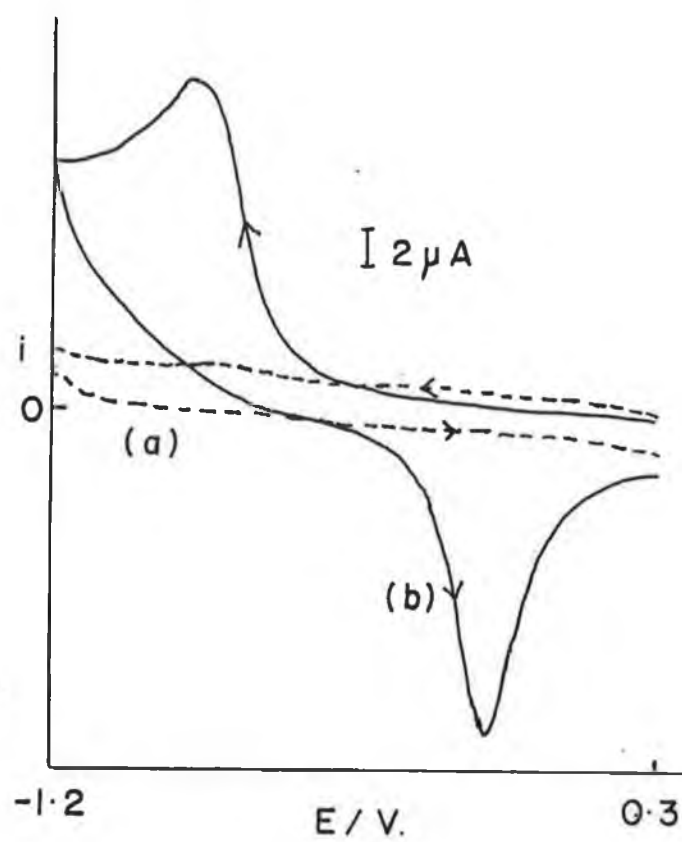


Figure 3.3 Cyclic voltammogram of O₂ reduction at a bare platinum electrode.
 (a) degassed with N₂
 (b) equilibrated with air. 50mVs⁻¹ = ν

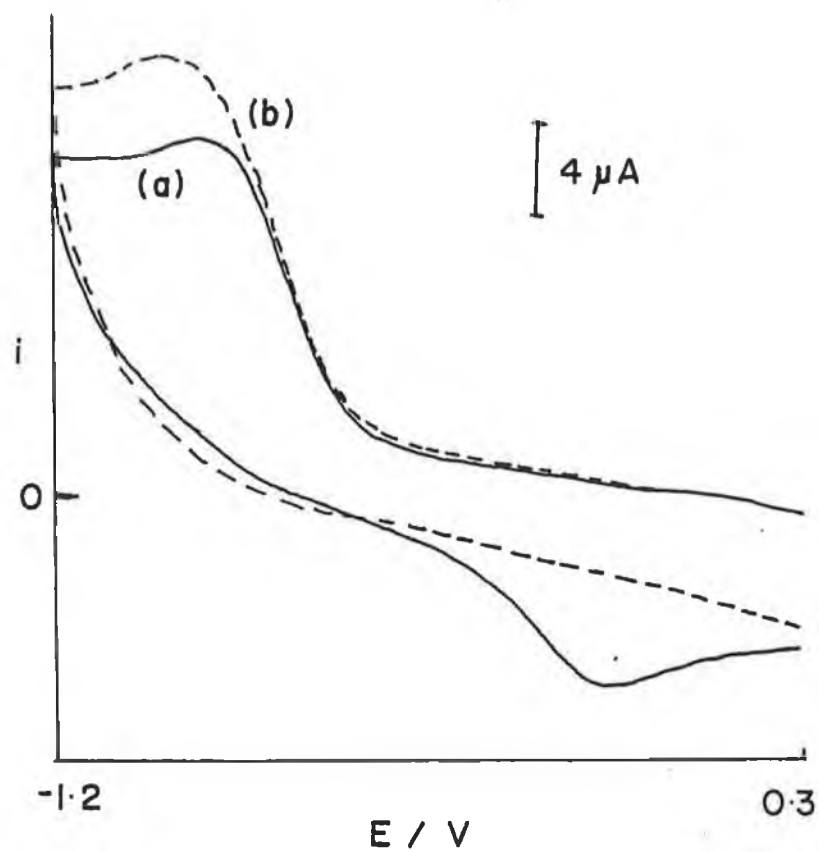


Figure 3.4 Voltammetry of O_2 reduction.
 (a) at a glassy carbon electrode with a PPy/Pt. layer.
 $50 \text{ mV/s} = v$
 (b) with addition of CCl_4 .

further reduced at the electrode.

A scan rate study of the peak cathodic current for O_2 reduction at each of the electrodes, bare glassy carbon, platinum, and a PPy/Pt. layer on a platinum electrode were carried out. Graphs of i_p versus $v^{1/2}$ are shown in figure 3.5. These are linear indicating that the O_2 reduction is diffusion controlled, occurring in the solution in each case. This linear behaviour of the PPy/Pt electrode indicates that the reduction is occurring in a region where the Pt. electrodes act as an array.

3.3.3 Rotating disc electrode experiment.

It was intended to use the rotating disc electrode experiment results to obtain some idea of diffusion coefficients and to obtain some kinetic parameters for O_2 reduction.

The variation in current at a rotating disc electrode with the square root of rotation rate is expected to be curved and tend toward the limit $i = i_k$ as $\omega \rightarrow \infty$. The following equation is expected to be linear [12].

$$\frac{1}{i} = \frac{1}{i_k} + \frac{1}{i_{lc}} = \frac{1}{i_k} + \frac{1}{0.629 n F A C_{O_2}^* D^{2/3} v^{1/6} \omega^{1/2}} \quad 3.3$$

where $1/i_{lc}$ is the limiting cathodic current in the region of mass transport control and the other symbols have their usual meaning. Therefore a plot of $1/i$ versus $1/\omega^{1/2}$ should be linear with an intercept of $1/i_k$. If i_k is found for different values of potential, then kinetic parameters can be obtained by using the following expression [12]

$$\ln i_k = \ln (n F A C_{O_2}^* k_0) - \alpha n F (E - E^0) \quad 3.4$$

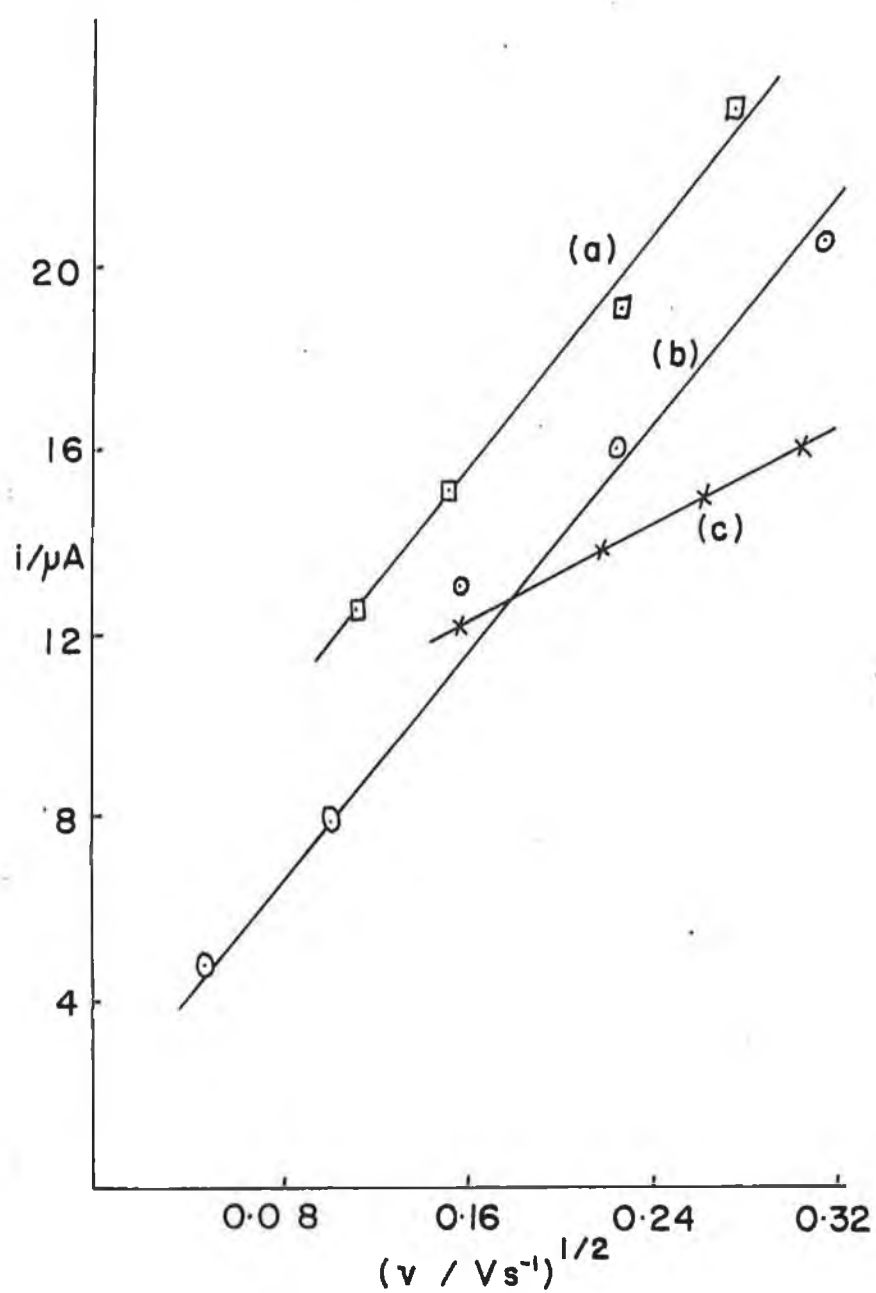


Figure 3.5 Scan rate study of O_2 reduction at
 (a) bare glassy carbon
 (b) bare platinum and
 (c) PPy/Pt. layer on glassy carbon electrodes.

This expression also allows calculation of α , the transfer coefficient.

If figure 3.6 is examined a number of conclusions can be drawn. The shape of the voltammogram obtained when O_2 is reduced at bare platinum shows that at fast rates of reaction, ie. fast rotation rates, there is fouling or poisoning of the electrode surface as the shape of the voltammogram is not like that normally obtained in this type of experiment. The cyclic voltammetry was fairly reversible, so perhaps the fouling is due to some side reaction of the $O_2^{\bullet-}$ with the DMSO. If the potential is allowed to return to the initial value, hysteresis, indicative of fouling, is observed, as can be seen in figure 3.6 (a) for 2000 RPM. Figure 3.6 (b) is a similar reduction carried out at a glassy carbon electrode with the composite PPy/Pt. Layer. Here the voltammetry appears to be kinetically hindered. As the incorporated Pt. particles behave as a sort of array of microelectrodes, there would be expected to be less of a difference between currents observed at various rotation rates. This would be due to the increased flux of material due to the edge effect of an array of microelectrodes [13]. This can be seen in figure 3.6 (b). The behaviour of the superoxide ion does not follow the behaviour predicted by equation 3.3 and 3.4. The graphs of $1/i$ versus $1/\omega^{1/2}$ were not very linear in character. Hence "intercepts" obtained from these graphs would contain a significant error so it was thought that any kinetic data obtained would be invalid.

3.3.4. PPy/Pt. modified stainless steel electrodes.

The final experimental stage was to examine the voltammetry of O_2 reduction at stainless steel electrodes coated with the PPy/Pt. layer Figure 3.7 shows a cyclic voltammogram for the reduction of oxygen at a platinum-containing polypyrrole coating on stainless steel. It can be seen here that the reduction appears to reach a steady state value unlike the behaviour observed at the bare electrodes. This behaviour is indicative of an array of microelectrodes [14,15]. Figure 3.7 (b) shows that there is some residual current, although at these potentials the

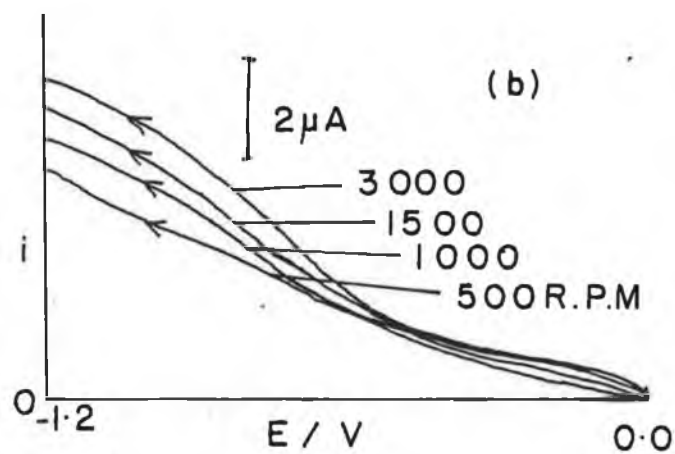
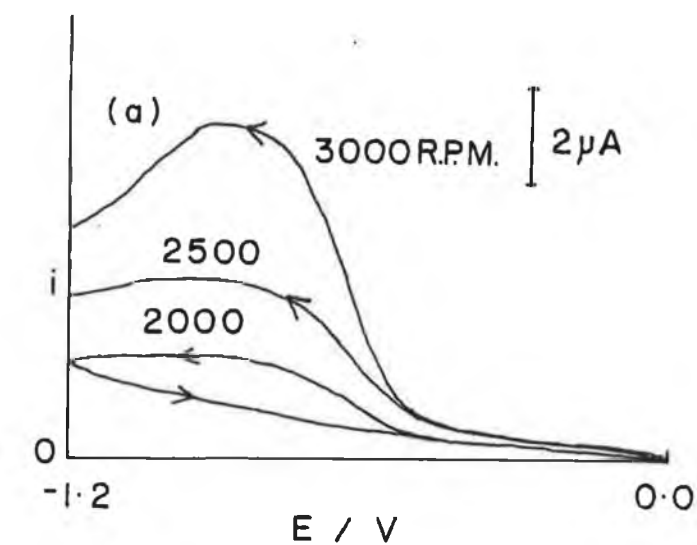


Figure 3.6 Rotating disk study of oxygen reduction in DMSO (0.1 M $LiClO_4$) at (a) a platinum electrode and (b) a PPy/Pt coated glassy carbon electrode.

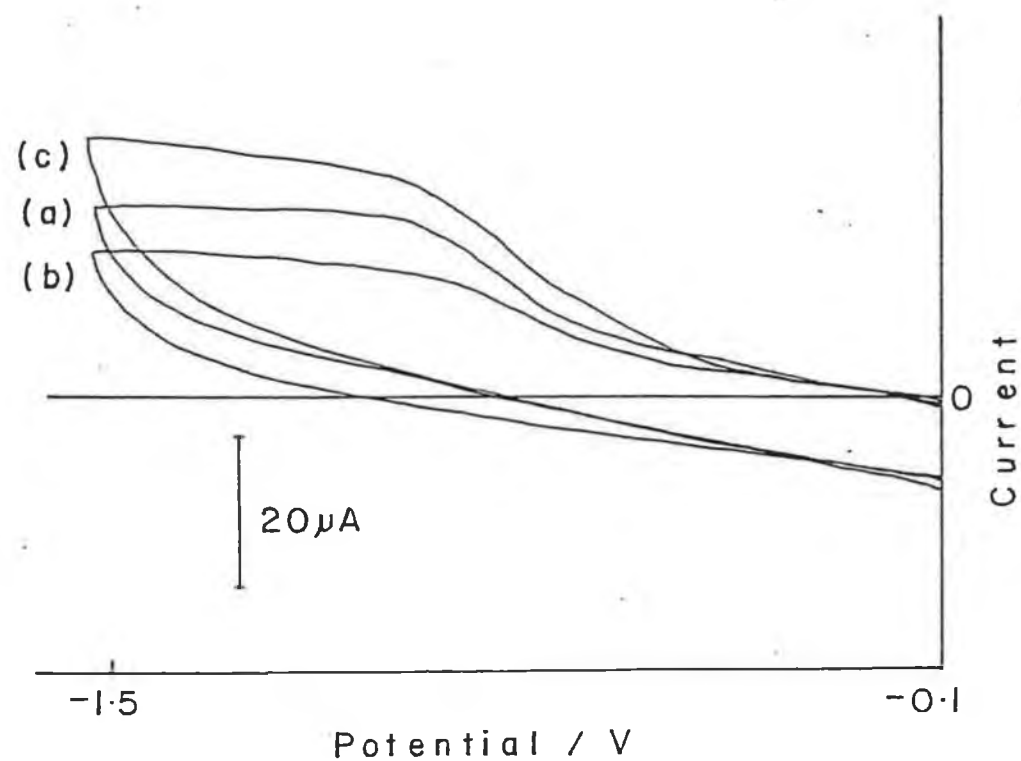


Figure 3.7 Cyclic voltammogram of a PPy/Pt coated stainless steel electrode in DMSO (0.1M LiClO₄), scan rate 50 mVs⁻¹, Pt deposition time = 20 min, PP dep time = 4 min., (a) a solution equilibrated with air, (b) solution degassed with N₂ and (c) as solution (a) but with CCl₄ added to a concentration of 42 mMdm⁻³.

polypyrrole should be in reduced form. This may be due to incomplete removal of oxygen. Figure 3.8 shows the limiting current as a function of polypyrrole layer thickness for a given amount of platinum deposited. It can be seen here that the most efficient oxygen reduction occurs at thinner layer of polypyrrole. This corresponds to a high density of platinum sites, unlike in thicker polypyrrole layers where the platinum is more dispersed, which may cause problems with contact with the substrate electrode, since then the electrical contact is through the distribution of platinum particles suspended in the layer [16]. Wang [17], suggested that as the electropolymerised layers become thicker the permeability decreases. This would imply that a two-dimensional coating is more feasible than a three-dimensional coating is more feasible than a three-dimensional one.

As can be seen from figure 3.9, as the loading of Pt. increases, for a given thickness of polypyrrole, the limiting oxygen reduction current also marginally increases. The effect of varying platinum deposition time is not as great as that of the polypyrrole. So, optimum layers are thin PPy layers with a high Pt. loading. In this work Pt. loading varied from $1.75 \times 10^{-7} \text{ mol cm}^{-2}$ to $3.0 \times 10^{-7} \text{ mol cm}^{-2}$.

As was done with the composite layer on the bare platinum electrode, the decomposition properties of the superoxide were studied using CCl_4 as a model compound. As was seen previously the limiting current increases corresponding to the catalytic decomposition of the CCl_4 (figure 3.7 (c)). The increase in current is due to the catalytic regeneration of oxygen where the reaction follows equations 3.1 and 3.2. The CO_4^{2-} reacts with DMSO to form dimethylsulphone and CO_3^{2-} which was determined by titration with HCl [6]. Assuming the oxygen concentration to be approximately 4mM [6], the CCl_4 is destroyed at a rate of $10^{-9} \text{ mol min}^{-1}$ for an electrode area of 0.1 cm^2 . From the conditions achieved here, taking residual current into account, a current density of 0.1 A cm^{-2} can be obtained for O_2 reduction which compares favourably with a peak current at a bare platinum electrode [6]. The effective area is greater due to the edge effect of an array of microelectrodes [13,18].

A problem that was found to exist in all experiments involving the superoxide

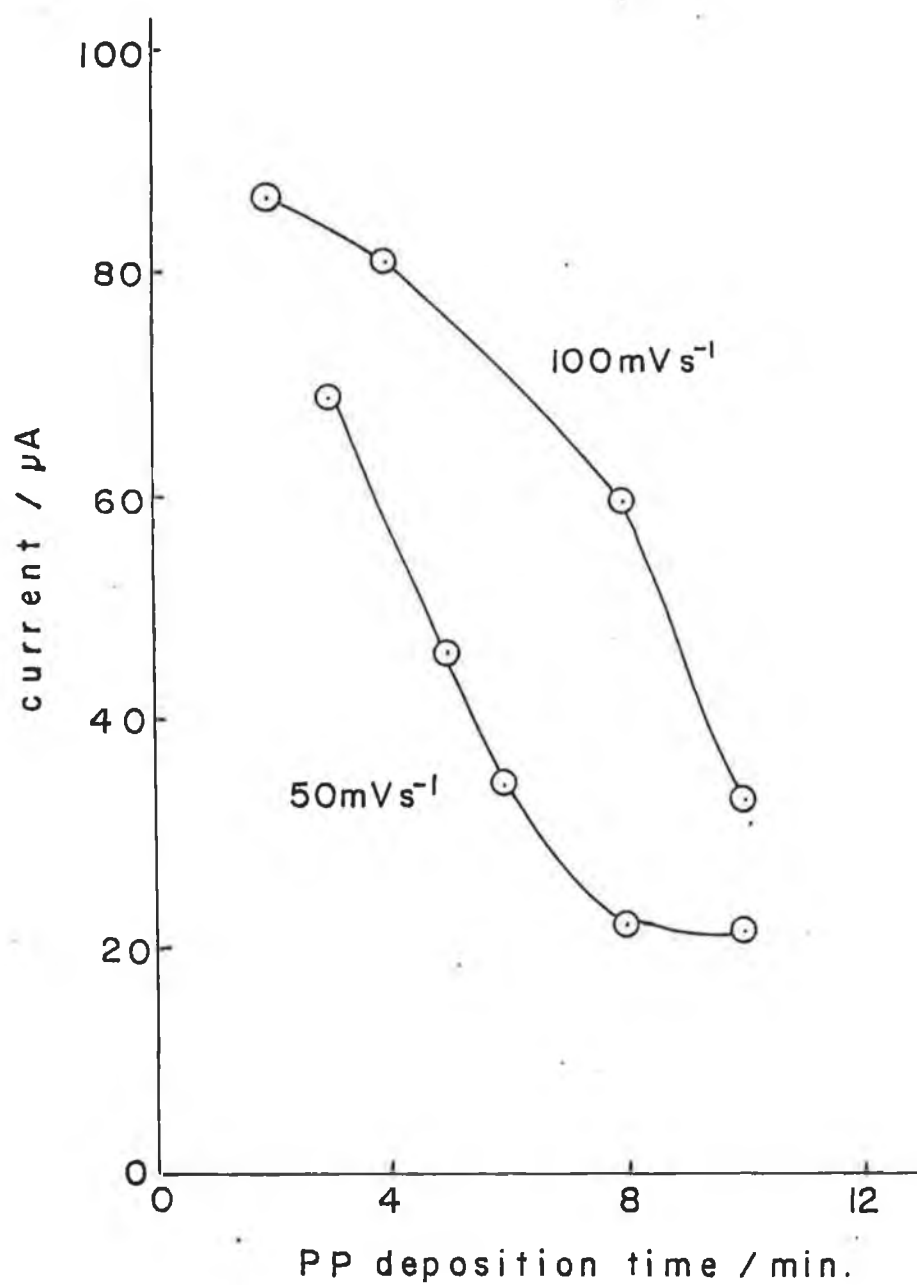


Figure 3.8 Variation of limiting current for oxygen reduction with PPy deposition time with a constant amount of Pt. Same conditions at Figure 3.7.

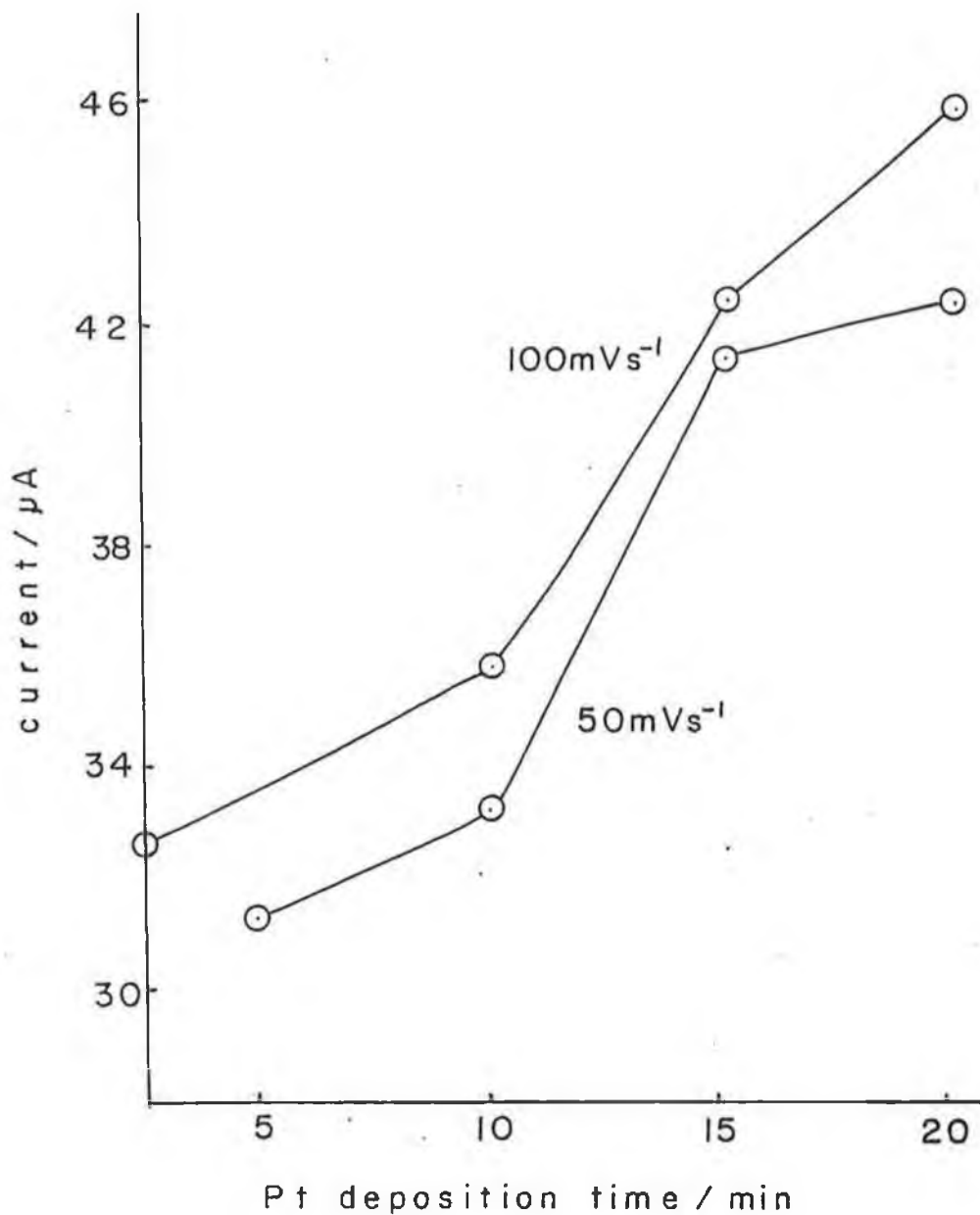
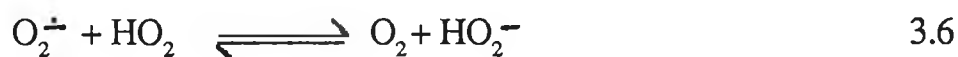


Figure 3.9 Variation of limiting current for oxygen reduction as a function of platinum loading with a constant amount of PPy, deposited for 4 min. Conditions as in Figure 3.7.

ion was the presence of water, even in miniscule quantities. Previous workers have found that the superoxide reacts preferentially with water rather than the chlorinated organics [19,20]. The following reaction scheme indicates the degree to which reaction with water is more preferential than that with, for example CCl_4 . For the reaction 3.2, k_2 is of the order of $1300 \text{ M}^{-1} \text{ s}^{-1}$. When water is present the following reactions occur.



The rate constant for reaction 3.6 is of the order of $1.0 \times 10^8 \text{ M}^{-1} \text{ s}^{-1}$ [20].. This reaction would lead to decomposition of the $\text{O}_2^{\cdot-}$ without any utilization of the product for CCl_4 destruction, although Sawyer et al [6], believed that the contribution of these reactions to the total reaction rate with CCl_4 would be in the order of 5%. Initial experiments carried out with “undried” DMSO, in this work, would suggest that there is a significant effect on the production of $\text{O}_2^{\cdot-}$ due to reticent water in the solvent. This would generally mean that in the case of industrial waste some drying step would be required prior to decomposition.

3.4 CONCLUSIONS

The method used in this work to deposit polypyrrole films on various substrate electrodes and then to incorporate platinum microparticles into the polymer layer was successful, in that the platinum could be used to catalyse O_2 reduction. Once formed, these layers have the advantage of needing very small amounts of platinum to have an active electrode, as compared to bulk platinum CCl_4 decomposition was successfully carried out at these modified electrodes. The

voltammetry of O_2 reduction at these PPy/Pt. electrodes was diffusion controlled and the Pt. behaved as a microelectrode. The high reactivity of $O_2^{\bullet -}$ with water and trace contaminants was a constant problem in DMSO. The optimum nature of the layers are thin polypyrrole layers with a high platinum loading.

The superoxide has its disadvantages for use as a reagent; It is highly reactive, reacting with even trace amounts of water preferentially to reaction with CCl_4 . This would mean that superoxide would not be viable for industrial waste samples as their composition would be so heterogeneous. There is also evidence that perhaps the superoxide may react with the DMSO if the reaction rate is increased. Again this is unwanted. Finally the concentration of O_2 in DMSO is too small to allow effective use of superoxide ion to decompose chlorinated organic molecules. The concentration of the mediating catalyst is therefore difficult to control, unless pure O_2 is bubbled through the solution. Another disadvantage of the system used in this work is that the polypyrrole does not fully passivate the stainless steel and some pitting was observed. With this in mind it was decided to change direction and attempt polychlorinated molecule decomposition using a catalyst incorporated in a surfactant micelle in aqueous solutions. This is the subject of the next chapter.

3.5 REFERENCES

- [1] A. Kowal, K. Doblhofer, S. Krause and G. Weinberg, *Journal of Applied Electrochemistry*, (1987) **17**, 1246 - 1253
- [2] D. Belanger, E. Brassard and G. Fortier, *Analytica Chimica. Acta*, (1990), **228**, 311 - 315
- [3] H. Laborde, J.M. Leger, C. Lamy, F. Gamier and A. Yasser, *Journal of Applied Electrochemistry*, (1990), **20**
- [4] M. Gholamian, A.W. Contractor, *J. Electroanal. Chem.*, (1990), **289**, 69-83
- [5] D.E. Weisshaar and T. Kuwana, *J. Electroanal. Chem.*, (1984), **163**, 395 - 399
- [6] J.L. Roberts and D.T. Sawyer, *J. Am. Chem. Soc.* (1951), **103**, 712
- [7] D.T. Schiffrin, *The Electrochemistry of Oxygen, Specialist Periodical Reports*, (1983), Vol. 8., *Electrochem.*, Royal Soc. Chem., London, pp 161 - 165
- [8] O. Ikeda, K. Okabayashi, N. Yoshida, H. Tamura, *J. Electroanal. Chem.* 1985, **191**, 157 - 174
- [9] E.E. Kalu and R.E. White, *J. Electrochem. Soc.*, December 1991, Vol. 138, No. 12
- [10] W. Breen, PhD Thesis, University of Dublin, 1991.
- [11] A.R. Hillman, E.F. Mallen, *J. Electroanal. Chem.* (1987), **220**, 351
- [12] A.J. Bard and L.R. Faulkner, *Electrochemical Methods, Fundamentals and Applications*, Wiley, New York, (1980), pp 290 - 300
- [13] J.F. Cassidy, J. Ghoroghchian, F. Sarfarasi, S. Pons, *Can., J. Chem.*, (1985), **63**, 3577
- [14] W.H. Kao and T. Kuwana, *J. Am. Chem. Soc.*, (1984) **106**, 473

- [15] K. Aoki and J. Osteryoung, J. Electroanal. Chem. 1980, **125**, 315
- [16] S. Holdcroft and B.L. Funt, J. Electroanal. Chem., 1988, **240**, 89
- [17] J. Wang, S.P. Chem., M.S. Lin, J. Electroanal. Chem, (1989), **273**, 231
- [18] M.O. Iwunze, J.F. Rusling, *ibid*, (1989), **266**,197
- [19] D.T. Sawyer and M.J. Gabian, Tetrahedron, (1979), **35**, 1471.
- [20] K. Yamaguchi, T.S. Calderwood and D.T. Sawyer, Inorg. Chem., 1986, **25** , 1289 - 1290

4. DECOMPOSITION OF CHLORINATED ORGANIC MOLECULES IN A HOMOGENOUS MEDIATION SYSTEM

4.1 INTRODUCTION

Electrocatalysis using micelles enable redox reactions of non-polar substrates to be carried in aqueous media. The use of surfactants to solubilize non-polar organic compounds in water for electrochemical measurement was first described by Proske in 1952 [1]. Micelles are dynamic surfactant aggregates able to combine with soluble molecules via hydrophobic and coulombic interactions. The hydrocarbon tails of the surfactant were found to be directed towards an organic core, while the charged tails pointed out towards the polar solvent [2].

Because of the compartmentalization of reactants in the micellar layer, the reactions observed have featured considerable kinetic enhancement compared to the same reaction carried out in the bulk organic solvent [3 -6]. Rusling has reported a range of examples of electrochemical catalysis in aqueous micelles and water-in-oil microemulsions [6]. A microemulsion is a three-component solution that contains water, water immiscible hydrocarbon and a surfactant. An alcohol is frequently added as a co-surfactant. Microemulsions are thermodynamically stable and macroscopically homogenous [7]. The use of microemulsions as media for the voltammetric reduction of Ru(III) hexaamine, ferrocyanide, ferrocene and several polycyclic aromatic hydrocarbons has been studied by Rusling [7].

A typical reaction observed when the catalyst is incorporated in a micellar phase, features diffusion to an electrode surface of a micelle-bound species, it's acceptance of an electron, and subsequent transfer of the electron to a micelle-bound substrate [8]. Surfactant assemblies have also been used to suppress

unwanted electrode side reactions, and to form catalytic films on electrodes [10,11]. Previous reports have said that ion radicals produced at electrodes could be stabilized by aqueous micelles. MacIntire, Blount and co-workers [12 - 14] found that micelles of sodium dodecylsulphate (SDS), stabilized both 10 - methylphenolthiazine cation radical and nitrobenzene anion radical. Saveant et al [15], claimed stabilization of phthalonitrile anion by micelles of cetyltrimethylammonium bromide (CTAB). The stability of organic ion radicals in micelles depends on interactions of the ion with the surface charge and with hydrophobic sites of the micelle [4]. Electrochemically generated anion radicals, if sufficiently stable in the hydrophobic region of a micelle, should be able to transfer an electron rapidly to a suitable organic substrate resident in the same micelle. Such a reaction regenerates the parent of the anion radical to complete the catalytic cycle.

Rusling and co-workers have carried out much work in electrocatalysis, including work utilizing surfactant systems [3 - 9]. Of particular interest to this work was the catalysed reduction of allyl halides to 1,5 hexadiene at glassy carbon electrodes [4,5]. Rusling catalysed this reaction using this (2 - 2' bipyridyl) cobalt (ii) in 0.1M SDS and 0.1M CTAB in aqueous solutions.

This work proposes the use of a similar catalyst system, in both CTAB and didodecyldimethylammonium bromide (DDAB), with the purpose of developing an electrolysis system for the decomposition of chlorinated wastes. DDAB was used as a surfactant as it had previously been used as a medium for the decomposition of Aroclors, which are commercial mixtures of PCB's [16]. In that work the unique properties of the DDAB solutions, which were reported to be more like a suspension, were thought to contribute to the better decomposition observed when DDAB was used rather than CTAB. Preliminary work involved the study of the catalyst reduction in varying surfactant concentrations.

4.2 EXPERIMENTAL

4.2.1. Instrumentation, cells, electrodes and chemicals

A Metrohm, 3 electrode, single compartment cell was employed for all electrochemical experiments. A glassy carbon disc of surface area 0.07cm^2 , sealed in Teflon was employed as a working electrode. A carbon rod was used as an auxiliary electrode, while all potentials are quoted with respect to the saturated calomel electrode in aqueous saturated KCl. The working electrode was pretreated by polishing with $0.3\mu\text{m}$ alumina slurry on felt, prior to each experiment.

Potential control and current measurement was performed using a H.B. Thompson potentiostat linked to a J.J. Lloyd PL3 X-Y recorder.

All chemicals employed were reagent grade and used without further purification. Water was distilled and deionised.

4.2.2. Catalyst incorporation in surfactant micelles

The catalyst employed in this work was tris (2, 2'-bipyridyl) cobalt (II). The surfactants used were cetyltrimethylammonium bromide, (CTAB) and didodecyldimethylammonium bromide (DDAB). For reasons that will be explained later it was necessary that the ratio of bipyridine to cobalt was maintained at 3:1 in all solutions. Typically this meant 9mM bipyridine and 3 mM CoCl_2 were used. To make up the surfactant/catalyst solutions the following procedure was followed;

In the case of CTAB solutions, sufficient weights of CTAB, CoCl_2 and bipyridine were dissolved by heating the reagents to between 35°C and 40°C in 0.1 M KCl. When made up to the mark, the solutions were left to reach equilibrium for a number of days. If necessary the solutions were placed in an ultrasonic bath prior to experiment. All electrochemistry experiments were carried out approximately

35°C.

In the case of DDAB solutions, a similar procedure was followed, but in this case the solutions were heated to 50°C to dissolve the chemicals while all electrochemical experiments were carried out at a similar temperature.

4.2.3 Bulk electrolysis experiments

Solutions of CoCl_2 (3mM), bipyridine (9mM), KCl (0.05M), KBr (0.05M) and the appropriate surfactant, CTAB or DDAB, were made up in deionised water. 25cm³ of the solution was placed in the working electrode compartment of figure 4.1. The working electrode consisted of a glassy carbon plate (geometric area approximately 12 cm²). The reference electrode was a saturated calomel electrode and the auxiliary electrode was a glassy carbon rod. A solution of KCl (0.02M) and KBr (0.02M) in Na_2SO_4 (0.05M) was placed in the auxiliary compartment of the cell. The cell was connected up to an EDT potentiostat, model ECP 100, and a potential of -1.8V was applied to the working electrode. The solution in the working compartment was stirred and degassed with N_2 .

The solution changed colour from orange to pink during the electrolysis indicating a change in oxidation state of the cobalt. CCl_4 (1ml), was added to the cell (whose volume was 25 ml) and the electrolysis was carried out for different periods of time. A sample of the solution (10cm³) was taken and after dilution was titrated with 0.05M AgNO_3 with potentiometric detection. This consisted of a silver flag electrode linked to a saturated calomel electrode and its potential was measured as a function of Ag^+ added.

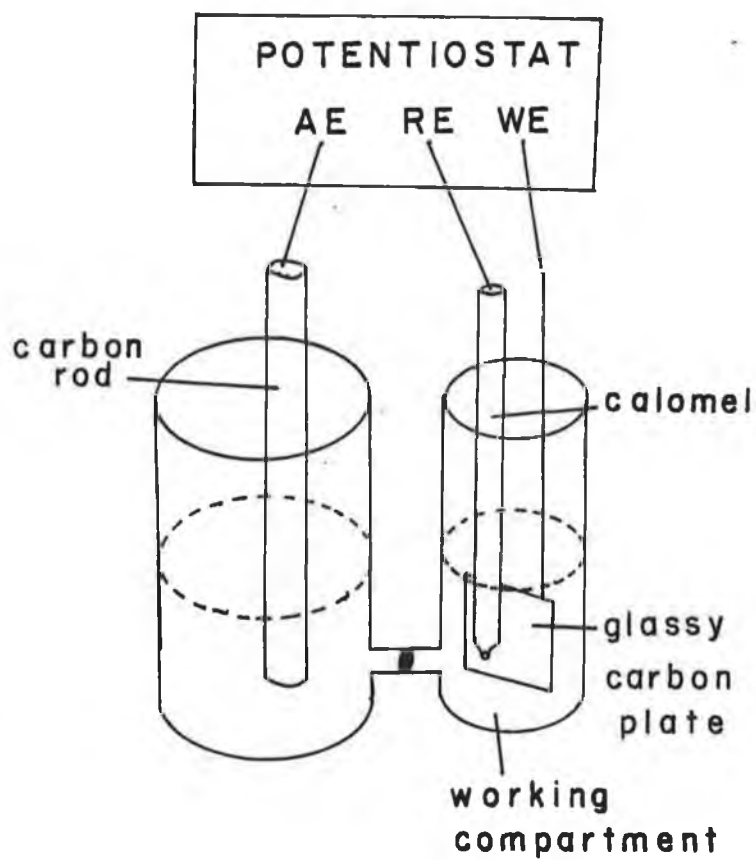


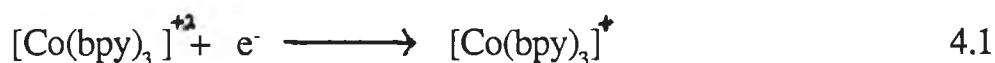
Figure 4.1 Diagram of bulk Electrolysis cell. The working electrode compartment was also degassed with N_2 which is not shown on the diagram.

4.3 RESULTS AND DISCUSSION

4.3.1. Cyclic voltammetry experiments

Initially cyclic voltammetry was carried out in solutions containing $[\text{Co}(\text{bpy})_3]^{2+}$ catalyst (3mM) only, in 0.1M KCl. A cyclic voltammogram of the cobalt reduction is shown in figure 4.2. As can be seen from figure 4.2 there is no well defined first peak for the initial cobalt reduction from Co(III) to Co(I) . The second reduction peak shows thin-layer characteristics and is indicative of the Co(I) to Co(-I) reduction [5]. The reoxidation peaks are characteristically thin-layer, indicative of species adsorbed at the electrode surface. The voltammetry can be seen to be fairly irreproducible since as many as four small peaks were observed on reduction at slower scan rates. It is not clear whether the reduction occurs on the cobalt centre or on the bipyridal ligands, However in this discussion, Co(-I) is assumed.

Figure 4.3 shows that by the addition of a small quantity of CTAB (0.01M), quite similar behaviour is observed, although a better defined first reduction peak is observed. On increasing the CTAB concentration to 0.1M, as shown in figure 4.4, better electrochemical behaviour is observed. The first reduction is fairly reversible and corresponds to [5].



The second reduction peak is approximately twice the height of the first peak and is the two electron reduction of the Co(I) species corresponding to



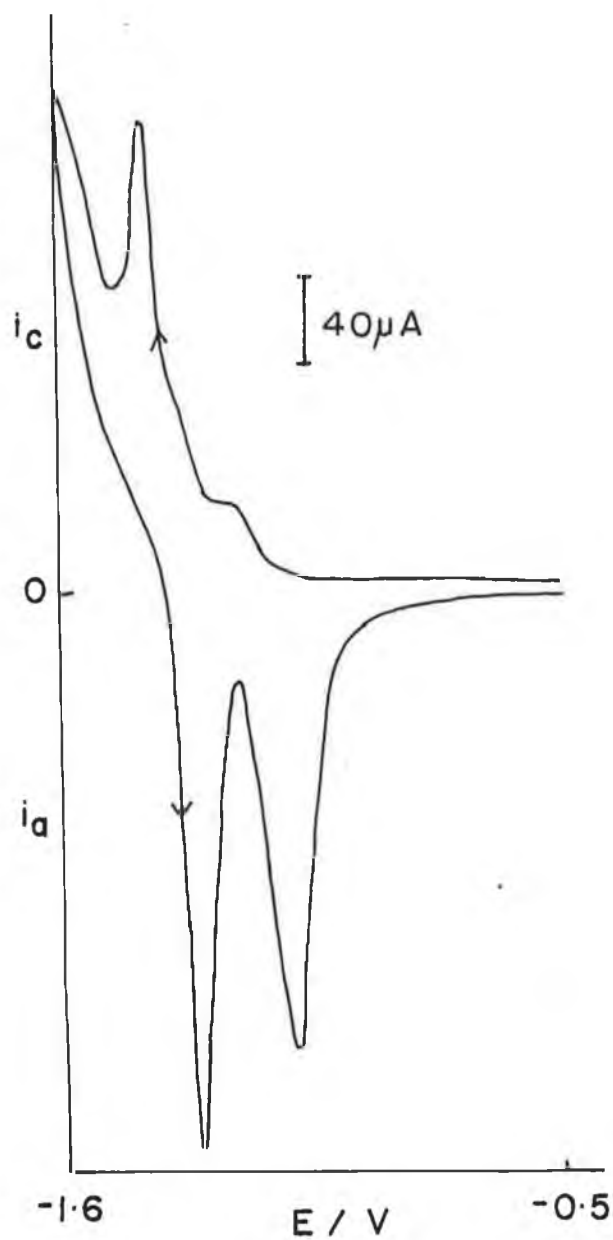


Figure 4.2. Voltammogram of a solution of 3 mM Co^{2+} , 9mM bpy in 0.1 M KCl at a bare glassy carbon electrode. scan rate = 100 mVs^{-1} .

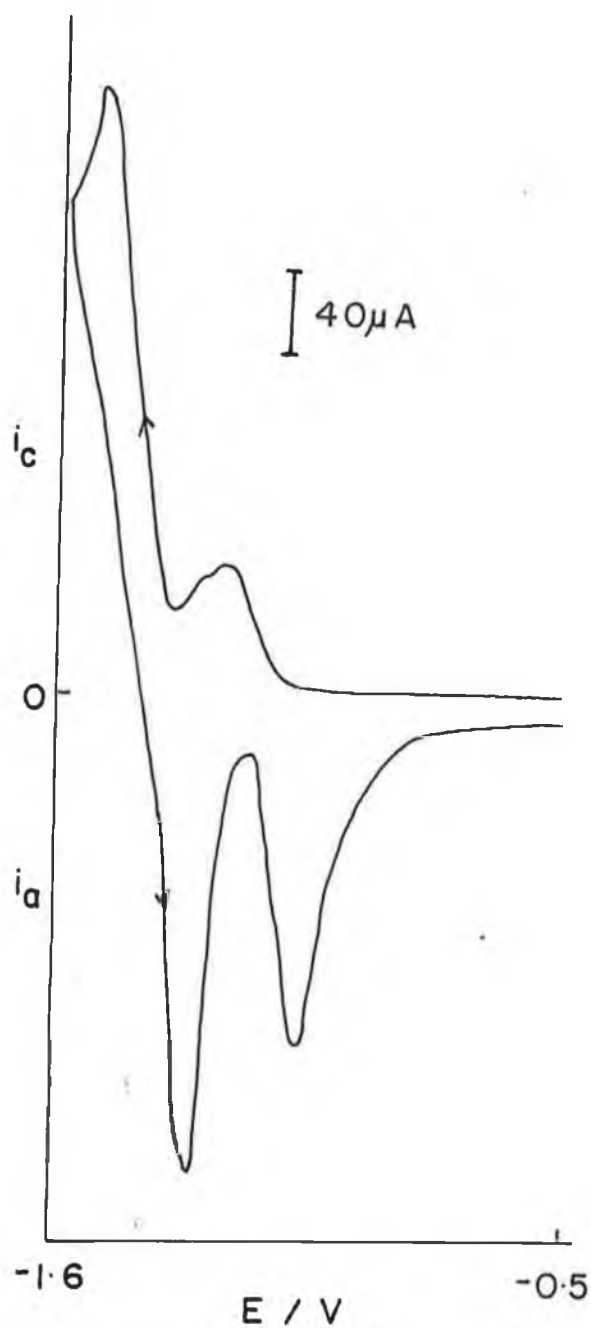


Figure 4.3. Voltammogram of a solution of 3 mM Co^{2+} , 9 mM bpy and 10mM CTAB in 0.1 M KCl at a glassy carbon electrode, scan rate = 100 mV/s

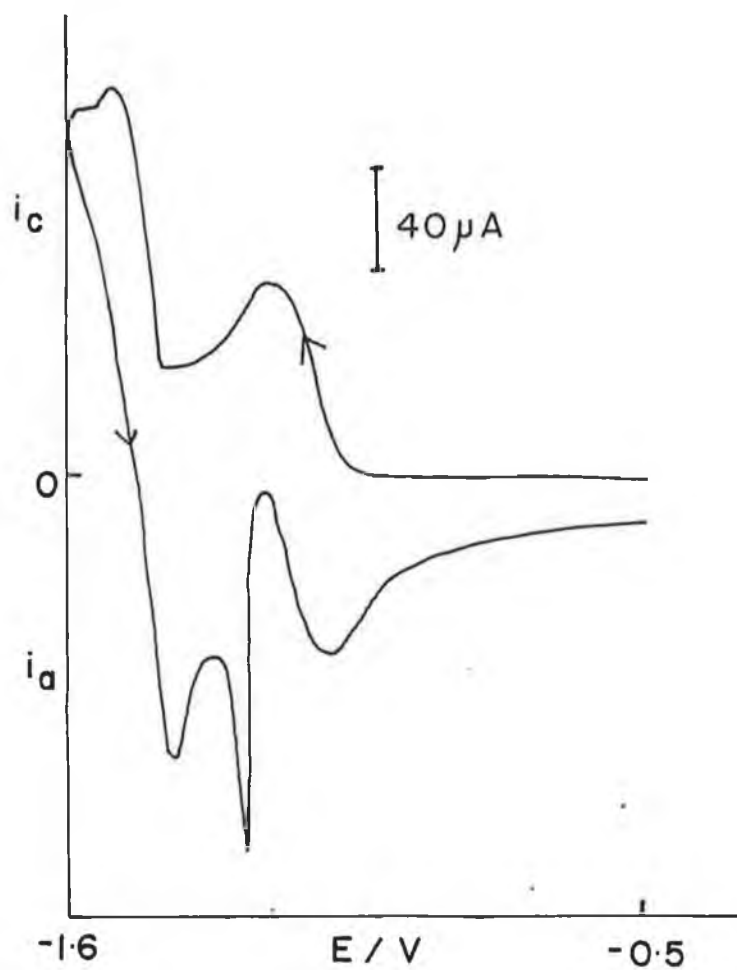
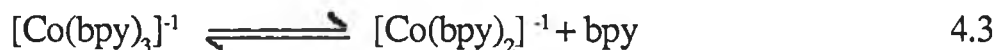


Figure 4.4. Voltammogram of a solution of 3 mM Co^{2+} , 9 mM bpy and 0.1M CTAB in 0.1 M KCl at a glassy carbon electrode, scan rate = 100 mV/s

The species formed by the second reduction may dissociate as follows



It is the dipyridyl species which gives the sharp reoxidation peak seen in figure 4.3. This peak is due to the adsorption of the $[\text{Co}(\text{bpy})_2]^{-1}$. Therefore if excess bpy was present then reaction 4.3 would not go towards the right hand side.

If figure 4.2, 4.3 and 4.4 are compared it can be seen that the current observed for figure 4.4 is much smaller than that observed for the other two. This would indicate that the species diffusing through the solution is, in fact, the micelle, ie. $[\text{Co}(\text{bpy})_3]^{+2}$ bound in the micelle, rather than the solution $[\text{Co}(\text{bpy})_3]^{+2}$ complex itself. Also the current for the second reduction is decreased by a factor of 0.64. Therefore the diffusion coefficient would decrease by a factor of $(0.64)^2$, as the appropriate Randle-Sevcik equation is [8]

$$i_p = 0.4463 \text{ FAC}_x (F/RT)^{1/2} v^{1/2} D^{1/2} \quad 4.4$$

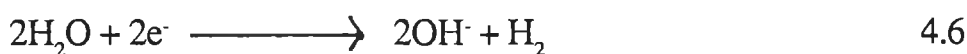
where all the expressions have their usual meanings. The concentration of CTAB is an important parameter as it effects equation 4.3. If figure 4.3 is examined, it can be seen that the voltammetric behaviour observed is a combination of the electrochemistry of $[\text{Co}(\text{bpy})_3]^{+2}$ in solution and $[\text{Co}(\text{bpy})]^{+2}$ within the micelle, due to some $[\text{Co}(\text{bpy})_3]^{+2}$ being at the outer edge of the micelle. There is no splitting of the first oxidation peak, at all scan rates, for voltammograms run in 0.01M CTAB.

Diffusion coefficients of micelle-bound molecules in solutions of surfactants have been evaluated by Rusling [8] using equation 4.4. From the data obtained in this work graphs of peak current versus root scan rate, for the first electron transfer were linear, indicating diffusion control (concentrations of CTAB used were 0.1M and 0.15M). The intercepts of these plots were found to be non-zero. This deviation from the expected theoretical behaviour may be due to interference caused by

adsorbed surfactant at the electrode surface. The behaviour of the subsequent reduction peaks was deemed to be too complex to be subjected to this type of analysis because of the catalytic reactions occurring.

It is known that glassy carbon is hydrophobic and perhaps the $[\text{Co}(\text{bpy})_3]^{-1}$ and $[\text{Co}(\text{bpy})_2]^{-1}$ adsorbed onto the surface, whereas when the micelle is present, the electron transfer occurs from within the micellar hemisphere, on the electrode surface. If a hemi-micelle formed at the electrode surface this would give rise to thin layer like voltammetry, which is observed to some degree. Rusling and others have found that when working in CTAB, that a thick film of CTAB on the electrode surface traps reactants, and the reaction between the substrate and the active form of the catalyst occurs in this hydrophobic film [5,17].

Figure 4.5 shows the behaviour of the system at even higher surfactant concentration. Again the Co(I)/Co(II) couple is reversible. Here the adsorption peak has increased in magnitude relative to the other peaks. This increase occurs at the expense of the other oxidation peak at -1.4V. From this result it can be seen that the dissociation of $[\text{Co}(\text{bpy})_3]^{-1}$ increases with the concentration of CTAB. So CTAB appears destabilize the $[\text{Co}(\text{bpy})_3]^{-1}$ complex leading to the formation of the $[\text{Co}(\text{bpy})_2]^{-1}$ species. By decreasing the scan rate to allow a greater time for reaction at the electrode, voltammetric behaviour like that seen in figure 4.6 is observed. The second reduction peak magnitude is much greater than twice that of the first reduction peak. By comparing figure 4.4 and 4.6 it can be seen that a catalytic current is evident, perhaps due to



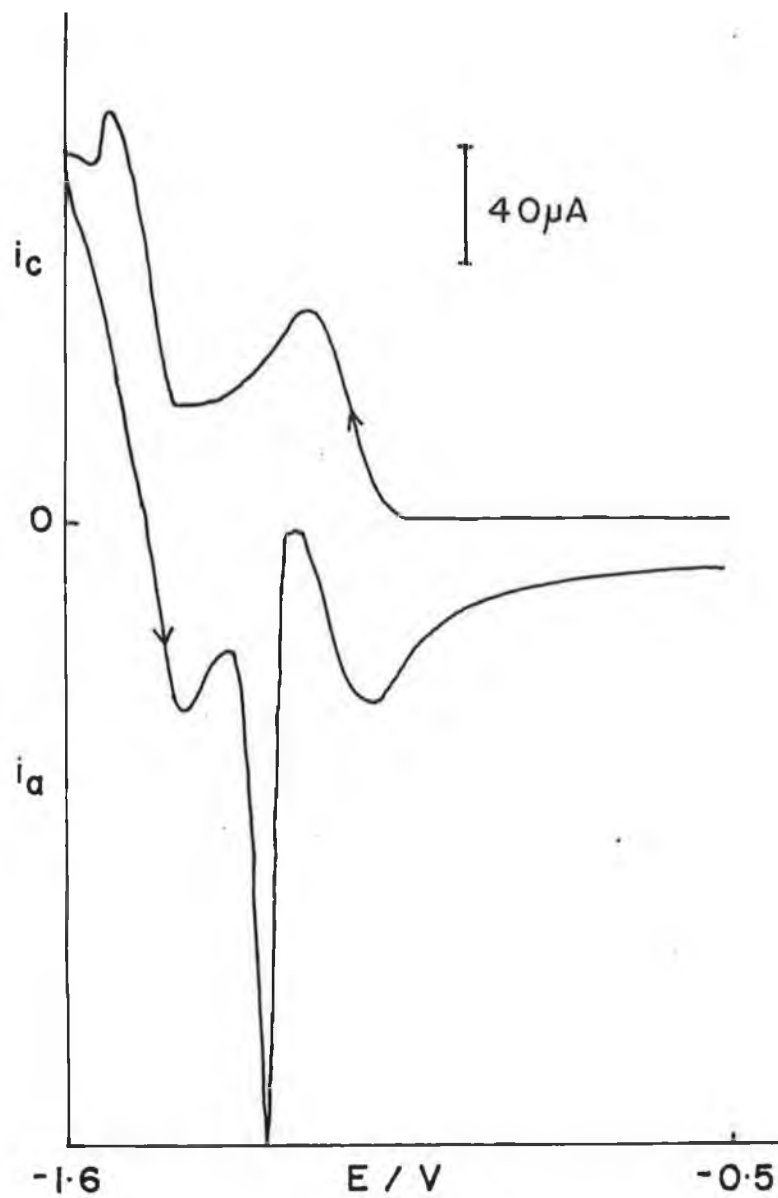


Figure 4.5. Voltammogram of a solution of 3 mM Co^{2+} , 9 mM bpy and 0.2M CTAB in 0.1 M KCl at a glassy carbon electrode, scan rate = 100 mV/s

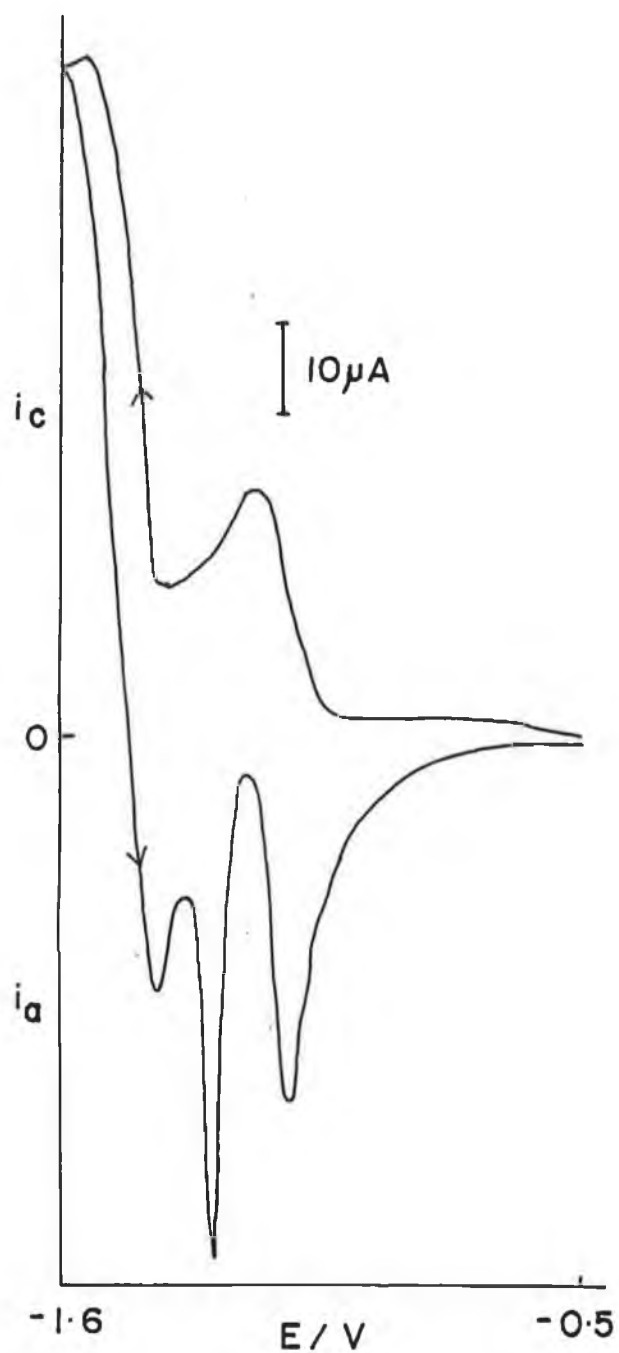


Figure 4.6 Voltammogram of a solution of 3 mM Co^{2+} , 9 mM bpy and 0.1M CTAB in 0.1 M KCl at a glassy carbon electrode, scan rate = 10 mV/s

Overall reaction is



If DDAB is used as surfactant different voltammetry is observed, as can be seen in figure 4.7 (0.2M DDAB). It can be seen that there is no dissociation of $[\text{Co}(\text{bpy})_3]^{-1}$ to $[\text{Co}(\text{bpy})_2]^{-1}$, and bpy, as there is no adsorption peak observed, even at this high concentration of DDAB. By comparing figure 4.5 and figure 4.6, it can be seen that the first reduction peak is much smaller for DDAB, indicating that perhaps the micelle size is greater and diffusion coefficient smaller. Mediation is occurring since the reverse of the second peak is smaller than the forward peak. This means that the $[\text{Co}(\text{bpy})_3]^{-1}$ once formed, must undergo reaction with the water as it is not all available for reoxidation (as shown in equation 4.7). The single electron redox couple exhibits reversible voltammetry as observed in the CTAB case, although the peak to peak separation is greater than for CTAB.

At lower scan rates (figure 4.8), the mediation at the second reduction peak can be seen by the low reoxidation peak. The $[\text{Co}(\text{bpy})_2]^{-1}$ species can be observed as the concentration of DDAB is decreased. Figure 4.9 shows a voltammogram of the $[\text{Co}(\text{bpy})_3]^{+2}$ in 0.01 M DDAB there the peak due to the reoxidation of the $[\text{Co}(\text{bpy})_3]^{+2}$ is similar in magnitude to that of $[\text{Co}(\text{bpy})_3]^{-1}$. The reason for the unusual voltammetry observed when using DDAB solutions is that the solutions of DDAB may have an emulsion/liquid crystal type of behaviour. Iwunze and Rusling [16], suggested that DDAB does not actually form micelles but insoluble milky suspensions in water. This result supports this claim. They suggested that the adsorption observed when using DDAB was due to adsorption of DDAB aggregates onto the electrode. As exhibited by CTAB solutions, the voltammetry of the DDAB solution shows diffusion controlled voltammetry for the Co(III)/Co(I) couple only.

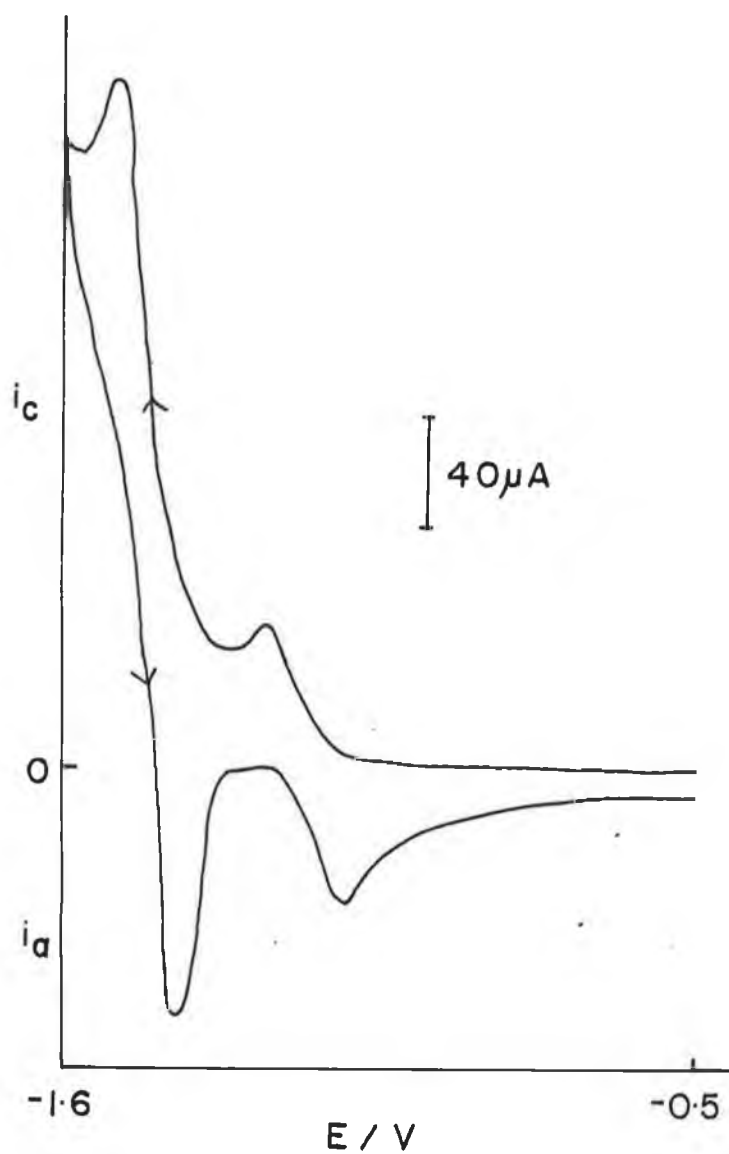


Figure 4.7. Voltammogram of a solution of 3 mM Co^{2+} , 9 mM bpy and 0.2 M DDAB in 0.1 M KCl at a glassy carbon electrode, scan rate = 50 mV/s and $T=40^{\circ}\text{C}$

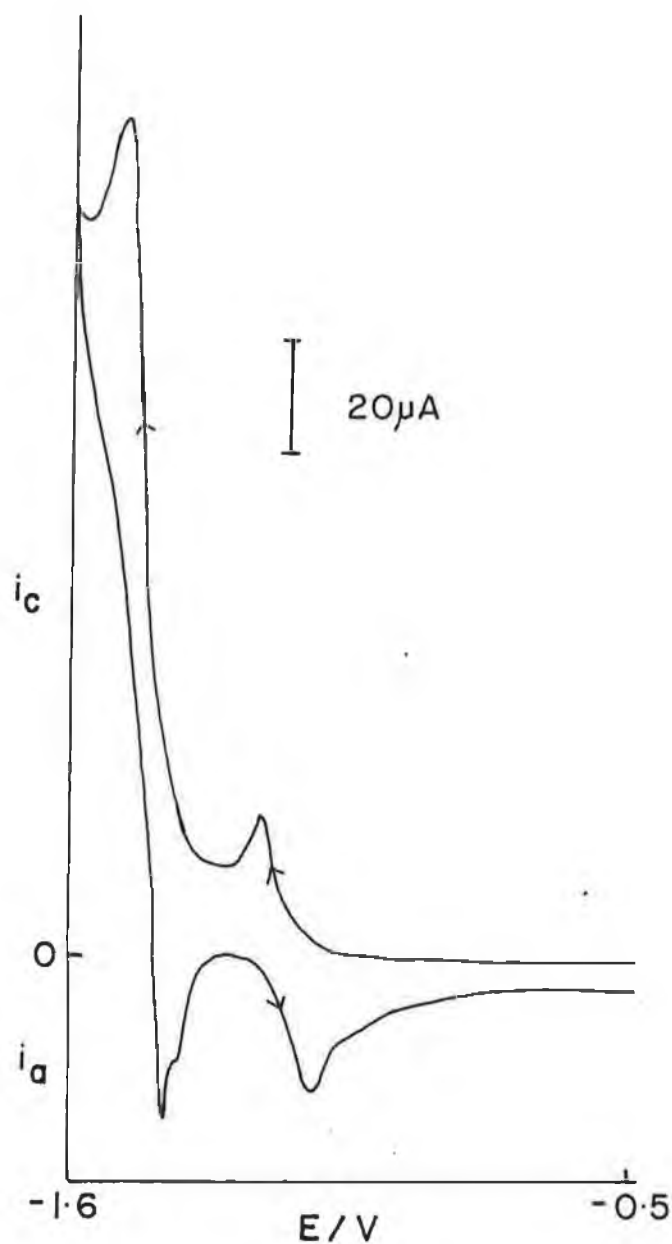


Figure 4.8. Voltammogram of a solution of 3 mM Co^{2+} , 9 mM bpy and 0.2M DDAB in 0.1 M KCl at a glassy carbon electrode, scan rate = 10 mV/s and $T = 40^{\circ}C$.

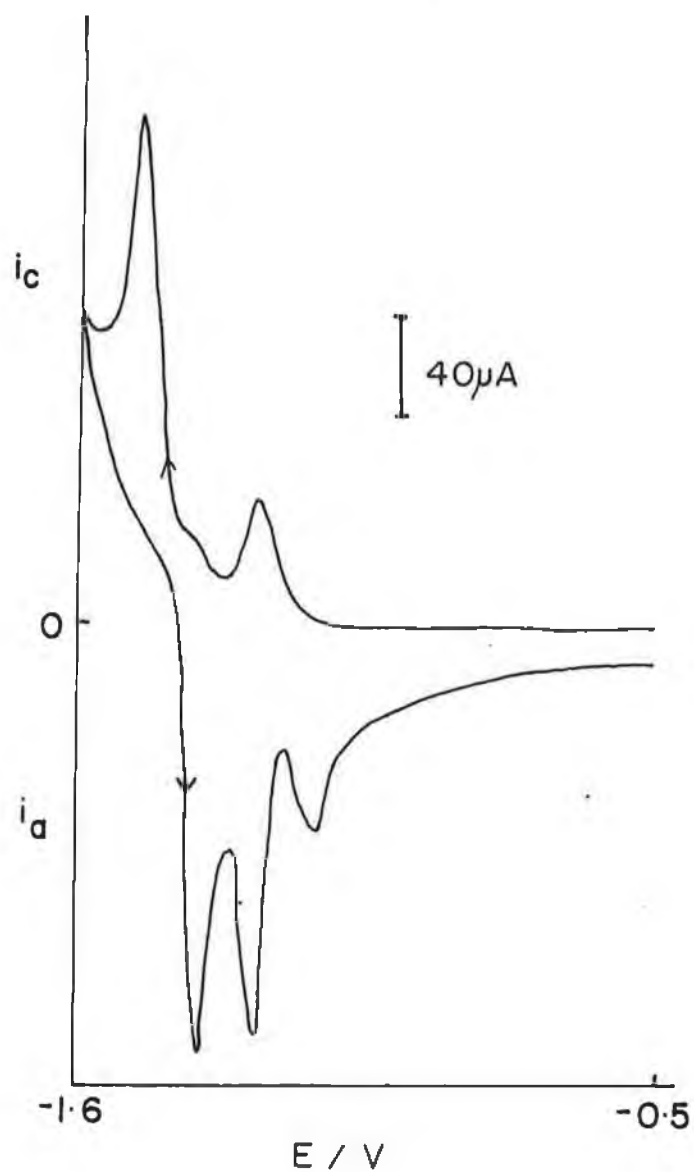


Figure 4.9. Voltammogram of a solution of 3 mM Co^{2+} , 9 mM bpy and 0.01M DDAB in 0.1 M KCl at a glassy carbon electrode, scan rate = 50 mV/s and $T = 40^\circ C$.

It was decided to use DDAB solutions to analyse the decomposition of CCl_4 , primarily as the voltammetry is apparently more consistent than in the CTAB solutions. It is also possible to use smaller concentrations of DDAB than CTAB to achieve decomposition. There is a greater degree of mediation in DDAB solutions. Figure 4.10 shows the effect of adding 2.5 mls of CCl_4 to a solution of $[\text{Co}(\text{bpy})_3]^{+2}$ in 0.05M DDAB. The enhancement of the reduction peaks indicates that the CCl_4 is being decomposed by the electrocatalysed $\text{Co}(-\text{I})$ species. If the concentration of DDAB is further decreased, the behaviour exhibited in figure 4.11 is observed, upon addition of 2.5 mls of CCl_4 . As can be seen there is a considerable increase in current observed upon reduction. The reoxidation peaks appear to disappear, but it was felt that the considerable enhancement of the catalytic current seen here would suggest that more efficient decomposition of CCl_4 would be achieved using this DDAB concentration. This would again suggest that dissociation of the $[\text{Co}(\text{bpy})_3]^{-1}$ is necessary.

The next step was to attempt bulk electrolysis utilizing $[\text{Co}(\text{bpy})_3]^{+2}$ in DDAB solutions to decompose CCl_4 . This will be discussed next.

4.3.2. Bulk electrolysis

Figure 4.12 depicts a series of potentiometric titrations for a preliminary bulk electrolysis of solutions of cobalt(II) tris (bipyridal) in the presence of DDAB as surfactant. The cell used for bulk electrolysis was degassed and this caused some difficulty, in that the surfactant induced bubbling of the solution. It can be seen that there are two end-points in the titration, the second is due to chloride. It is interesting to note that the Br^- from the surfactant was observable using this technique. After some electrolysis it can be seen that while the positive of the end point for bromide does not change the concentration of chloride increases. This is presumably due to the electrocatalytic reduction of CCl_4 mediated by the cobalt complex yielding ultimately Cl^- . Ideally analysis of the solution for the chlorinated hydrocarbon should have carried out to determine the composition of

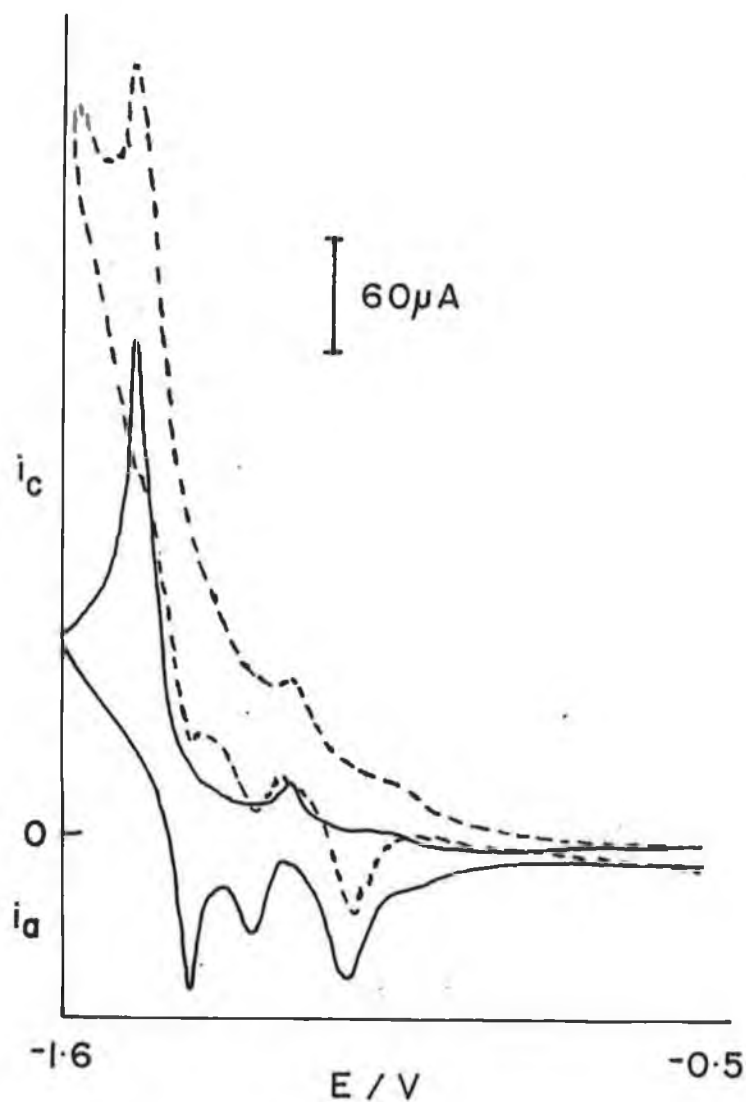


Figure 4.10 Voltammogram of a solution of 3mM Co^{2+} , 9mM bpy, 0.05 M DDAB in 0.1M KCl at a bare glassy carbon electrode, scan rate = 10 mV/sec,. Dashed line is the same following an addition of 2.5 cm³ of CCl_4 to the solution.

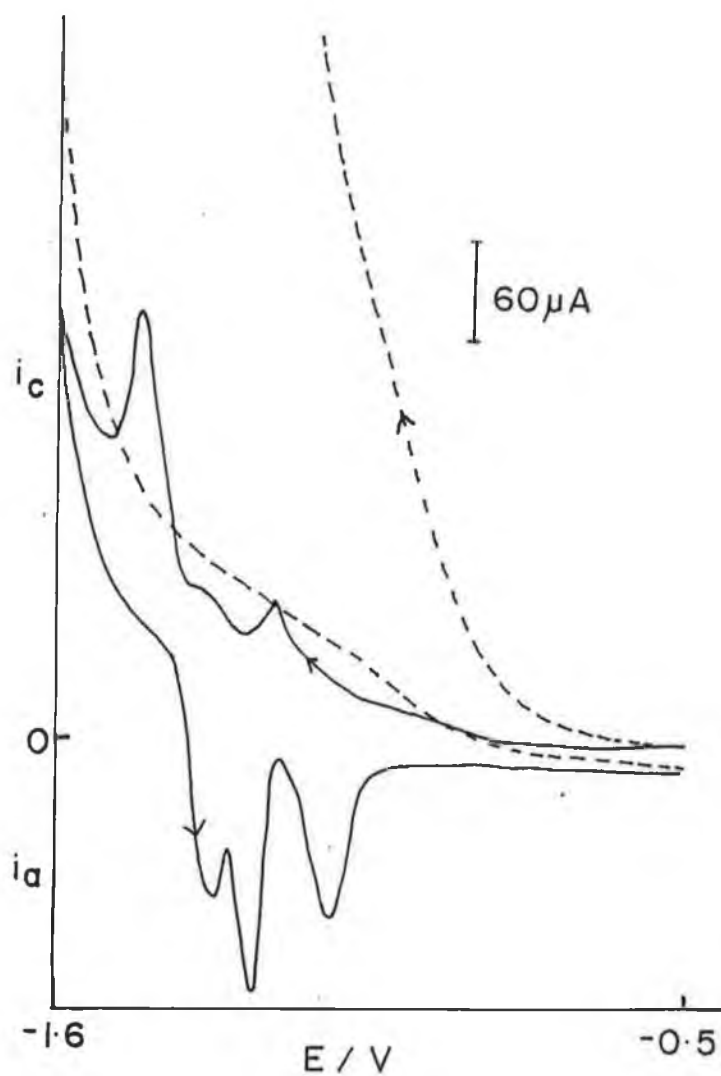


Figure 4.11 Voltammogram of a solution of 3mM Co^{2+} , 9mM bpy, 0.01 M DDAB in 0.1M KCl at a bare glassy carbon electrode, scan rate = 10 mV/sec, Dashed line is the same following an addition of 2.5 cm³ of CCl_4 to the solution.

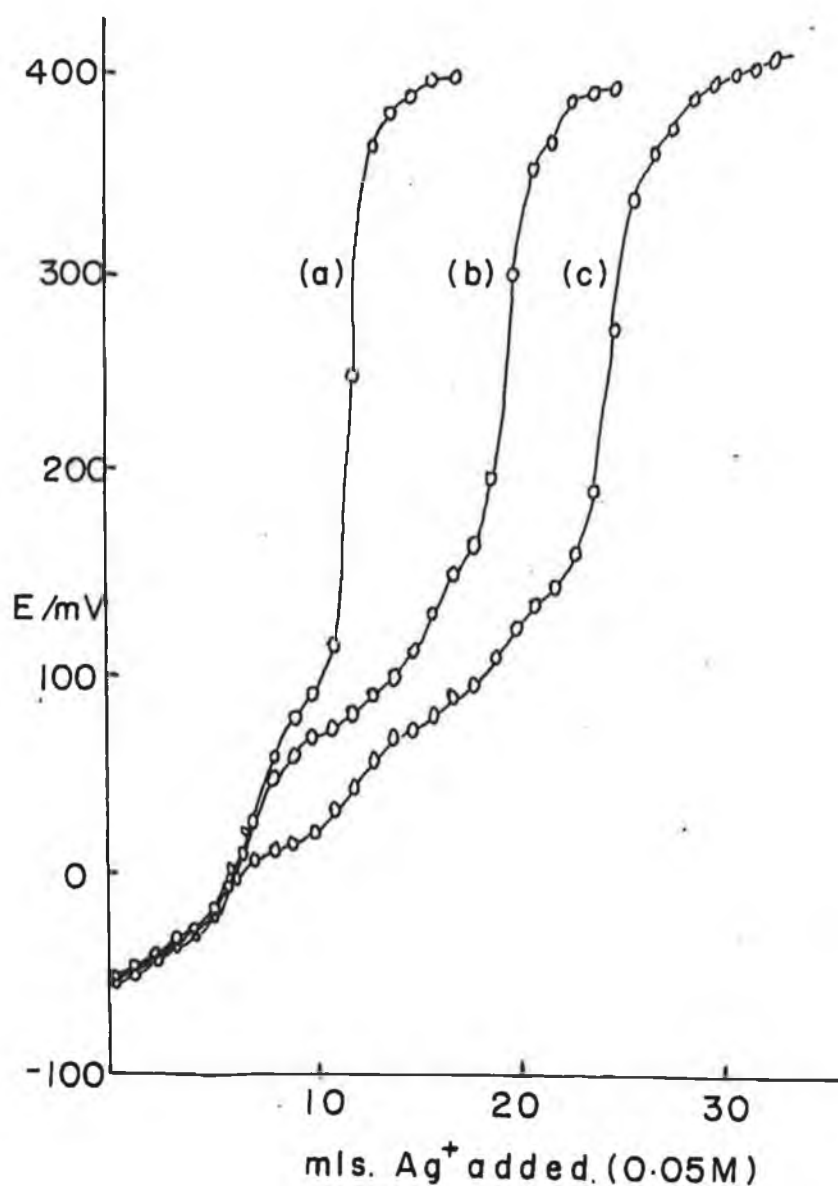


Figure 4.12 Potentiometric plot for a solution of 25 ml. of 0.05 M Na₂SO₄, 0.02 M NaCl, 0.02 M KBr, 0.05 M DDAB, 3mM CoCl₂ and 9 mM bpy, with 1 ml. CCl₄ added. (a) before electrolysis, (b) after 3 hours electrolysis, and (c) after 6 hours electrolysis. The sample taken in each case was 10 ml., the titrant was 0.05 M Ag⁺ and the indicating electrode was a Ag/AgCl electrode.

the other reduced forms of CCl_4 . It may be seen that for longer electrolysis times the end point for bromide increases indicating possible degradation of the micellar phase. However the first end point corresponds to a $[\text{Br}^-]$ of about 0.07 M. The increase in chloride concentration was 0.045M after three hours (curve 4.12(b)), indicating that the increase in concentration of Cl^- in the cell, which corresponds to a percentage decomposition of 2.7% for the initial CCl_4 added to the cell after three hours and 3.9% conversion after six hours.

It is difficult to estimate the current efficiency of this process because there was a reasonable fluctuation in the current during the electrolysis, but it appears that the values were close to 100%. Further work is necessary. It should be noted that the bulk electrolysis took place at room temperature, with stirring, where the solution took on an opalescent colour. Similar experiments were carried out at higher DDAB concentrations and with CTAB instead and with sodium acetate instead of Na_2SO_4 as a background electrolyte. However these were largely unsuccessful.

A pH study would be useful since an optimum pH region is expected; low enough to provide H^+ for the reduced CCl_4 but not too low so as to precipitate out the surfactant. Furthermore, a test for the presence of CO_3^{2-} would be useful in characterizing the products of the electrolysis. In order to make the electrolysis viable a layer cell configuration would be necessary and the problems associated with the clean up of the resultant solutions and recovery of the cobalt complex solved. This is also a relatively expensive technique since the DDAB and bpy are expensive and if chloride could be removed periodically then a batch operation may be possible.

4.4 CONCLUSIONS

This work was concerned primarily with comparing the voltammetry of $[\text{Co}(\text{bpy})_3]^{+2}$ complexes in CTAB and DDAB micelles with variations in surfactant concentration and scan rate. The surfactant was necessary as it was seen to stabilize the Co(I) complex allowing it to undergo reduction to the Co(-I) species. In CTAB the Co(II)/Co(I) couple was relatively reversible electrochemically, especially at high concentrations of CTAB run at fast scan rates. The voltammetry of this couple was not so reversible in DDAB solutions.

The micelles do appear to provide protection of the catalyst from decomposition. The peaks due to the $[\text{Co}(\text{bpy})_2]^{-1}$ are thin-layer indicating that the complex is adsorbed at the electrode surface in solutions of both surfactants. The adsorption appears to increase with concentration of CTAB and also with decreasing scan rate. The scan rate dependence is to be expected as there is less time available for reaction at the electrode surface at fast scan rates. If the concentration of CTAB is decreased voltammetry characteristic of a non-surfactant containing solution is observed, indicating that concentrations of the order of 0.1M CTAB are required to fully compartmentalize the $[\text{Co}(\text{bpy})_3]^{+2}$, although this is a concentration much greater than the critical micelle concentration, (CMC) The CMC is the minimum concentration of surfactant needed so that micelles form. The fact that greater adsorption is observed in CTAB solutions of highest concentrations may also support the idea that the electrochemistry occurs in a hydrophobic CTAB film adsorbed at the electrode surface. CTAB also seems to destabilize the $[\text{Co}(\text{bpy})_3]^{-1}$ complex leading to the formation of the adsorbing $[\text{Co}(\text{bpy})_2]^{-1}$ species.

In DDAB the adsorption peak does not exhibit as much of a scan rate dependence as in CTAB. Perhaps the micelles are easier formed in DDAB, or maybe diffusion is inhibited due to the greater viscosity. The voltammetry also exhibits less of a concentration dependence in DDAB. The effect of the viscosity can be seen if one considers the fact that the $[\text{Co}(\text{bpy})_2]^{-1}$ species only seems to

appear at low DDAB concentrations, indicating that any cobalt species in a 'micellar' phase, at higher DDAB concentrations do not appear capable of diffusing to the electrode surface to undergo reduction. This behaviour may be in keeping with the idea that DDAB does not actually form micelles, but non-micellar suspensions instead. In DDAB the magnitude of the second reduction peak is not as reversible as that observed in CTAB solutions. There is considerable mediation at the second reduction peak as can be seen by the much smaller reoxidation peaks observed.

Because of the compartmentalization of catalyst in the micellar layer the decomposition of CCl_4 features considerable kinetic enhancement. When low concentrations of DDAB are used at slow scan rates, the reoxidation peaks totally disappear indicating the reaction of electrogenerated species with CCl_4 . At higher surfactant concentrations, only the $[\text{Co}(\text{bpy})_3]^{-1}$ peak was diminished.

Initial bulk electrolysis experiments showed a fairly low rate of conversion of CCl_4 to Cl^- . Further work is needed to optimise conditions and to further develop the system. An advantage of using the DDAB, is that lower DDAB concentrations can be used to compartmentalize the reactants while much greater CTAB concentrations are needed.

There are a number of disadvantages of using surfactant systems. The very nature of the surfactant means that it is difficult to make a degas solutions without unwanted bubble formation. All solutions had to be made very carefully and allowed to reach equilibrium for a number of days prior to use. Degassing had to be done very carefully. All solutions were heated as they were being prepared to solubilize the reactants and voltammograms were run at temperatures greater than room temperature. This meant the use of an insulated cell and industrially would mean an extra energy requirement on the system. In the bulk electrolysis experiments, the DDAB solutions were solubilized by continual stirring of the solution during electrolysis. This has the advantage of driving flux of electrolyte to the electrode surface while removing the need for heating of the solution. Finally DDAB is an irritant and care must be taken when handling the gel and its solutions.

4.5 REFERENCES

- [1] G.E.O. Proske, Anal Chem., (1952), **24**, 1834
- [2] E. Outkiewicz, B.H. Robinson, J. Electroanal. Chem., (1988), **251**, 11 - 20
- [3] J.F. Rusling, Chun-Nian Shi and S.L. Snuib, J. Electroanal. Chem., 1988, **245**, 331 - 307.
- [4] J.F. Rusling, Chun- Nian Shi, D.K. Gosser and S.S. Shukle, J. Electroanal Chem., 1988, **240**, 201 - 216
- [5] J.F. Rusling, G.N. Kamau, J. Electroanal. Chem., 1988, **240**, 217 - 270
- [6] M.O. Iwunze and J.F. Rusling, J. Electroanal. Chem., (1991), **303**, 267 - 270
- [7] M.O. Iwunze, A. Sucheta and J.F. Rusling, Anal. Chem., 1991, **62**, 644 - 649
- [8] J.F. Rusling, Chun-Nian Shi and T.F. Kumosiniski, Anal. Chem., 1988, **60**, 1260 - 1267
- [9] T.F. Connors and J.F. Rusling, J. Electrochem. Soc., (1983), **130**, 1120.
- [10] T.C. Franklin and M.O. Iwunze, J. Electroanal. Chem., (1980), **108**, 97
- [11] T.C. Franklin and M.O. Iwunze, Anal. Chem., (1980), **52**, 973
- [12] G.L. McIntire and H.N. Blount, J. Am. Chem. Soc., (1979), **101**, 7720.
- [13] G.L. McIntire, H.N. Blount in K.L. Mitell and E.J. Fendler (Eds), "Solution behaviour of surfactants,"
- [14] G.L. McIntire, D.M. Chiappardi, R.L. Casselberry and H.N. Blount, J. Phys. Chem., (1982), **82**, 2632
- [15] G. Meyer, L. Nadyo and J.M. Saveant, J. Electroanal. Chem., (1981), **119**, 417
- [16] M.O. Iwunze and J.F. Rusling, J. Electroanal. Chem., (1989), **266**, 197 - 201
- [17] J. Georges and S. Desmettre, Electrochem. Acta., (1984), **29**, 521

5. GENERAL CONCLUSION

This work carried out preliminary investigations into the feasibility of using electrochemical methods to decompose polychlorinated organic molecules. Initial attempts of carrying out the decomposition in aprotic media, using superoxide ion as a reagent were hindered by low oxygen concentration and the fact that $O_2^{\cdot-}$ is a very reactive species and preferentially reacts with residual water in the system. This would mean that the use of this reagent, in a scaled-up mode, would not be feasible as the nature of industrial samples would be expected to very heterogeneous. A final disadvantage of this system would be the fact that platinum is required, leading to increased cost of reactor. In this work an active electrode was prepared using a very small amount of platinum incorporated into a polypyrrole matrix. This electrode was shown to exhibit electrochemistry indicative of an array of microelectrodes and thus would reduce the cost of electrodes.

The use of conducting polymers is a fast growing area for new electrode material research. Polypyrrole layers with various incorporated counterions were studied. In the case of PPyDBS and PPyDDS layers, in aqueous solution, low charging current was observed, unlike PPyClO₄ or PPyBF₄. The voltammetry of the layers studied were shown to be due in some part to the incorporated anion and not just to differences in morphology of the layers. The layers formed with DBS⁻ and DDS⁻ counterions are more compact and adherent than the layers with smaller anions, suggesting that these layers have a greater degree of order. Charge neutrality is maintained by cation movement in aqueous solutions, while anion movement appears to occur in the THF/water mixture. The relative size of which ever species moves to maintain charge neutrality within the layer appears to affect the electrochemistry of the layer.

The polymer layers formed on the transparent ITO electrodes were fairly heterogeneous in nature. Large charging currents were observed at very high potentials. Very unusual formal potentials were observed when the background electrolyte was changed. A simple graphical method was used to approximate the

bandgap energy of the neutral polypyrrole layer, and this was found to be 2.76 eV.

Carbon tetrachloride was successfully decomposed using a cobalt trisbipyridyl complex incorporated in a micellar system. The surfactant was found to stabilize the cobalt complex, allowing it to undergo further reduction and reoxidation. The electrochemistry of these solutions appears to be complicated, with adsorption of electrogenerated species being dependant upon both scan rate and surfactant concentration. This is particularly true in the case of CTAB micellar solutions. DDAB solutions do not show much of a scan rate dependence. The voltammetry of the cobalt reduction is different depending upon which surfactant is used. Fairly reversible behaviour occurs in CTAB solutions, while this is not true of the DDAB solutions. In DDAB there is considerable mediation occurring. The decomposition of the CCl_4 which was decomposed by this technique was small. Much further work is required to better characterize the system. Perhaps a pH study, changing the surfactant or varying the temperature, might prove useful. It should be noted here that the working electrode was relatively small (12cm^2), and to make the electrolysis viable a larger cell configuration would be necessary. The system would also be run a batch mode.

The use of catalyst incorporated into a micellar phase was found to have a number of advantages;

- (1) It is possible to get selective decomposition of material in micelles,
- (2) It is also possible to stabilize the cobalt complex using a surfactant,
- (3) It is also possible to deliberately vary the concentration of mediator, unlike in the case of O_2 reduction, to achieve specific aims,
- (4) Only a cheap electrode material such as carbon is needed, whereas Pt. is required for O_2 reduction.

Balanced against this are the disadvantages of expense of reagents, problems encountered due to frothing of surfactant, complicated mix of chemicals and the fact that a potentially dangerous heavy metal is required. The $[\text{Co}(\text{bpy})_3]^{+1}$ has been shown a useful reagent and further work is needed to better characterize it's

use for chlorinated molecule decomposition is needed.

At the moment this complex would ideally be useful for decomposing chlorinated "fine chemicals" present in aqueous wash-water from pharmaceutical plants. Further work is necessary to determine if this technique may be economically expanded to a larger scale.